

NECROBIOME SEASONAL VARIATION IN MICHIGAN AND POTENTIAL
POSTMORTEM MICROBIAL BIOMARKERS OF INFANT DEATH INVESTIGATION

By

Bethany G. Mikles

A THESIS

Submitted to
Michigan State University
in partial fulfillment of the requirements
for the degree of

Entomology – Master of Science

2023

ABSTRACT

Death and decomposition usher in a complex community of decomposers to break down and recycle organic matter. Two understudied, key players in this necrobiome are postmortem microbiota and necrophagous insects. The objectives of this study were to characterize these interkingdom dynamics within two postmortem contexts: 1) active insect colonization and carrion decomposition in contrasting seasons; and 2) a snapshot of human infant microbiota pre-insect colonization, to investigate their potential to inform forensic science, carrion ecology, and human health. It was predicted that postmortem microbial communities would change over time and by season. It was also hypothesized that active insect colonization of carrion by blow flies would facilitate the introduction of microbes, altering carrion microbiota. For microbiomes pre-insect colonization, it was predicted that microbiome composition would be structured by body site microbiota and manner of death (MOD), which could indicate potential biomarkers related to MOD. Seasonal comparisons demonstrated significantly distinct microbiota over time and between carcass and fly microbes and significantly slowed decomposition in the fall, greater blow fly diversity in the fall, increasing alpha diversity over decomposition time in the summer, and evidence for the introduction of microbes by flies. In addition, manner of death and body site had a statistically significant structuring effect on postmortem microbiota, and significant interactions (age, race, sex) were identified with manner of death. A potential biomarker of infant death, *Sneathia*, associated with preterm birth and labor was also discovered. These studies present new data that further our understanding of complex postmortem microbiome dynamics and promote standardization of practical and applicable analyses within the fields of forensic science and carrion ecology.

To my parents, for their unconditional support through the good, the bad, and the weird.
To Nate, for holding me steady.
And to Al, for just being a part of it. Thank you.

ACKNOWLEDGEMENTS

I firstly must extend my thanks to my guidance committee. Thank you to Dr. Jen Pechal, for taking a chance on me and granting me this immense learning experience, and for her patience and honest advice. I am so grateful for the opportunity to step outside of my comfort zone and grow as an individual during my time here. Thank you to Dr. M. Eric Benbow, for his wisdom, kindness, and encouragement. And thank you to Dr. Rebecca Knickmeyer, for taking the time to listen and provide valuable perspective and insight. I know it's been a journey to get here, and I appreciate each of your support and mentorship along the way.

The completion of these projects would not have been possible without the help, time, and counsel of many others. Thank you to Dr. Anthony Cognato for helping me improve my skills in beetle identification. I thank my fellow students and peers that have come through the Benbow lab; we all learned so much from each other. Thank you to my amazingly cool undergrads Emily Schnettler, Kat Yoskowitz, and Alexandria Verner, whose genuine enthusiasm for our work never failed to encourage me. I thank Dr. Sophie Picq for her sincerity and guidance in and out of the lab, at all times of day, and Alexandra Bauer and Alex Rakestraw for sharing their knowledge with me. A huge thank you to Anthony Grigsby and Kelly Waters for their hard work, long days out in the field, and assistance with sample collection; I'm so excited to see what you will discover and accomplish. I must also give an extra, emphatic thank you to Kelly for lending me countless hours of her limited time, and for her invaluable friendship during the long nights and challenging weeks when the lab became our home away from home.

I must lastly extend one final thank you to my friends, family, my wonderful partner Nate, and my cat Bella. You have supported me all the way, mostly from hundreds of miles away. Thank you all for believing in me.

TABLE OF CONTENTS

LIST OF ABBREVIATIONS.....	vi
CHAPTER 1: NECROBIOME SEASONAL VARIATION IN MICHIGAN	1
CHAPTER 2: POTENTIAL POSTMORTEM MICROBIAL BIOMARKERS OF INFANT DEATH INVESTIGATION.....	53
LITERATURE CITED	85
APPENDIX A: RECORD OF DEPOSITION OF VOUCHER SPECIMENS	96
APPENDIX B: SUPPLEMENTARY MATERIALS.....	97

LIST OF ABBREVIATIONS

ADH - Accumulated Degree Hours

CB – Cardiac blood

CI – Confidence Interval

FDR – False Discovery Rate

IF – Interhemispheric fissure

KW – Kruskal-Wallis

LEFSe – Linear discriminant analysis Effect Size

MOD – Manner of death

ND – No Data

NIJ – National Institute of Justice

PCoA – Principal Coordinates Analysis

PCR – Polymerase Chain Reaction

PERMANOVA – Permutational Multivariate Analysis of Variance

PMI - Postmortem Interval

SE - Standard Error

TAE – Tris-acetate-EDTA

TS – Trabecular space

CHAPTER 1: NECROBIOME SEASONAL VARIATION IN MICHIGAN

Abstract

Decomposing remains provide ephemeral resources to a diverse host of organisms, supporting a dynamic framework that drives the essential recycling of nutrients back into ecosystems. These interactions are complex and often overlooked, particularly those among insects and microbes. Diptera, especially blow flies (Diptera: Calliphoridae), may play a significant mechanistic role in this system as primary colonizers of forensic importance. This study aimed to investigate these interkingdom relationships and community dynamics to improve our understanding of the ecological structure and functioning of the necrobiome over time. Insect succession, carcass epinecrotic microbial communities, and internal blow fly microbiomes were sampled from swine carcasses (N = 6) in East Lansing, Michigan, during decomposition in the summer and fall. Carcass decomposition and accumulated degree days (ADH) in the fall occurred nearly five times slower than summer carcass decomposition and ADH. Insect communities also differed, with greater blow fly species diversity observed in the fall. Amplicon-based 16SrRNA sequence analyses revealed statistically significant daily temporal effects on bacterial succession of carcasses for both seasons, as well as significant interactions between internal blow fly and carcass microbiota. Summer early decomposition was represented by high relative abundances of Moraxellaceae, while fall was represented by Enterobacteriaceae. Alpha diversity increased over decomposition time in the summer, and abundances of Vagococcaceae appeared in correlation with blow fly catches as decomposition progressed for the summer and fall. Blow fly internal microbiomes were characterized by high relative abundances of Vagococcaceae compared to carcass microbes, providing support for the potential introduction of exogenous microbes into carrion decomposition by blow flies.

Introduction

Decay is a dynamic, complex process that supports critical ecosystem services, seen and unseen (Barton, Cunningham, Lindenmayer, et al., 2013). After death, carrion becomes a concentrated nutrient-rich patch for a diverse assemblage of vertebrate scavengers, insects, and microbes to exploit and redistribute back into the ecosystem (Barton et al., 2019). The culmination of these organisms and their interkingdom interactions make up the necrobiome, an efficient, intricate framework that can profoundly impact ecosystem structure and function over time (Barton, Cunningham, Lindenmayer, et al., 2013; Barton et al., 2019; Benbow et al., 2019; Parmenter & Macmahon, 2009). Despite the wide impacts of carrion decomposition, however, its scope of study has been primarily limited to individual components of the necrobiome framework, such as arthropod succession or microbial succession, and few studies have examined their potential interactions simultaneously.

Many studies have documented the predictable assembly of necrophagous invertebrate taxa on carrion over time in various ecosystems, which can be used as a means of determining the minimum postmortem interval (PMI_{min}) or a minimum time elapsed since death (Anderson, 2011; Archer, 2004; Benbow et al., 2013; Early & Goff, 1986; Matuszewski et al., 2008). Because their development is highly temperature dependent and they are known to visit vertebrate carrion at differing stages of decomposition depending on their nutritional, reproductive, or habitat needs, insects can be used as a tool to better predict when death occurred (Byrd & Caster, 2009; Payne, 1965). For example, Diptera, such as blow flies (Diptera: Calliphoridae) and flesh flies (Diptera: Sarcophagidae), are among the first insects to detect and arrive at a carcass, while other insects, such as skin beetles (Coleoptera: Dermestidae), are typically attracted to skin and hair of drier, older carcasses (De Jong & Merritt, 2015;

Kulshrestha & Satpathy, 2001). Studies have also demonstrated that preventing or delaying insect access to decomposing remains significantly reduces biomass removal rates, slows decomposition processes, and can even alter insect community succession patterns (Payne, 1965; Pechal, Benbow, et al., 2014). These associations are critical to informing the field of forensic entomology, the analysis and use of arthropod evidence within the judicial system for use in criminal and civil litigation (Byrd & Caster, 2009).

Other studies have examined the succession of postmortem bacterial communities, also demonstrating their potential as a standardized tool for estimating a PMI_{min} range (Guo et al., 2016; Metcalf et al., 2013). The human microbiome has proven to be a highly dynamic community reflective of its host's antemortem lifestyle, environment, and physiology over time, with distinct variations observed in the microbiomes of individual body sites (*i.e.*, mouth, nose, skin) (Costello et al., 2009; Turnbaugh et al., 2007). Recent metagenomic data have also indicated potential correlations between host microbiota structure and function, and health conditions such as inflammatory bowel disease, colorectal cancer, and obesity (Cho & Blaser, 2012). This pattern continues after death, with antemortem host microbiomes remaining viable for 48-72 hours postmortem, and significant temporal changes observed in bacterial communities as decomposition progresses (Adserias-Garriga et al., 2017; Hyde et al., 2015; Pechal, Crippen, et al., 2014; Pechal et al., 2018).

While the individual importance of microbes and insects in carrion decomposition is well described, the extent of their interactions has yet to be fully evaluated. Research has demonstrated that microbes play a role in multiple fly lifecycles from egg to adult, such as the black soldier fly (Diptera: Stratiomyidae), blow fly, fruit fly (Diptera: Drosophilidae), house fly (Diptera: Muscidae), and the primary vector of malaria, *Anopheles* mosquitoes (Diptera:

Culicidae) (Ahmad et al., 2006; Majumder et al., 2020; Wang et al., 2011; Zheng, Crippen, Singh, et al., 2013; Zurek et al., 2000). Flies are also well-established vectors of more than 100 bacterial pathogens, such as *Staphylococcus aureus*, a leading cause of many skin infections like “staph”, *Camylobacter* spp., a leading cause of food poisoning, and *Escherichia coli* O157:H7, the primary cause of hemorrhagic colitis and hemolytic uremic syndrome in North America (Armstrong et al., 1996; Graczyk et al., 2001; Greenberg, 1991). It subsequently stands to reason that flies could be capable of introducing their own exogenous microbiota to epinecrotic microbial communities during colonization and oviposition, potentially altering the postmortem microbiome in undiscovered ways. Findings from Weatherbee et al. (2017) suggested significant temporal interactions between epinecrotic communities on carcasses, dipteran larval masses, and the internal larval blow fly microbiome, while results from Iancu et al. (2015) and Metcalf et al. (2016) show support for the introduction of new microbial taxa on a carcass by necrophagous flies. Zheng (2013) also found evidence that black soldier flies and blow flies are attracted to volatiles released by specific bacteria deposited on carrion by conspecifics, and may be repelled by bacteria from competing species, suggesting that microbes may drive competition for ephemeral resources and selection of oviposition sites.

Studies documenting the extent of the role adult flies may play in the exchange of microbes are lacking, and there is a need for further study of this interkingdom relationship to better understand how these ubiquitous organisms shift necrobiome dynamics in various ecological settings and environmental conditions. To investigate these interactions, we conducted two seasonal decomposition trials to: 1) characterize insect communities and document decomposition processes; 2) evaluate postmortem microbial community succession across different body sites on carrion and the internal microbiome of necrophagous flies using high-

throughput sequencing; and 3) compare the findings across each season to identify potential exchanged microbial taxa in carcass and fly microbiomes.

We hypothesized that progression of decomposition would be slower in the fall than the summer, and that microbial and insect diversity would also decrease with cooler temperatures with Diptera being the dominant observed insect taxa. We also hypothesized that temporal shifts in relative abundances of microbial taxa would occur during decomposition, on each carcass as well as between individual body sites, and that the timing of these shifts would correlate with the introduction of microbial taxa by flies, with similar community composition observed in carcass and fly microbiomes.

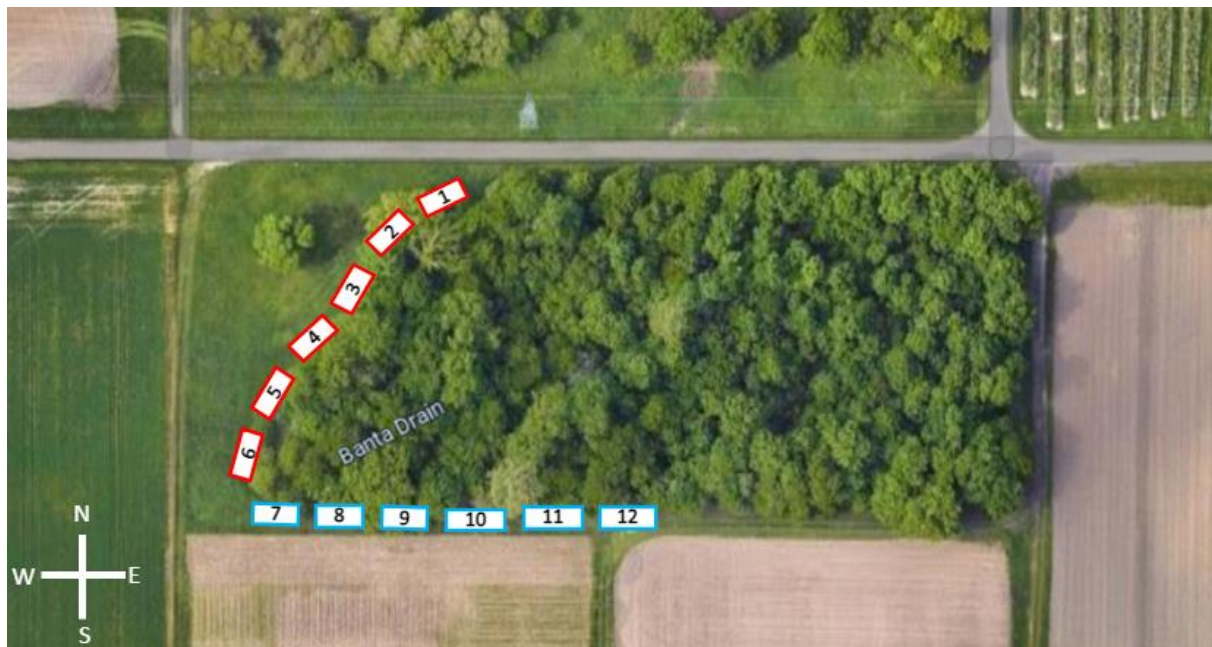


Figure 1. Placement of swine carcasses in the field. Red markers 1-6 represent placement for the summer trial, and blue markers 7-12 represent the fall trial.

Materials and Methods

Study Site

The study was conducted at Box Woodland on Michigan State University's Entomology Research Farm in Lansing, Michigan (42.689789 N, -84.491081 W). Box Woodland is a 5-acre natural area rich in herbaceous flora and contains several maple species (*Acer* spp. L.), white ash (*Fraxinus americana* L.), basswood (*Tilia americana* L.), sycamore (*Platanus occidentalis* L.), several oak species (*Quercus* spp. L.), and red mulberry (*Morus rubra* L.). To model human decomposition, six stillborn swine carcasses (*Sus scrofa* L.) weighing 0.7 to 2.2 kg were placed for two seasonal trials: summer (5 – 11 August 2022) and fall (14 October – 13 November 2022). Studies have shown that swine carcasses closely represent decomposition of human remains, and can be used to model this process in the absence of human cadavers (Catts & Goff, 1992). The size and age of carcasses used for this study were based on availability.

Carcasses were obtained from the Michigan State University Swine Teaching and Research Center in East Lansing, Michigan on 3 June 2022 (N = 6) and 30 September 2022 (N = 6). Carcasses were received frozen and wrapped securely in plastic bags; they were immediately transported from the research center to the Pechal Laboratory at Michigan State University and placed in -20°C storage. Prior to placement at the field site, carcasses were allowed to thaw at room temperature (22-24°C) for 24 h, and then placed in 0°C storage for 12 h to prevent early onset of decomposition. Carcasses were placed directly on the ground on their right side at 11:50 h (5 August 2022) and 9:30 h (14 October 2022), with each carcass approximately 10 m apart (**Figure 1**). For the summer trial, carcasses were laid in a transect running northeast-southwest against the west edge of the Box Woodland, with heads facing northeast, and labelled alphanumerically C1-C6. Carcasses for the fall trial were placed in a west-south transect along

the south edge of the woodland with heads facing west, and labelled C7-C12. No previous decomposition trials had taken place at the study site (Figure 2).

To prevent scavenger disturbance, each carcass was covered by a wooden cage (0.6 x 0.3m x 0.3m) constructed of poultry netting (0.3m x 1.2m x 15m, 20 gauge, 2.5cm mesh) (Midwest Air Technologies Inc., Long Grove, IL) and untreated pine lumber (Figure 3). For added security, anti-scavenger cages were tied down with nylon-polypropylene cord (0.32cm x 15m) (Everbilt, Home Depot Inc, Atlanta, GA) and wooden stakes (2.5cm x 5cm x 46 cm) secured in the ground and were also weighed down at each corner with a burnt clay brick. For the summer trial a single NexSens DS1921G micro-T temperature logger (Fondriest Environmental, Inc., Alpha, OH) was affixed to the front-left of each cage with a zip tie (Commercial Electric, Cleveland, OH), and ambient temperature was recorded every 15 min until 18:30 h on 26 August 2022. For the fall trial, a single Kestrel DROP D3 wireless data logger (Nielsen-Kellermen Co., Boothwyn, PA) was affixed to each cage as in the summer trial, and ambient temperature was recorded every 10-15 min until 17:20 h on 13 November 2022.

To observe insect succession, a butterfly trap (BugDorm, MegaView Science Co.,Ltd., Taiwan) hung from a steel shepherds hook (1.2 m) (Vigoro, Chicago, IL) was positioned approximately 1 m from each carcass (Figure 3). Written field notes were taken and carcasses were photographed using an iPhone XS (Apple, Cupertino, CA) to document and track decomposition progress. Photos were taken of each carcass in entirety, of the head, abdomen, and rear, and of any present larval masses or other noteworthy observations.



Figure 2. Panoramic view of field sites taken on sampling day one of each trial, (A) Summer and (B) Fall.



Figure 3. Example of the field set-up (anti-scavenger cage, data logger, and butterfly trap) for a swine carcass.

Microbe and Insect Sampling

Postmortem bacterial communities of the skin, mouth, and rectum were collected from each carcass twice daily for each trial, at 10:00 h and 14:00 h in the summer, and at 7:00 h and 13:00 h in the fall. Microbial samples were taken from each body site with a 15 cm sterile DNA-free cotton-tipped swab (Puritan Medical Products, Guilford, ME), by physically rubbing and rotating the swab for 30 s. Skin samples were taken by swabbing three areas of a posterior-

anterior transect along the carcass, with care taken not to resample areas as described in Weatherbee et al. (2017). The cotton tip of each swab was then broken off into a 1.5 ml tube containing 200 μ l of RNAlater stabilization solution (AM7021, Thermo Fisher Scientific, Waltham, MA, USA), later modified to 500 μ l for the fall trial, and transported to the Pechal laboratory to be placed in -20°C storage until further processing.

In the summer trial, insects were sampled every 12 h by placing butterfly traps in -20°C storage overnight and emptying the contents of each into a sterile 15 ml conical tube (VWR International, Radnor, PA). Insect samples were stored at -20°C until further processing, and empty traps were replaced by the next sampling event. In the fall trial, butterfly traps were emptied in the field due to prolonged decomposition and decreased insect activity during the colder weather. All insects were identified to family under a stereoscope using dichotomous keys from Triplehorn et al. (2004), Whitworth (2006), and Marshal et al. (2019), and stored in 100% molecular grade ethanol in 1.5 ml tubes at -20°C. All adult Diptera identified as Calliphoridae (N = 42) were further identified to species using Whitworth (2006) and Marshal et al (2011).

DNA Isolation and Quantification

Microbial body site samples from all time points of the summer trial were selected for DNA analysis due to the quick progression of decomposition in the warmer months and number of sampling events (N = 14), for a total of 252 summer samples. Due to the longer duration and number of sampling events (N = 62) in the fall trial, samples were chosen by calculating ADH across both seasons and choosing comparable sampling events representative of decomposition stages. In the fall trial, 252 samples from 14 sampling events were chosen at 0, 100, 381, 439, 788, 901, 1166, 1250, 1470, 1526, 1690, 1723, 1912, and 2041 ADH or 0, 171, 202, 207, 250,

273, 418, 430, 477, 482, 501, 506, 564, and 608 h after trial start. All blow flies from both trials were also selected for DNA analysis due to their limited quantity. Temperature data were converted to ADH using a base temperature of 10°C (VanLaerhoven, 2008). A summary of sampled substrates for each day, sampling event, and ADH for both seasons can be found in Table 1.

DNA was extracted from the swab samples and blow flies under a biological safety cabinet using a modified QIAGEN DNeasy Blood & Tissue Kit protocol (QIAGEN, Hilden, Germany). Swabs were first prepared for lysis on Parafilm sheets (Bemis Company, Inc, Neenah, WI, USA) by using sterilized general-purpose stainless steel pinning forceps (10-270, Thermo Fisher Scientific, Waltham, MA, USA) and scalpel handles (12-000-164, Thermo Fisher Scientific, Waltham, MA, USA) with sterile, single-use carbon steel blades (22-079-697, Surgical Design Inc. Lorton, VA, USA) to carefully cut the cotton tip off the wooden handle. The cotton was then placed back into its respective 1.5 ml tube, and the wooden handle and Parafilm were discarded. To preserve the individual microbial communities, a new piece of Parafilm and pair of sterile dissecting forceps and scalpel were used to prepare each sample.

Table 1. A summary of all substrates sampled across each seasonal trial, by sampling day, sampling event, and ADH. X indicates that a substrate was sampled that day and **X** (in bold) indicates that a particular sample was processed and sequenced for analysis. While all summer samples were processed due to the short study duration, * indicates the exact event fall samples were chosen from for processing due to their quantity.

Sampling Day	1	2	3	4	5	6	7	8	9	10	11	12
Sampling Events	0*-1	2-3	4-5	6-7	8-9	10-11	12-13	14-15*	16-17	18*-19*	20-21	22*-23
Summer												
ADH	0-91	367-448	806-882	1160-1259	1437-1509	1648-1750	1964-2053					
Insects	X	X	X	X	X	X	X					
Calliphoridae	X	X	X									
Microbes	X	X	X	X	X	X	X					
Decomposition Photos and Taphonomy	X	X	X	X	X	X	X					
Fall												
ADH	0-8	21-25	32-47	57-57	57-57	57-57	57-61	63-100	198-275	381-439	575-647	788-765
Insects	X	X	X	X	X	X	X	X	X	X	X	X
Calliphoridae							X	X	X	X		
Microbes	X	X	X	X	X	X	X	X	X	X	X	X
Decomposition Photos and Taphonomy	X	X	X	X	X	X	X	X	X	X	X	X

Table 1 (cont'd)

Sampling Day	13	14	15	16	17	18	19	20	21	22	23
Sampling Events	24*-25*	26*-27	28-29	30-31	32-33	34-35	36*-37	38*-39	40-41	42*-43*	44*-45*
Summer											
ADH											
Insects											
Calliphoridae											
Microbes											
Decomposition Photos and Taphonomy											
Fall											
ADH	901-901	901-935	935-963	992-1017	1057-1049	1103-1123	1166-1205	1250-1283	1345-1393	1470-1526	1690-1723
Insects	X	X	X	X	X	X	X	X	X	X	X
Calliphoridae	X			X		X	X				
Microbes	X	X	X	X	X	X	X	X	X	X	X
Decomposition Photos and Taphonomy	X	X	X	X	X	X	X	X	X	X	X

Table 1 (cont'd)

Sampling Day	24	25	26	27	28	29	30	31
Sampling Events	46*-47	48-49	50-51*	52-53	54*-55	56-57	58-59	60-61
Summer								
ADH								
Insects								
Calliphoridae								
Microbes								
Decomposition Photos and Taphonomy								
Fall								
ADH	1782-1811	1843-1875	1899-1912	1928-1969	2041-2126	2175-2213	2213-2213	2213-2215
Insects	X	X	X	X	X	X	X	X
Calliphoridae								
Microbes	X	X	X	X	X	X	X	X
Decomposition Photos and Taphonomy	X	X	X	X	X	X	X	X

Blow flies were prepared for DNA extraction by surface sterilizing with three, five-minute rinses of 10% bleach, and three rinses of sterile molecular biology grade water (Pechal & Benbow, 2016). Flies were allowed to dry and each placed into a 2 ml Lysing Z Matrix tube (6961-100, MP Biomedicals, Irvine, CA, USA), then submerged in liquid nitrogen for 20-30 s and immediately pulverized in a FastPrep-96 high-throughput bead beating grinder and lysis system (MP Biomedicals, Irvine, CA, USA) for 15-45 s as needed at 1400 oscillations/min. This pulverizing method was adapted for use with insects from a CTAB (Cetyltrimethyl ammonium bromide) extraction protocol from Tann and Yiap (2009) to promote increased DNA yield.

The manufacturer's protocol was then followed accordingly with the addition of 10 ul of 15 mg/ml lysozyme to promote increased microbial cell lysis. Samples were also treated with 4 ul 100mg/ml RNase A following incubation per the MSU Genomics Core Illumina sample sequencing requirements, and final DNA elution volume was modified from 200 ul to 50 ul. DNA was then quantified using a Qubit 2.0 and a 1x dsDNA High Sensitivity Assay (Thermo Fisher Scientific, Waltham, MA, USA). DNA was stored at -20°C to await further processing.

16S rRNA Confirmation

The microbial gene amplicon V4 region was amplified using conventional PCR with DreamTaq Green PCR Master Mix (2x) (Thermo Fisher Scientific, Waltham, MA, USA), PCR-grade nuclease free water, and region-specific primers 515f/806r (5' GTGCCAGCMGCCGCGGTAA, 5' GGACTACHVGGGTWTCTAAT). PCR samples were each prepared with 24 ul mastermix and 1 ul template DNA, loaded into 96-well plates (82006-636 VWR International, Radnor, PA, USA), and sealed with qPCR film (6091-078, VWR International, Radnor, PA, USA) in a biological safety cabinet. The positive and negative

controls run in each plate were *E. coli* and PCR-grade nuclease-free water, respectively. PCR samples were spun down in a Sorvall ST 8 centrifuge (Thermo Fisher Scientific, Waltham, MA, USA), placed into a Veriti 96-well thermal cycler (Thermo Fisher Scientific, Waltham, MA, USA) and amplified according to previously described methods (Caporaso et al., 2011). Resulting PCR product was stored at -20°C.

Visual 16S rRNA confirmation was then performed via gel electrophoresis. 3% agarose gels (3.6 g agarose in 120 ml 1X TAE) (N605-500G, VWR International, Radnor, PA, USA) were cast in a Thermo EC Midicell Primo EC-330 Horizontal Gel System (Thermo Fisher Scientific, Waltham, MA, USA). 5ul each of GeneRuler 1kb ladder (Thermo Fisher Scientific, Waltham, MA, USA), PCR product, and controls were loaded and run at 90 V for 40 minutes. Gels were then agitated in GelRed solution (60 ul GelRed in 200 ml DI water) (Thermo Fisher Scientific, Waltham, MA, USA) for 30 minutes on a 3D platform rotator (Thermo Fisher Scientific, Waltham, MA, USA). Gels were imaged using the Axygen Gel Documentation System (Corning Incorporated, Corning, NY, USA) at UV 302.

16S rRNA Gene Amplicon Sequencing

DNA sequencing and library construction for microbial body site samples (total N = 400, summer N = 203, fall N = 197) and blow flies (N = 42) was performed at the Michigan State University Genomics Core facility (East Lansing, MI, USA) on the Illumina MiSeq (2 x 250 bp paired-end reads). The V4 region of the 16S rRNA gene was amplified using dual indexed 515F/806R Illumina primers (5'-GTGCCAGCMGCCGCGG-3', 5'-

TACNVGGGTATCTAATCC-3') following the protocol described in Kozich, JJ, et al. (2013). PCR products were batch normalized using an Invitrogen SequelPrep DNA Normalization plate, and products were pooled and cleaned up using a QIAquick Spin column and AMPure XP magnetic beads. Library pools were quality controlled and quantified using a combination of Qubit dsDNA HS, Agilent 4200 TapeStation HS DNA1000, and Invitrogen Collibri Illumina Library Quantification qPCR assays. Amplicon pools were then loaded onto a MiSeq v2 standard flow cell and sequencing was carried out in a 2 x 250 bp paired-end format using a MiSeq v2 500 cycle reagent cartridge and custom sequencing and index primers complementary to the 515f/806r oligomers. Base calling was performed by Illumina Real Time Analysis (RTA) v1.18.54 and output of RTA was demultiplexed and converted to FastQ format with Illumina Bcl2fastq v2.20.0.

Sequence Analyses

QIIME2 (Quantitative Insights Into Microbial Ecology) (v2023.2) was used to filter and analyze raw 16S microbial sequencing data. Demultiplexed reads were assembled and quality filtered for chimeric reads and artifacts using DADA2. A Naïve Bayes classifier (V4, SILVA database v138-99) trained against the 16S rRNA region was used to classify filtered reads into taxonomic groups and assign taxonomy (Quast et al., 2013; Yilmaz et al., 2014). Sequences were aligned with a De novo multiple sequence alignment program in QIIME2 (Mafft v7) and contingency filtered to remove singletons and reads corresponding with mitochondria or chloroplasts (Kato & Standley, 2013). 16SrRNA relative abundances at the phylum and family levels of bacterial communities were visualized over decomposition time and between sample types (anatomical sites on carcasses and internal blowfly microbiota) in RStudio 4.3.1 (RStudio

Inc., Boston, MA) with the phyloseq, MicrobeR, microbiome, qiime2R, microbiomeSeq, microbiomeutilities packages.

Statistical Analysis

Pairwise Wilcoxon rank-sum tests of observed and Shannon diversity (False Discovery Rate (FDR) correction) were performed to determine significant differences in bacterial alpha diversity between seasons and among sample types (Benjamini & Hochberg, 1995). Permutational Multivariate Analysis of Variance (PERMANOVA, 999 iterations) and pairwise PERMANOVA (FDR corrections) tests using weighted UniFrac distances using the vegan R package (Oksanen et al., 2015) were conducted to explore differences in bacterial beta diversity between seasons, sample types, and over time. These differences were visualized using principal coordinate analyses (PCoA) of weighted UniFrac distance matrices generated by sequence analyses in QIIME2, and shown with ellipses representing 95% CIs for the mean of each group. Weighted UniFrac metrics were used for these analyses because they account for phylogenetic distances and relative abundances among microbes (Lozupone & Knight, 2005). All statistical analyses were performed in RStudio, and all p-values were considered significant with $\alpha \leq 0.05$.

Results

Seasonal Decomposition

Temperature data were used to calculate accumulated degree hours (ADH) to accurately compare rates of insect and decomposition development over time and between seasons. Summaries of ADH for each season are found in Figures 4 and 5, and in Tables 1 and 2. Distinct differences were observed in the progression of decomposition across each season, with all decomposition stages (fresh to dry) being observed in all carcasses in the summer within five days (2052 ADH), whereas each stage of decomposition was only observed in half of the fall carcasses during the entire trial period of 31 days (2215 ADH) (Figure 3). This difference was apparent from the first sampling event, as all summer carcasses reached bloat within five h of placement at a mean ADH of 137 (SEM = 50), compared to the beginning of bloat in the fall at a mean of 104 ADH (SEM = 27) at 172h, or eight days into sampling. Summer carcasses then progressed to active decomposition at a mean of 1176 ADH (SEM = 83) (72 h), to advanced at 1360 ADH (SEM =48) (84 h), and to dry at 2052 ADH (SEM = 51) (148 h) (Figure 11).

In contrast, fall carcasses progressed to active decomposition at a mean of 367 ADH (SEM = 112) (200 h), to advanced at 970 ADH (SEM = 115) (330 h), and dry at 1685 ADH (SEM =117) (501 h). Three carcasses in the fall (i.e., C8, C9, and C10) did not fully reach the criteria for dry stages of decomposition as defined by Payne (1965) and so are not included in mean fall ADH for that stage (Table 2, Figure 4). At the end of the fall study trial three carcasses were beginning to dry and a majority of flesh had been removed from the head and extremities, but some liquefying and disintegrating flesh remained in the abdominal cavities along with scattered fly larvae, and the underlying soil remained wet with decomposition fluid up until the final sampling event (n=62) at 2215 ADH (689 h) on day 31.

In addition to differences in ADH and decomposition stages, each season presented varying physical, taphonomic changes in carcass decomposition which can be seen in Figures 6 and 7. Due to higher average daily temperatures in the summer, bloat manifested very quickly and inconspicuously before carcasses were overtaken by larval masses at the face and umbilical regions. In contrast, the fall bloat stage lasted a little over five days and was visually more pronounced, with the abdomens of carcasses very distended and bloated with the gases of putrefaction, and the foaming or oozing of fluids from the mouth, nose, rectum, or umbilical area observed at each carcass. Fall carcasses were also observed with mottled red and purple discoloration of the abdomen during peak bloat, which shifted into a gray-green discoloration accompanied by strong fetid odors and some skin slippage on the surface of the abdomen. In addition, fall carcasses told conflicting stories as decomposition progressed, as the mouths and skin of fall carcasses visible from the top developed a tough, dry, almost leathery appearance, while the undersides and insides of the abdomen were wet with decomposition fluid, and skeletonized more quickly. Summer decomposition visually progressed more uniformly across each carcass, with no observed signs of green-gray discoloration, skin slippage, or purge as seen in the fall.

Seasonal Insect Communities

The colonization of carcasses by fly larvae also occurred differently between the summer and fall (Figures 6-7). While egg masses and hatched larvae were observed initially on and in protected areas like the mouths, noses, ears, rectum, and between the legs of each carcass, only the summer carcasses developed distinct larval masses that eventually grew to overtake the entire carcass. In contrast, larval activity and development in the fall was not apparent externally and

took place primarily internally, within the head, esophagus, chest, and abdominal cavities. This made the precise observation of larval activity difficult, as they were not obvious from the top of each carcass compared to summer. Discrete summer larval masses formed first on the mouth and face, and around the umbilical area (Figure 6), while fall larval masses were looser, with the concentration of activity varying among body cavities. Representative larval samples were collected over each seasonal trial, but their analysis is not included in this study.

A variety of adult insect taxa was also documented across each season (Figure S6). A total of 276 insects were collected and identified, with 206 from the summer and 70 from the fall. Diptera had by far the greatest relative abundance of any taxa across both seasons, 67% in the summer and 74.3% in the fall. Calliphoridae relative abundances for the fall were over three times greater than the summer, and three more calliphorid species, *Calliphora vomitoria*, *Cynomya cadaverina*, and *Lucilia sericata*, were observed in the fall than in the summer. However, there were 13 more Dipteran families observed in the summer than in the fall: Dolichopodidae, Drosophilidae, Mycetophilidae, Phoridae, Piophilidae, Pipunculidae, Poleniidae, Sarcophagidae, Sepsidae, Syrphidae, Tachinidae, and Tephritidae. Interestingly, Chloropidae was the most abundant family in the summer of all Diptera and family taxa, representing 14% of insect abundance, but was present at only 2.86% (n=2) in the fall. Summer Chloropidae abundances were also greater than order-level abundances of Coleoptera (6.31%) and Hemiptera (8.25%).

The second and third greatest relative abundant taxa after Diptera also differed by season, with Hymenoptera at 17.48% followed by Hemiptera at 8.25% in the summer, and Hemiptera at 12.86% followed by Coleoptera at 10% in the fall. Negligible numbers of Psocoptera (n = 2) and Lepidoptera (n = 1) were also collected in the summer and fall, respectively.

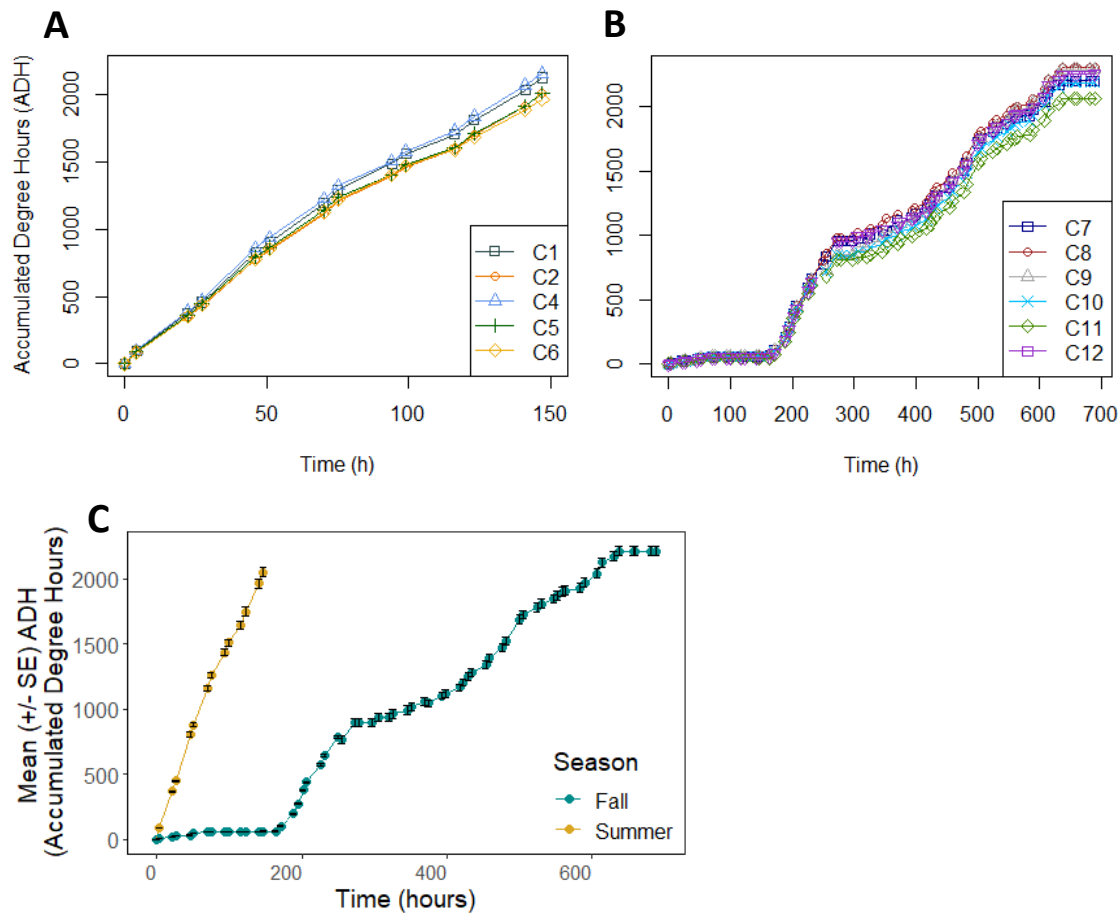


Figure 4. Seasonal variation in accumulated degree hours (ADH) expressed as time in hours. A) Summer intra-carcass variation in ADH. B) Fall intra-carcass variation in ADH. C) Mean ADH across both seasons. C3 is not represented in the summer due to a lack of available temperature data.

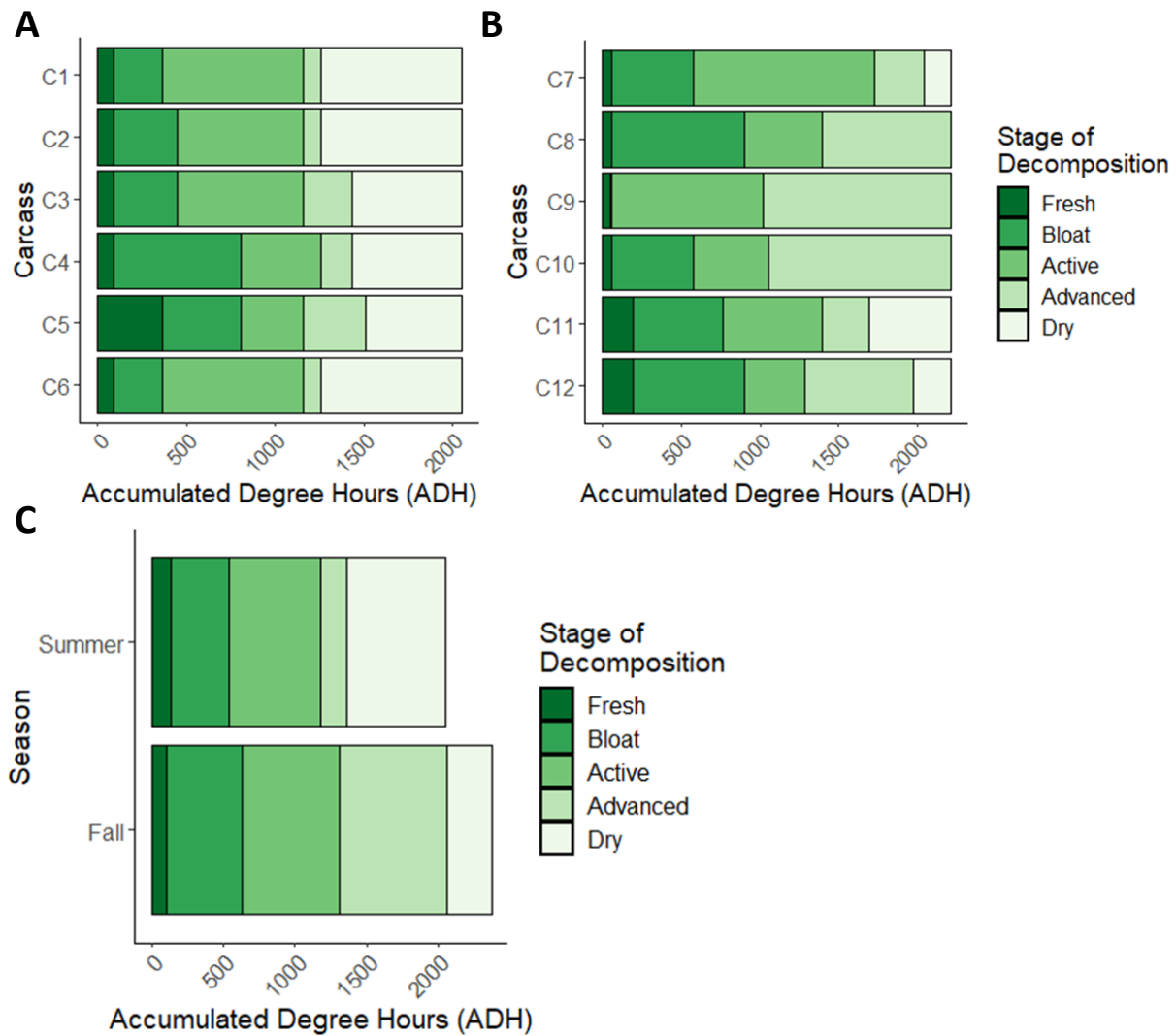


Figure 5. Differences in decomposition progression expressed as accumulated degree hours (ADH) between seasons. A) Intra-carcass variation in the summer. B) Intra-carcass variation in the fall. C) Mean accumulated degree hours (ADH) for both seasons. Decomposition stages (Payne 1965) were identified with a combination of written field observations, insect activity, and photographed taphonomy from each sampling event.

Table 2. Accumulated degree hour (ADH) ranges for each stage of decomposition as defined by Payne (1965) for each season. Ranges were estimated based on mean ADH, written field observations, and photographed taphonomy from each sampling event.

Stage	Summer	Fall
Fresh	0-91	0-61
Bloat	92-367	62-901
Active	368-1160	902-1782
Advanced	1161-1509	1783-2215
Dry	1510-2052	1691-2215

Table 3. Accumulated degree hour (ADH) ranges for each carcass during each season, according to decomposition stages as defined by Payne (1965). Ranges were determined using a combination of written field observations, insect activity, and photographed taphonomy at each sampling event. — indicates carcasses that did not reach that stage of decomposition.

Summer						
Stage	C1	C2	C3	C4	C5	C6
Fresh	0-91	0-91	0-91	0-91	0-367	0-91
Bloat	92-367	92-447	92-447	92-806	368-806	92-367
Active	368-1160	448-1160	448-1160	807-1259	807-1160	368-1160
Advanced	1161-1259	1161-1259	1161-1437	1260-1437	1161-1509	1161-1259
Dry	1260-2052	1260-2052	1438-2052	1438-2052	1510-2052	1260-2052
Fall						
Stage	C7	C8	C9	C10	C11	C12
Fresh	0-61	0-61	0-47	0-61	0-198	0-198
Bloat	62-575	62-901	48-57	62-575	199-768	199-901
Active	576-1723	902-1393	58-1017	576-1056	769-1393	902-1283
Advanced	1724-2041	1394-2215	1018-2215	1057-2215	1394-1690	1284-1875
Dry	2042-2215	-	-	-	1691-2215	1876-2215



Figure 6. Taphonomic changes from the summer of each carcass at 0, 24, 72, 96, 100, and 148 h, or 0, 406, 1197, 1462, 1510, and 2052 accumulated degree hours (ADH). Photos represent closest available visuals for mean decomposition stages as defined in table [mean table] and figures [stacked bars A and B].

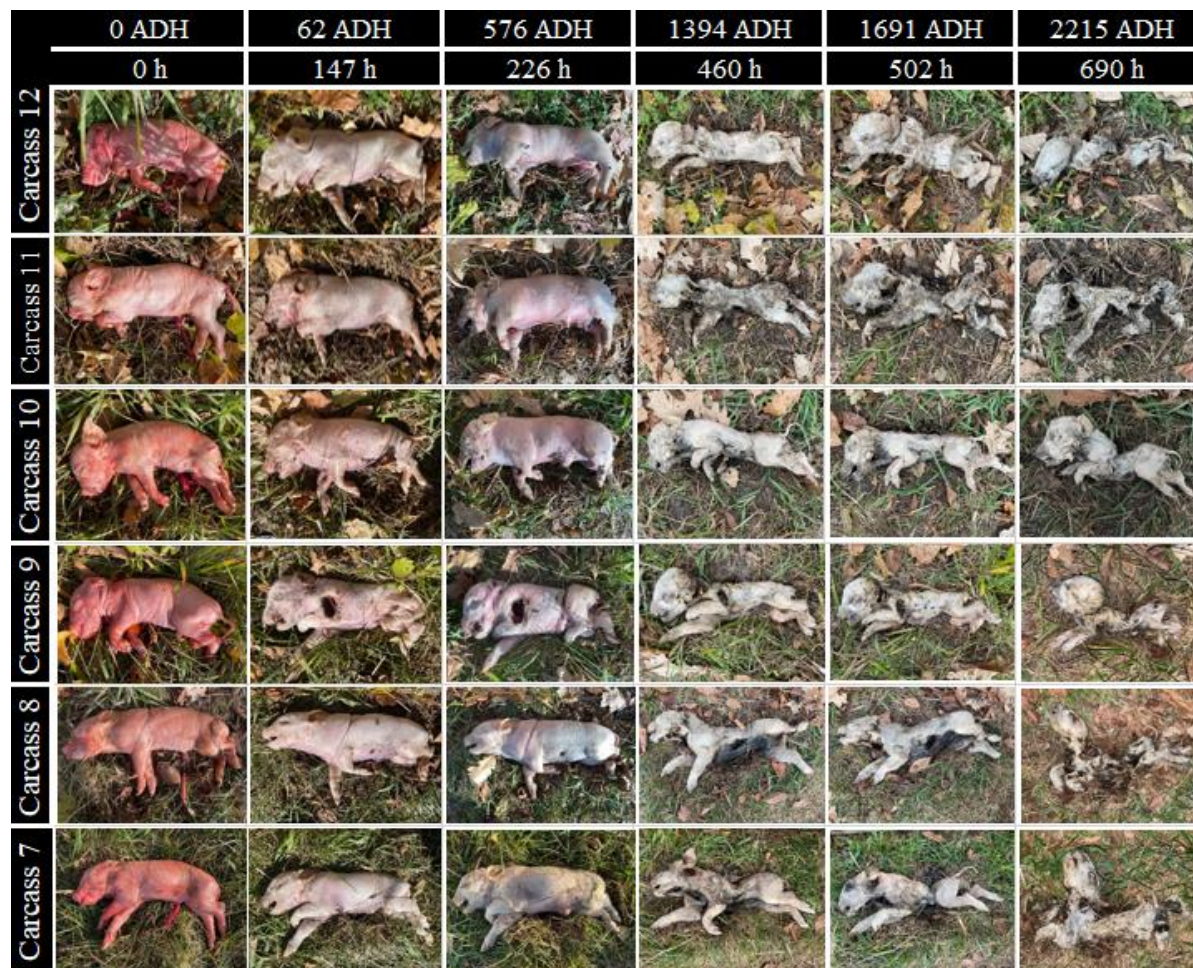


Figure 7. Taphonomic changes from the fall of each carcass at 0,147, 226, 460, 502, and 690 h, or 0, 62, 576, 1394, 1691, and 2215 accumulated degree hours (ADH). Photos represent closest available visuals for mean decomposition stages as defined in table [mean table] and figures [stacked bars A and B].

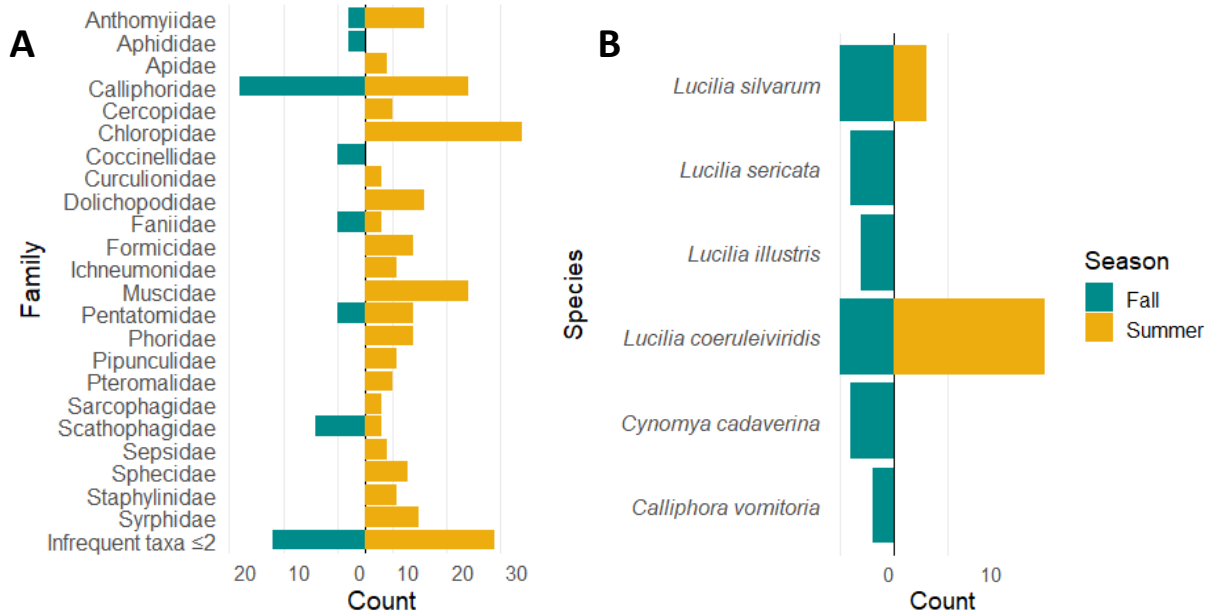


Figure 8. Counts of insect taxa between seasons. A) Insects identified to family. B) Calliphoridae identified to species. Infrequent taxa are families of which 2 or fewer specimens were collected for that season.

The recovery of blow flies from butterfly traps over time presented differently between seasons as well (Figure 8, Table 1), with 19 and 23 blow flies recovered from the summer and fall, respectively. Summer blow flies were collected on the first three days of decomposition, with the most recovered on day two (N = 12). Flies on day two were primarily *Lucilia coeruleiviridis* (N = 9), making up the majority species of all summer flies. In contrast, fall blow flies were recovered over eight non-consecutive days, with the most recovered on days eight and 15 (N = 6). There were five specimens of both adult *L. coeruleiviridis* and *Lucilia silvarum*.

Seasonal microbial community composition

Total relative abundance of bacterial taxa across all samples showed four primary phyla that most represented microbial community composition for each season: Actinobacteria,

Bacteroidota, Firmicutes, and Proteobacteria (Figure 9A). Of these phyla, Firmicutes and Proteobacteria were most dominant overall, accounting for >90% of relative abundance, with Proteobacteria being most abundant (>50%) regardless of season. Firmicutes and Proteobacteria also maintained >90% mean relative abundance over time and among sample types regardless of season (Figure 10, Figure 12). These four phyla were primarily represented by 8 families shared between seasons: Enterobacteriaceae, Enterococcaceae, Moraxellaceae, Morganellaceae, Planococcaceae, Streptococcaceae, Vagococcaceae, and Wohlfahrtiimonadaceae (Figure 9B). Wohlfahrtiimonadaceae was the most abundant overall (>20%) at the family level for each season, with the second overall being Moraxellaceae in the summer (20.6%) and Vagococcaceae in the fall (10.8%). Alpha diversity analyses among all samples found that season had a significant effect on microbial community composition (PERMANOVA, $F = 4.86$, $P = 0.012$) (Table), and measurements of Shannon and Observed alpha diversity (Wilcoxon rank-sum tests, FDR corrections) also indicated significant differences ($P < 0.001$) exist in seasonal diversity, with greater alpha diversity in the summer for both measures (Figure 9D).

Additional Permutational Analysis of Variance showed sample type (skin, mouth, rectum, or internal fly) had a significant effect in structuring communities for both summer ($F = 27.16$, $P = 0.001$) and fall ($F = 4.83$, $P = 0.001$) (Table 4). At the phylum level, Proteobacteria was the most relatively abundant among summer carcass microbiota (68%, 64%, and 58%, for the skin, mouth, and rectum, respectively) while summer fly microbes were primarily represented by Firmicutes (64% relative abundance) (Figure 10A). At the family level, summer carcass microbe relative abundances are comprised mostly of Moraxellaceae and Wohlfahrtiimonadaceae, which combined made up 48% of relative abundance of rectum samples, and >50% of all skin and mouth samples. Summer flies however were represented by

primarily Enterococcaceae (31% relative abundance) and Vagococcaceae (26% relative abundance) (Figure 10A).

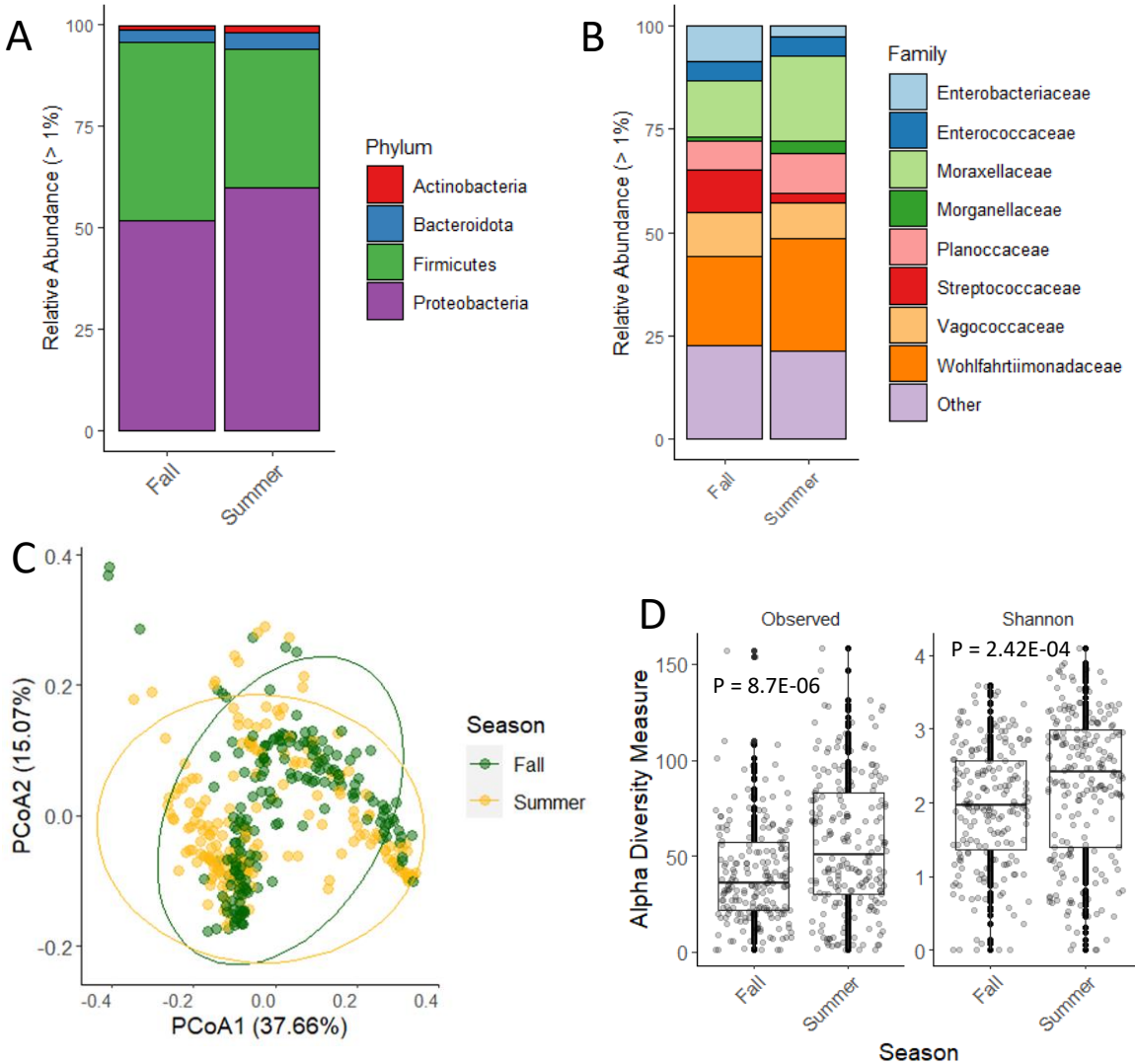


Figure 9. Differences in bacterial communities between seasons. Phylum (A) and family level (B) bacterial mean relative abundance between seasons. Only taxa which comprised greater than 1% of total abundance are shown. C) PCoA plot (weighted Unifrac distance) of all samples expressed as season. Ellipses indicate 95% confidence intervals (CI) for multivariate t-distributions. D) Differences in observed and shannon bacterial diversity (Wilcoxon rank-sum test, FDR correction).

Table 4. PERMANOVA of bacterial beta diversity between seasons. PERMANOVA test was conducted using weighted Unifrac distance and 999 permutations. DF = Degrees of Freedom. SS = Sum of Squares.

Factor	DF	SS	R²	F.Model	Pr(>F)
Season	1	0.0312	0.0115	4.8643	0.012
Residual	417	2.6714	0.9885		
Total	418	2.7026	1		

Phylum-level relative abundances among carcass microbiota in the fall were again dominated by Proteobacteria (>50% relative abundance), though rectal samples were split more evenly between Proteobacteria (48% relative abundance) and Firmicutes (50% relative abundance) (Figure 10B). Flies were also primarily represented by Firmicutes in the fall (52% relative abundance) but differed from summer flies at the family-level, with lower abundances of Enterococcaceae (<10%) and greater relative abundances of Enterobacteriaceae (5.4%) and Moraxellaceae (6.4%). Pairwise tests of Shannon and Observed diversity (Wilcoxon rank-sum test, FDR correction) among sample types for each season indicated that flies were less diverse overall and were significantly different ($P < 0.001$) from all other sample types for each measure (Figure 11). Significant pairwise differences in alpha diversity were also seen between all carcass sites in the fall for both measures except for mouth-rectum interactions (Observed $P = 0.68$, Shannon $P = 0.38$), while the only significant carcass site interaction in the summer was skin-rectum (Observed, $P = 0.007$).

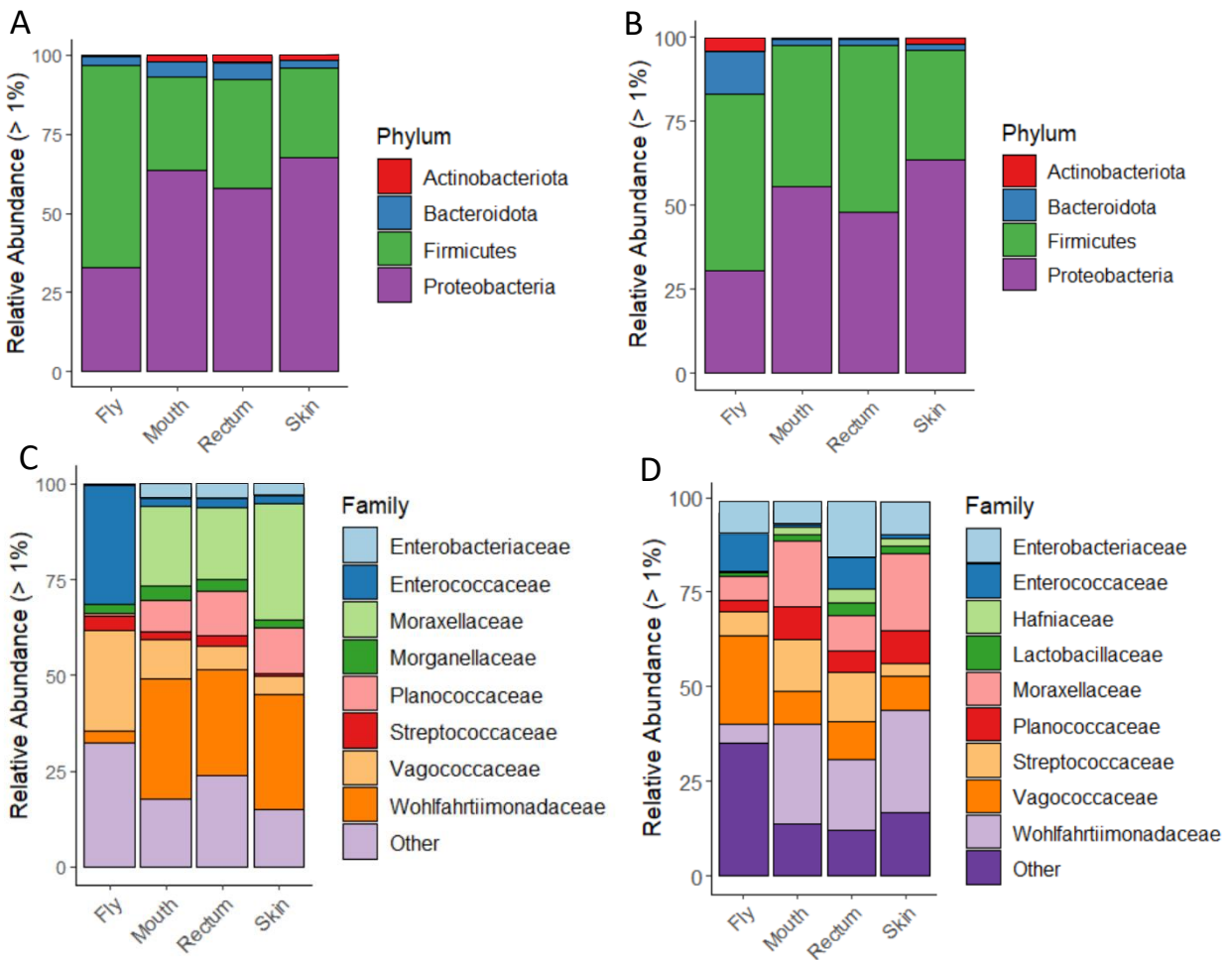


Figure 10. Bacterial communities by sample type (internal blow fly, mouth, rectum, or skin) for each season. A) Phylum and C) family level mean relative abundance for the summer. B) Phylum and D) family level relative abundance for the fall. Only taxa which comprised greater than 1% of total abundance are shown.

Pairwise PERMANOVA identified further specific significant interactions among sample types. Due to the significant differences in alpha diversity measures between flies and carcass samples regardless of season (Figure 11), tests of pairwise significance were conducted with and without flies for each season to better understand their effects on carcass microbial communities. Tests of all carcass and fly microbes (Table 6) showed significant differences between flies and

all carcass sites ($P = 0.002$) in the summer, while flies were only significantly distinct from rectal samples in the fall ($P = 0.023$). Distinct differences were also observed between the rectum and skin in the summer ($P = 0.023$), while skin microbiota were significantly different from the mouth and rectum in the fall ($P = 0.004$). Pairwise tests of exclusively carcass microbes showed that fall skin microbiota were again distinct from the mouth and rectum, but with greater significance ($P = 0.002$), and no significantly distinct microbiota were observed among carcass sites in the summer.

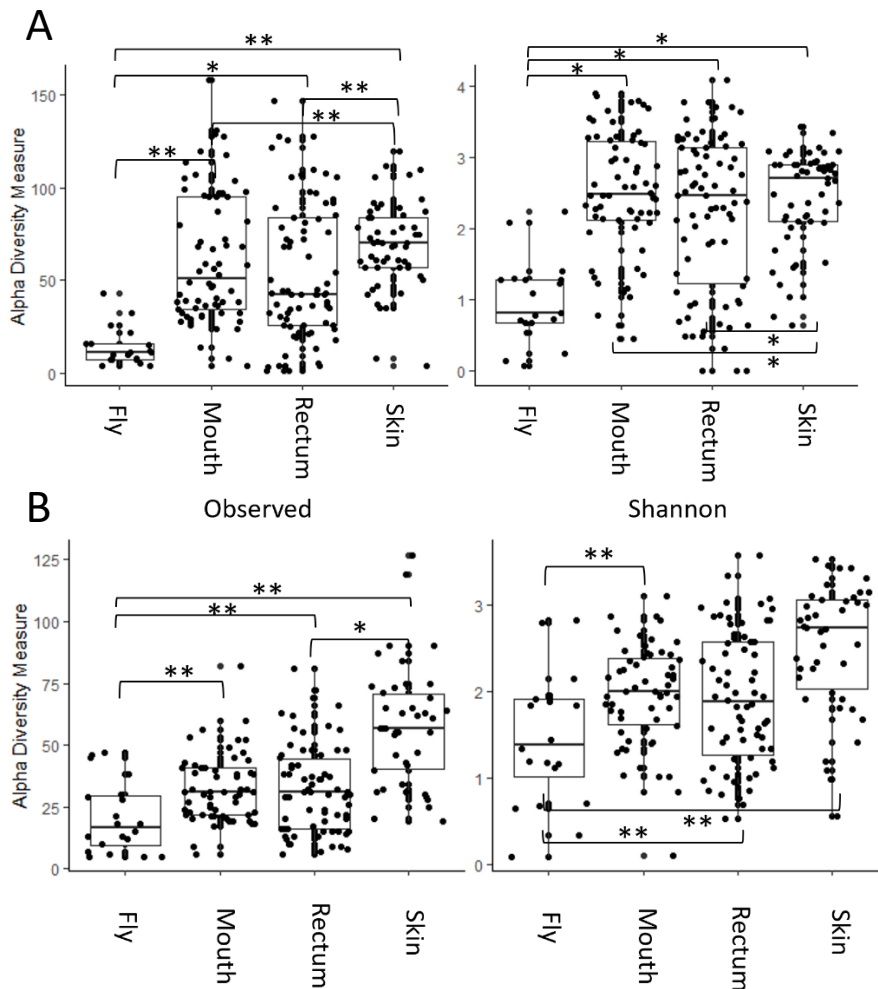


Figure 11. Pairwise tests of Observed and Shannon diversity (Wilcoxon rank-sum test, FDR correction) between sample types for the summer (A) and fall (B). Significant differences are denoted by brackets. * = $P\text{-adj} < 0.05$, ** = $P\text{-adj} < 0.01$.

Microbial community succession for each season was characterized by significant shifts in composition over time. In addition to mean relative abundance (Figure 12), total relative abundances for all samples over time were visualized to better identify temporal patterns among sample types (Figure 13). On day one of each seasonal trial, carcass bacterial communities are dominated by prominent abundances of Moraxellaceae, as well as Enterobacteriaceae in the fall. Day two of the summer was marked by a sudden increase in Vagococcaceae and decrease in Moraxellaceae, which continued to decrease daily. By day three Wohlfartiimonadaceae was the most dominant taxa with a mean relative abundance of 37%, which increased to 55% by day four (Figure 12A). By day five Wohlfartiimonadaceae abundance began to decrease as Planococcaceae increased in prevalence, eventually becoming the most dominant taxa by day seven at 26% mean relative abundance.

In the fall, similar successional patterns occurred but more gradually than in the summer (Figure 13). Moving from day one to day eight of decomposition, the most abundant family Enterobacteriaceae was replaced by Moraxellaceae, and Streptococcaceae appeared for the first time. By day 10 and moving into week two, Streptococcaceae and Moraxellaceae made up >40% of relative abundance, and microbial diversity increased as additional families including Lactobacillaceae, Leuconostocaceae, Enterococcaceae, and Hafniaceae grew in abundance as well. Notably, Lactobacillaceae, Leuconostocaceae, and Hafniaceae are families not observed in any summer carcass samples. Over days 19 – 26, Vagococcaceae grew in abundance with Wohlfahrtiimonadaceae, while Lactobacillaceae, Leuconostocaceae, and Hafniaceae decreased but maintained steady, low abundances into late decomposition. Planococcaceae was also present in analyses of individual body sites, though not in as high abundances as observed in the

summer. For the remainder of the fall trial, Enterobacteriaceae maintained a relative abundance of <2%.

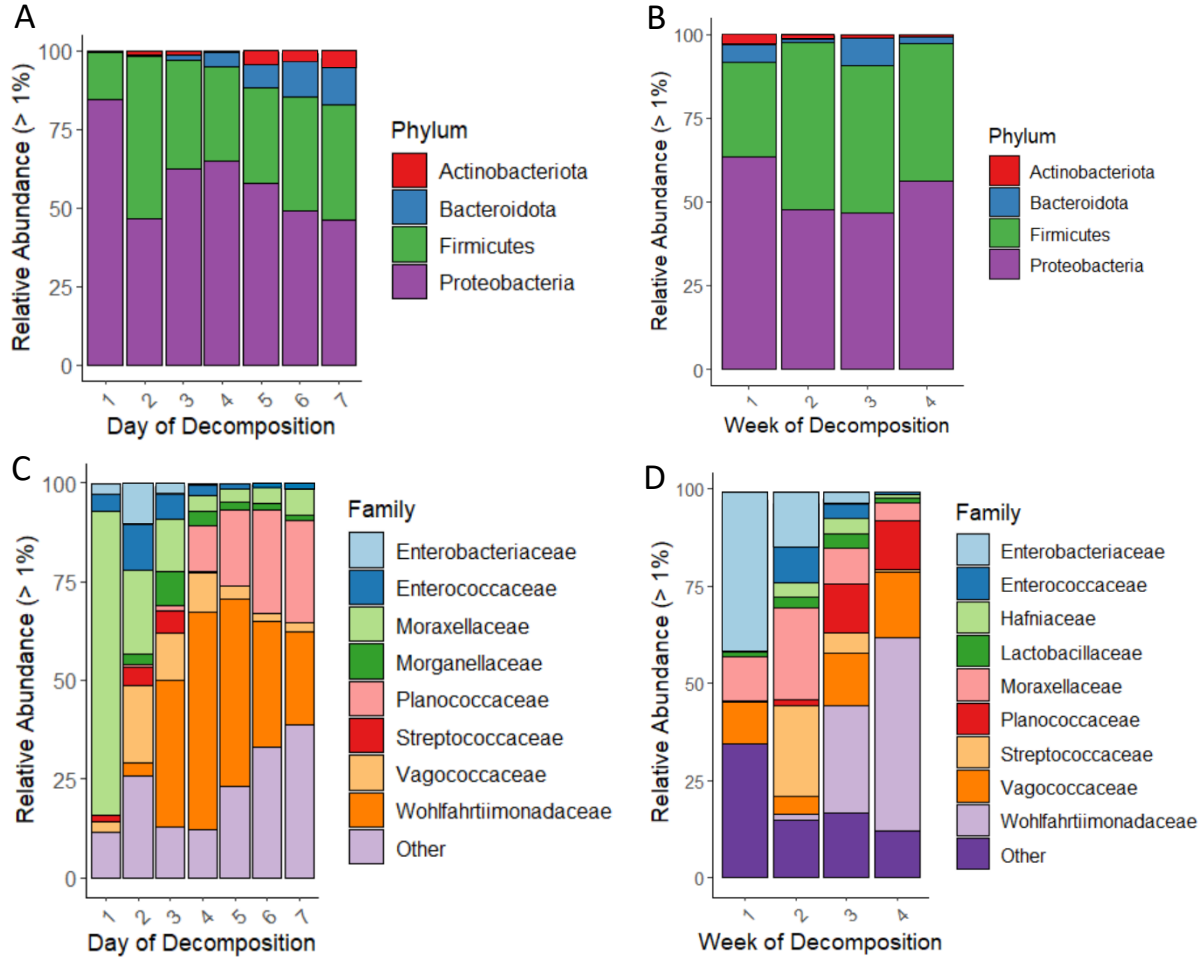


Figure 12. Bacterial communities over time for each season. A) Phylum and family-level mean relative abundance for the summer. B) Phylum and family-level relative abundance for the fall. Only taxa which comprised greater than 1% of total abundance are shown.

Shannon and Observed alpha diversity measures plotted daily (summer) and weekly (fall) suggested an increase in diversity over time, though this trend was not apparent in Observed fall diversity (Figure 13). Pairwise tests of Shannon and Observed diversity (Wilcoxon rank-sum test,

FDR correction) over time indicated significant differences between all days of decomposition in the summer except comparisons of days 1-2 and 1-3 (Observed), and 2-3, 4-5, and 6-7 (Shannon and Observed) (Figure 13A). Pairwise tests of fall Observed diversity indicated significant differences between comparisons of weeks 2-3, 2-4, and 3-4, and between all weeks except 3-4 for Shannon diversity (Figure 13B).

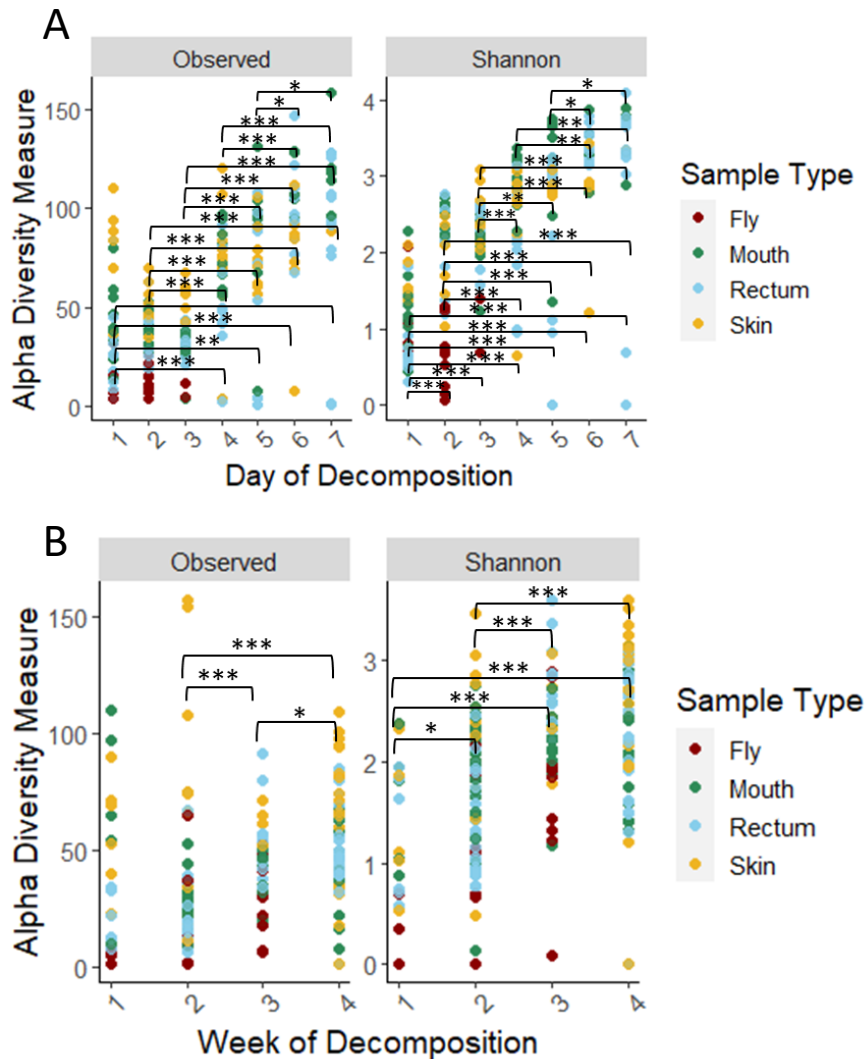


Figure 13. Pairwise tests of Observed and Shannon diversity (Wilcoxon rank-sum test, FDR correction) over time for each season expressed as sample type. A) Daily summer alpha diversity. B) Weekly fall alpha diversity. Significant differences are denoted by brackets. * = $P\text{-adj} < 0.05$, ** = $P\text{-adj} < 0.01$, *** = $P\text{-adj} < 0.001$.

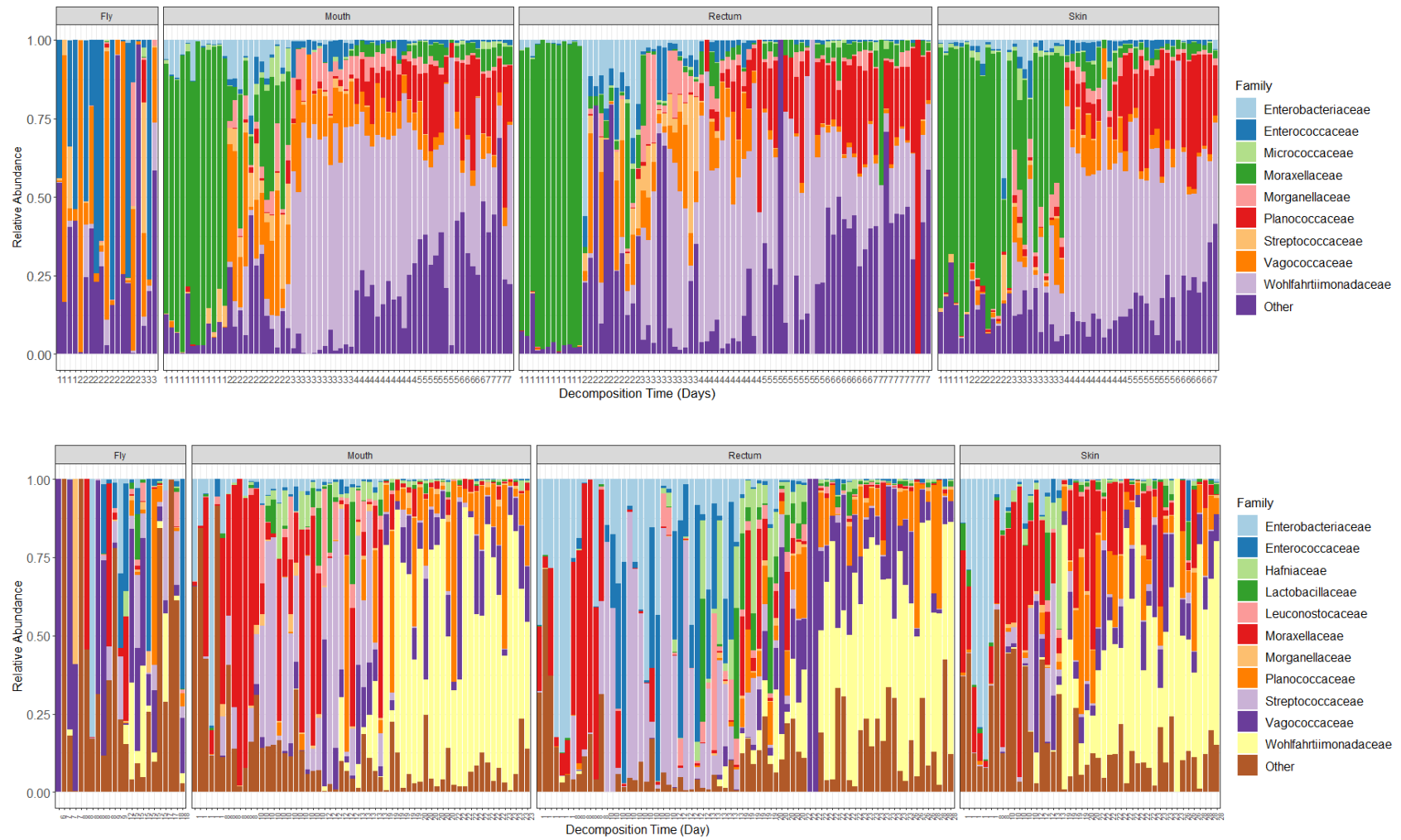


Figure 14. Total relative abundance of microbial taxa at the family level for the summer (top) and fall (bottom) grouped by sample type (internal fly, mouth, rectum, and skin) and sorted by day to show bacterial succession over time.

Table 5. Impact of sample type and time on seasonal bacterial beta diversity for carcass and fly microbes. Time in days was tested for both seasons, with an added factor of week for the fall due to study duration and to investigate the extent of temporal effects on fall decomposition. Significant values (<0.05) are indicated in bold. PERMANOVA test (weighted UniFrac distance) was conducted with 999 permutations. DF = Degrees of Freedom, SS = Sum of Squares.

Summer					
Factor	DF	SS	R²	F.Model	Pr(>F)
Sample Type	3	0.20021	0.2529	27.1628	0.001
Day	1	0.04505	0.0569	18.3342	0.001
Sample Type:Day	3	0.03535	0.04465	4.7959	0.007
Residual	208	0.51105	0.64554		
Total	215	0.79166	1		
Fall					
Factor	DF	SS	R²	F.Model	Pr(>F)
Sample Type	3	0.03046	0.06365	4.7278	0.001
Week	1	0.02115	0.04419	9.8468	0.001
Sample Type:Week	3	0.00817	0.01707	1.268	0.241
Residual	195	0.41876	0.87509		
Total	202	0.47853	1		
Sample Type	3	0.03046	0.06365	4.8342	0.001
Day	1	0.02592	0.05417	12.3434	0.001
Sample Type:Day	3	0.01261	0.02635	2.0012	0.059
Residual	195	0.40954	0.85583		
Total	202	0.47853	1		

Permutational Analysis of Variance also confirmed the significant ($P < 0.001$) effect of time on community composition regardless of season, in time measured in days, as well as time in weeks in the fall (Table 5). While time in days ($N = 32$) and weeks ($N = 4$) were both tested to investigate the extent of temporal effects on fall decomposition, a factor of week was chosen to best visualize fall microbial community structure in principal coordinates analysis (PCoA) (Figure 14). The same method used to test among sample types was applied to tests of bacterial communities over time. Within summer carcasses and flies, significant pairwise differences existed between all days of decomposition except for 1-2 ($P = 1.000$) and 6-7 ($P = 0.205$). In

tests of only carcass microbiota, significant pairwise differences also existed between all days of decomposition except for days six and seven ($P = 0.183$) (Table 7). However, comparisons of subsequent days such as 2-3 ($P = 0.02$), 4-5 ($P = 0.013$), and 5-6 ($P = 0.015$) were less highly significant than comparisons of non-subsequent days like 1-4 or 2-6 ($P = 0.001$). In addition, significant differences in tests of pairwise differences in carcass microbes were overall more significant than those in tests of carcasses and flies. These differences in community structuring were visualized in PCoA (Figure 14), and ordinations excluding flies explained a greater percentage of variation than those including flies.

Table 6. Comparison of seasonal Pairwise Permutational Analysis of Variance (PERMANOVA, FDR correction) among sample types.

Season	Comparison (Sample Type)	P adj.	
		Carcass microbes	Carcass and Fly microbes
Summer	Fly -Mouth	-	0.002
	Fly-Rectum	-	0.002
	Fly-Skin	-	0.002
	Mouth-Rectum	0.407	0.465
	Mouth-Skin	0.216	0.161
	Rectum-Skin	0.051	0.023
Fall	Fly-Mouth	-	0.065
	Fly-Rectum	-	0.004
	Fly-Skin	-	0.121
	Mouth-Rectum	0.492	0.370
	Mouth-Skin	0.002	0.004
	Rectum-Skin	0.002	0.004

Table 7. Pairwise PERMANOVA calculated from weighted UniFrac distances of summer bacterial communities by sampling day. Two tests were run, one including fly microbes and one excluding them. Values indicating significantly distinct microbiota (<0.05) are shown in bold.

Comparison (Day)	P adj.	
	Carcass microbes	Carcass and Fly microbes
1-2	0.001	1.000
1-3	0.001	0.002
1-4	0.001	0.002
1-5	0.001	0.002
1-6	0.001	0.002
1-7	0.001	0.002
2-3	0.02	0.022
2-4	0.001	0.002
2-5	0.001	0.002
2-6	0.001	0.004
3-4	0.001	0.002
3-5	0.001	0.002
3-6	0.001	0.002
4-5	0.013	0.019
4-6	0.001	0.002
5-6	0.015	0.009
7-2	0.001	0.022
7-3	0.001	0.002
7-4	0.001	0.002
7-5	0.001	0.002
7-6	0.183	0.205

Table 8. Pairwise PERMANOVA calculated from weighted UniFrac distances of fall bacterial communities by week of decomposition. To examine the impact of fly microbes on communities, tests were run with and without flies. Values indicating significantly distinct microbiota (<0.05) are shown in bold.

Comparison (Week)	P adj.	
	Carcass microbes	Carcass and Fly microbes
1-2	0.001	0.082
1-3	0.001	0.009
1-4	0.001	0.003
2-3	0.001	0.037
2-4	0.001	0.003
3-4	0.002	0.009

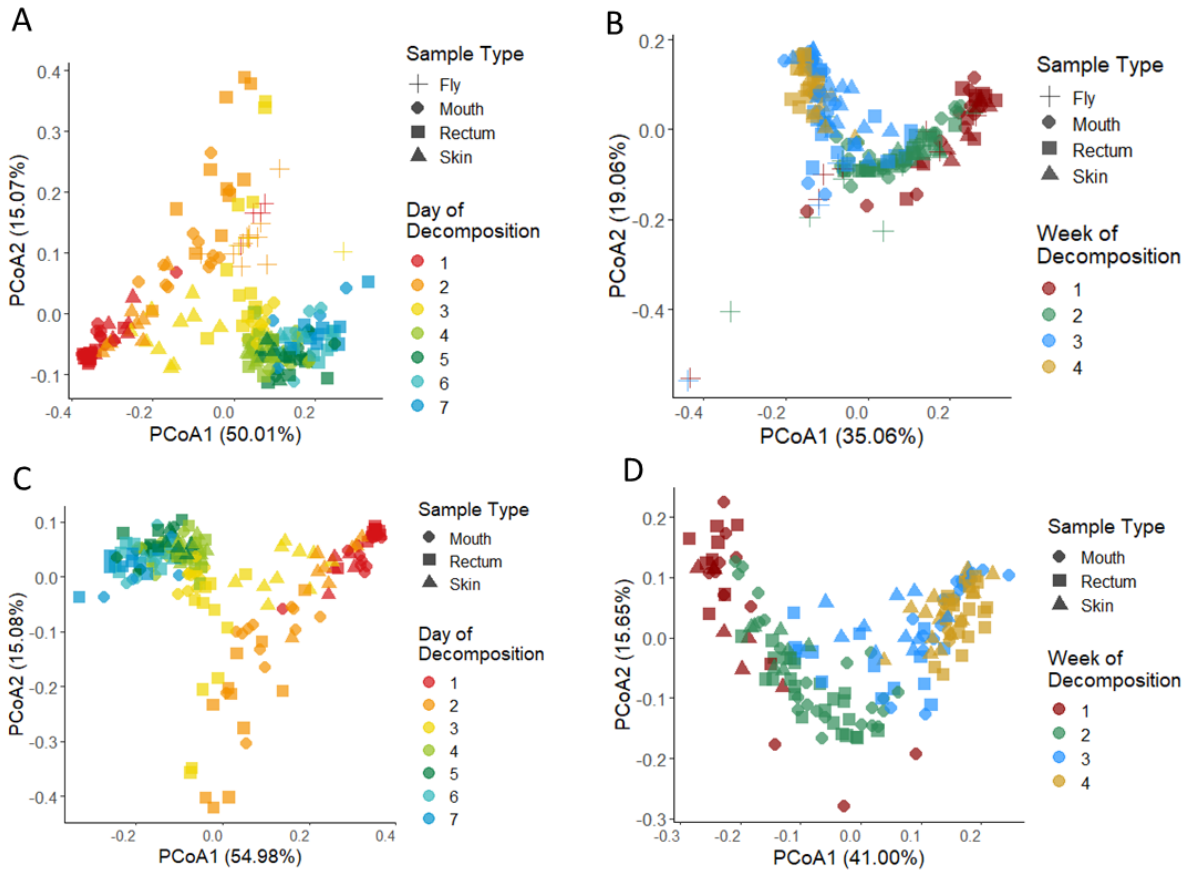


Figure 15. Seasonal comparison of principal coordinates analyses (PCoA) of weighted UniFrac distances with and without flies, expressed as sample type and time in days (summer) or weeks (fall). A) Summer fly and carcass microbes. B) Summer carcass microbes only. C) Fall fly and carcass microbes. D) Fall carcass microbes only.

Fly microbial communities

Internal blow fly communities were predominantly composed of Enterococcaceae and Vagococcaceae, but in overall mean relative abundances (Figure 10) possessed more “other” taxa (>20%) than other sample types, suggesting some underlying diversity or other untapped differences in community structure may exist. Fly bacterial relative abundances were also visualized individually at the family level and grouped by day caught (Figure 15), which revealed a few families not apparent in previous analyses including carcass microbiota. For

example, Anaplasmataceae made up >20% relative abundance for 12 flies in the summer but was absent from flies in the fall. Dysgonomodaceae was also detected at >50% relative abundance in one fly identified as *L. silvarum* in the summer but was similarly absent from the fall. However, four flies from the fall, *L. silvarum* (N=2), *L. coeruleiviridis* (N=1), and *L. illustris* (N=2) contained low abundances of Leuconostocaceae not detected elsewhere. Additionally, seven fall flies, *C. vomitoria* (N=1), *C. cadaverina* (N=2), *L. sericata* (N=1), *L. illustris* (N=2), *L. silvarum* (N=1), contained low abundances of Pseudomonadaceae also not detected elsewhere. Principal coordinates analyses of flies by species and season were conducted to visualize internal blow fly bacterial communities (Figure 15), and due to species sample sizes 95% confidence intervals could only be calculated for *L. coeruleiviridis*, *L. sericata*, and *L. silvarum*.

Fly-carcass interactions

Heatmaps of family-level taxa for each season grouped by day of decomposition and sample type were created to visualize potential exchanges of taxa between internal fly microbiota and carcasses (Figures 17 and 18). Heatmaps indicate high relative abundances of Moraxellaceae on day one for each season and among carcass samples, with comparatively low or absent abundances in flies. In the summer, high Vagococcaceae and Enterobacteriaceae abundances are seen on days two, three, and four, in correlation with fly sampling and activity. In the fall a similar trend occurs, with sudden high abundances of Vagococcaceae on days six and seven.

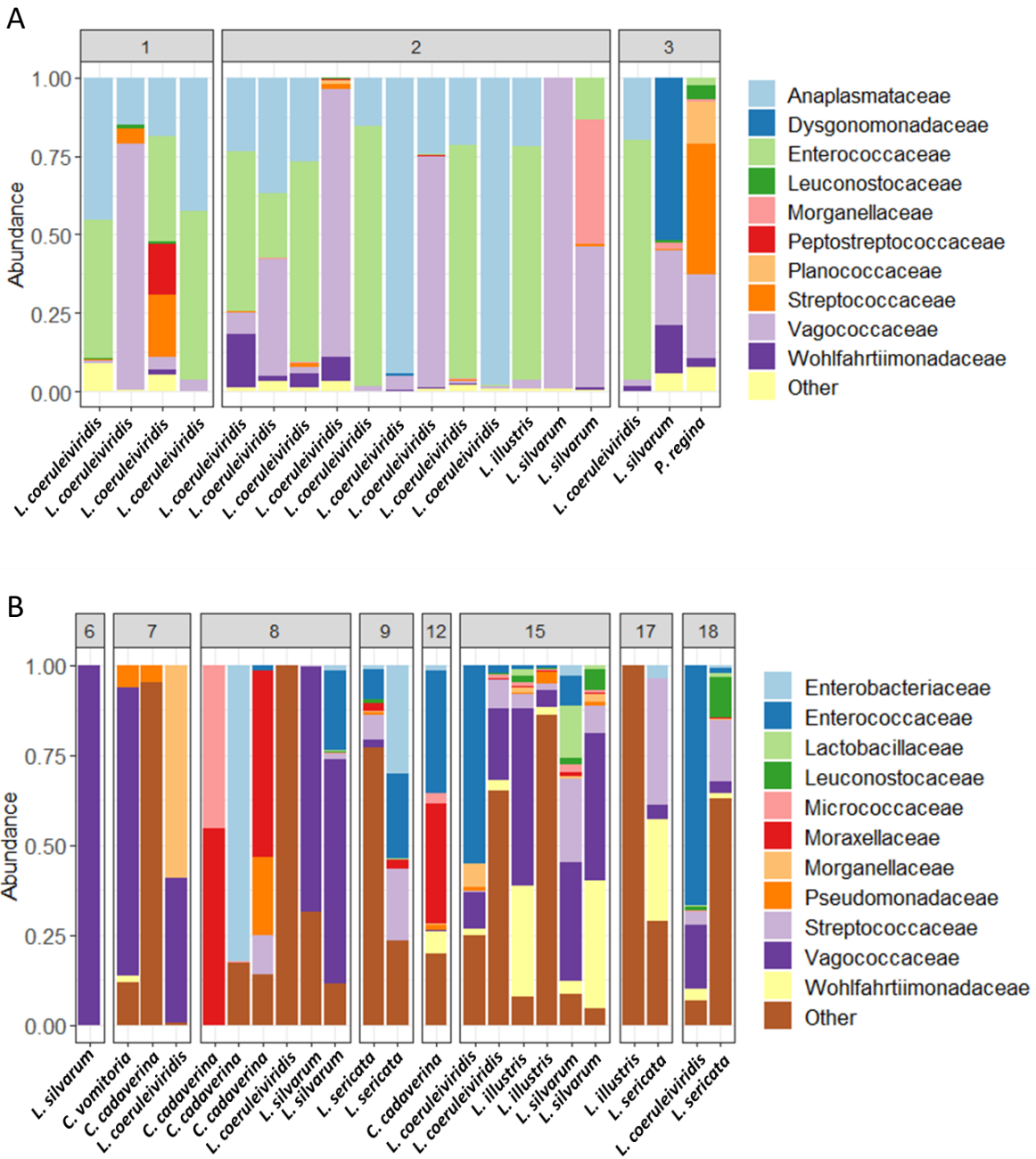


Figure 16. Total relative abundance of internal microbiota for all sampled blow fly species, grouped by day of decomposition for the A) summer and B) fall.

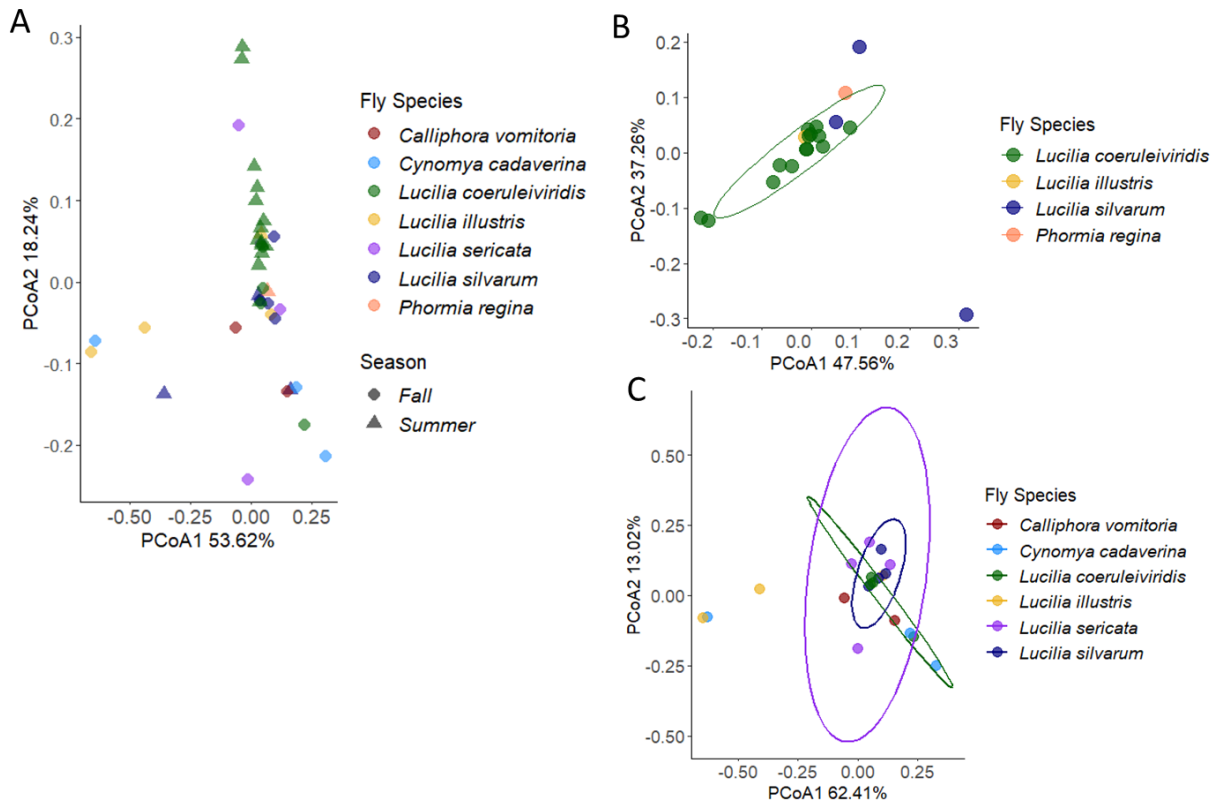


Figure 17. Seasonal comparison of principal coordinates analysis (PCoA) of weighted UniFrac distances for blow fly species. A) Summer and fall blow fly species. B) Summer blow fly species. C) Fall blow fly species. Ellipses indicate 95% confidence intervals (CI) for multivariate t-distributions.

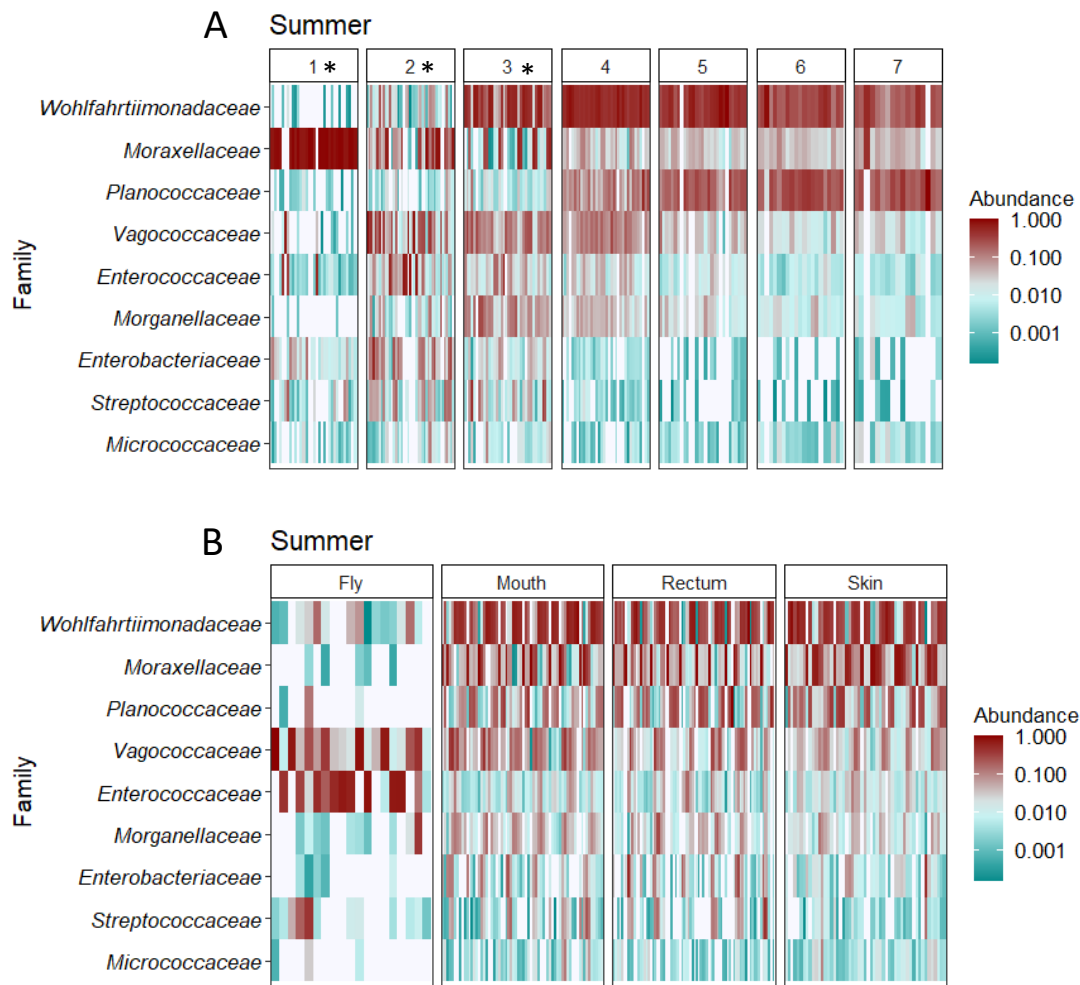


Figure 18. Heatmap of family level bacterial relative abundance by day of decomposition (A) and by sample type (B) for the summer. (*) indicates days on which blow flies were recovered from butterfly traps. Only taxa which comprised < 1% of total abundance are shown.

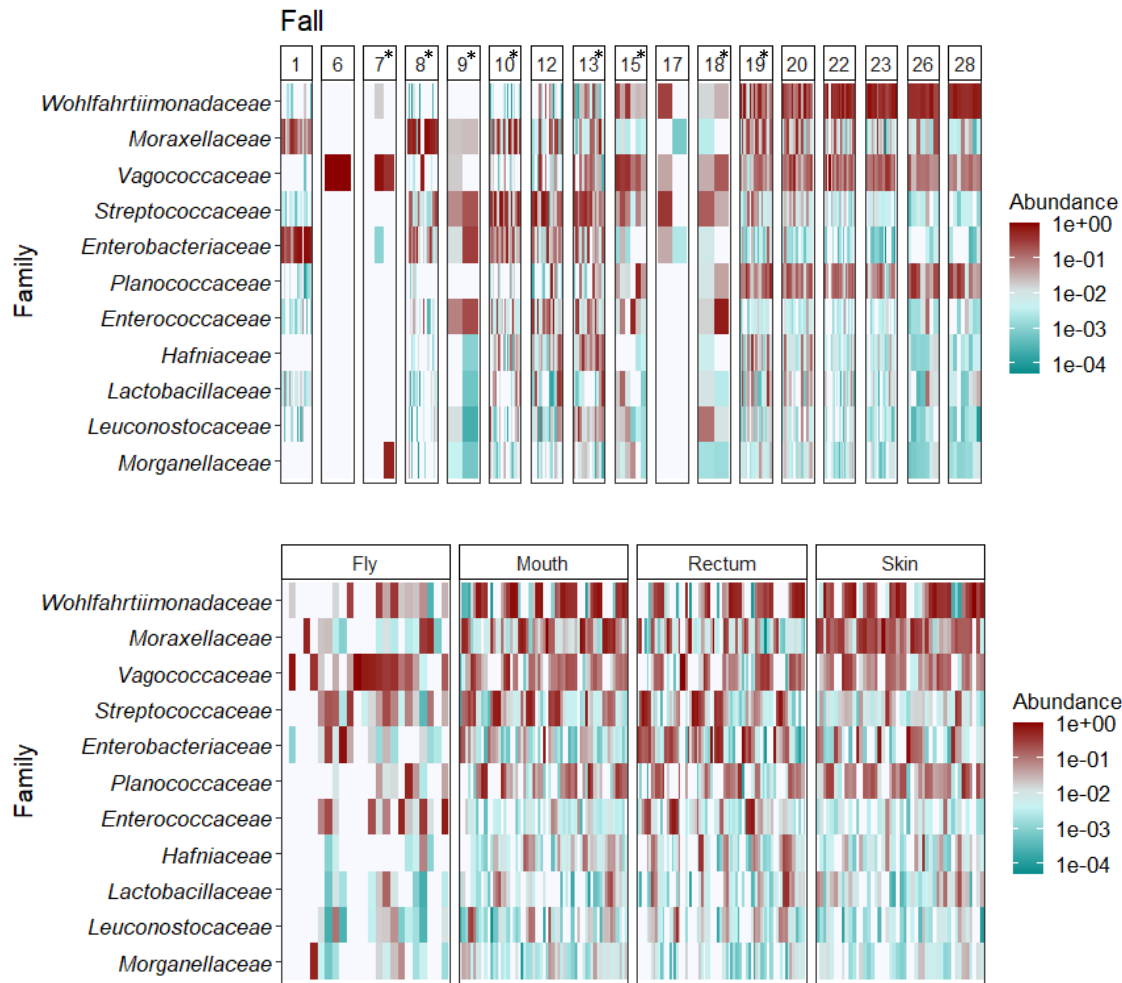


Figure 19. Heatmap of family level bacterial relative abundance by day of decomposition (A) and by sample type (B) for the fall. (*) indicates days on which blow flies were recovered from butterfly traps. Only taxa which comprised greater than 1% of total abundance are shown.

Discussion

The objectives of this study were to observe and characterize insect-microbe interactions within the necrobiome by comparing insect communities, decomposition patterns, postmortem microbial communities on mammalian carcasses, and internal calliphorid microbiomes between summer and fall. The necrobiome is a complex system and decomposition is a highly variable process shaped by many biotic and abiotic factors, making them challenging to uniformly describe or quantify at times. In spite of this, studies have attempted to do so by examining patterns of seasonal decomposition and insect succession, and postmortem microbiomes in a variety of animal models such as swine (Benbow et al., 2013; Pechal, Benbow, et al., 2014), humans (Hyde et al., 2015; Metcalf et al., 2013; Pechal et al., 2018), mice (Metcalf et al., 2013), cats (Early & Goff, 1986), salmon (Pechal & Benbow, 2016), kangaroos (Barton, Cunningham, Macdonald, et al., 2013), white-tailed deer, bears, and even alligators (Watson & Carlton, 2005). However, despite demonstrating the critical role that microbes and arthropod colonizers, particularly blowflies, individually play in the recycling of carrion within ecosystems (Metcalf et al., 2013; Pechal, Benbow, et al., 2014), few studies have attempted to investigate how necrophagous flies influence postmortem microbial community succession. The results of this study represent an important addition to improving our foundational understanding of intricate necrobiome dynamics, and the extent of the role that microbe-insect interactions play.

As predicted, a more diverse assemblage of insect taxa was observed in the summer (Figure 10) and Diptera were the most abundant insect order regardless of season. However, greater blow fly species diversity was observed in the fall, which could be attributed to prolonged decomposition providing significantly longer windows of colonization for necrophagous flies, or by differences in thermal tolerance of observed fall species. Additionally,

unlike the fall, Chloropidae were the most abundant family collected. Chloropidae, also known as eye gnats or frit flies, are generalist scavengers of decaying organic matter, such as feces, plants and fruit, and rotting wood (Merritt et al., 2009; Nartshuk, 2014). Chloropidae larvae feed on and develop in decomposing habitats, and have been documented previously in vertebrate decomposition (Early & Goff, 1986), but are not described as taxa of particular forensic interest or ecological significance. Additionally, it is important to note that the data presented here of blow fly communities cannot be assumed to be an absolute representation of blow fly diversity at these sites, and trapping results shared here vary from that of other studies. For example, a survey by Babcock et al. (2020) of adult blow fly community structure in Michigan cited catches of anywhere from 25 to just over 3,000 Calliphoridae per trap when left in the field for 4 h per day, demonstrating the abundance of blow flies in this area.

Bacterial community succession for each season was characterized by two significant shifts over time: 1) a sudden decrease in the abundance of endogenous taxa associated with fresh carcasses in correlation with bloat stage, leading to 2) increasing bacterial community diversity as decomposition progressed into active and advanced stages. A third shift may have also occurred in the summer, where increasingly dry stages of decomposition and larval migration away from carcasses caused a levelling off in bacterial diversity. This event was not as distinguishable in the fall, which could be due to differences in patterns of larval colonization and development, as well as prolonged active and advanced stages due to low temperatures. Similar trends towards homogeneity over time have also been observed in late decomposition of human cadavers (Hyde et al., 2015), perhaps in correlation with the increased risk of desiccation and decrease in larval activity.

In support of our hypothesis, marked differences were observed in the progression of decay and microbial community succession between seasons (Tables 4-7, Figures 4-5, 13-15). This contrast between summer and fall was anticipated due to the highly temperature dependent nature of both decomposition and insect development (Wall et al., 1992), with higher temperatures accelerating and low temperatures slowing or halting it entirely. Fall decomposition lasted nearly five times as long as the summer and was characterized by taphonomic changes such as prolonged periods of purge, skin slippage, and gray-green abdominal discoloration. These results are consistent with previous observations of swine carcass decomposition in cold seasons, and the colorful gray-green discoloration is thought to be caused by a delay in the formation of propionic and butyric acid volatiles that allow for the fermentation and breakdown of tissues by anaerobic bacteria in cold temperatures (Iancu et al., 2015). Inhibition of these anaerobic bacteria by the cold may be pivotal in delaying major shifts in microbial communities, as it is assumed that decreased metabolic activity would set back body cavity rupture and the beginnings of purge (Vass, 2001). Previous studies have proposed that abdominal purge is the pre-cursor to significant changes in soil microbial communities and pH as carcass nutrients are introduced to the surrounding habitat, which in turn likely alters endogenous carcass microbiota (Evans, 1963; Hyde et al., 2015; Metcalf et al., 2013).

The results of this study show some support for the proposed impact of abdominal purge on microbial communities, with highly significant ($P < 0.001$) shifts in Shannon diversity occurring between days one and two in the summer, corresponding with bloat and purge (Figure 13). This significance over time was confirmed with pairwise PERMANOVA ($P = 0.001$) and visualized by PCoA (Table 6, Figure 15). Relative abundances over time in the summer also support the effects of purge on communities, and showed a sudden decrease in abundance of

Moraxellaceae, and increases in Enterococcaceae, Enterobacteriaceae, and Morganellaceae from day one to day two. Where Moraxellaceae is an aerobic taxon, the increasingly abundant taxa following purge are known to be anaerobic, suggesting that these are endogenous bacteria that have escaped from the abdominal cavity causing shifts in community structure. This high abundance in fresh stages and subsequent decrease in Moraxellaceae in swine decomposition has also been reported by Pechal et al (2014), but differs from observations of this taxa in late stages of human decomposition (Hyde et al., 2015).

Relative to the fall, purge was not very noticeable in the summer, due to the accelerated rate of decomposition caused by higher seasonal temperatures. Also contributing to the swiftness of decomposition is presumably the smaller size of the stillborn swine carcasses used in these trials (mean weight of 1.87 kg in the summer and 1.32 kg in the fall). These sizes differ greatly from that of the adult pigs typically used in similar studies, which can range in weight from 14 kg up to 79 kg (Benbow et al., 2013; Díaz-Aranda et al., 2018; Matuszewski et al., 2008; Sharanowski et al., 2008). The limited biomass provided by these smaller carcasses likely also shortened the window of opportunity for insect exploitation, thereby limiting our ability to observe the full extent of insect communities associated with the summer necrobiome here.

Another potential explanation for the significant temporal shifts in seasonal bacterial communities could be the introduction of exogenous microbes via blow fly oviposition and larval development. The previously described decreases in abundances of endogenous taxa following fresh stages also correlate with observations of blow fly oviposition and larval mass activity (Tables 1-2, Figures 4-5). This correlation is supported by the appearance of bacterial taxa prevalent in internal blow fly microbiota such as Enterococcaceae, Vagococcaceae, and Wohlfahrtiimonadaceae in carcass microbiota on days blow flies were caught and observed

interacting with carcasses (Figures 10, 12, and 14). Pairwise PERMANOVA comparing daily and weekly bacterial communities trended towards less highly significant temporal differences with the inclusion of flies than without flies, and pairwise comparisons of sample types indicated a lack of significant differences between fly internal microbiota and mouth samples in the fall (Tables 5-7, Figure 15). Taxa heatmaps support the potential introduction of Enterococaceae, Vagococcaceae, and Wohlfahrtiimonadaceae by flies to carcass microbial communities (Figures 18-19) but further analyses of differentially abundant microbiota among sample types over time are needed to confirm and assign significance to this proposal.

This introduction of exogenous microbiota by blowflies could occur mechanically in different ways: via salivary secretions when feeding on carcass tissues, via tarsal contact as flies land to investigate the ephemeral resource, via regurgitation or defecation, or via oviposition of eggs by females on carcasses (Talley et al., 2009). Due to the significant role blow fly larvae play in consuming and transforming carrion, the latter mechanism could be more likely. In a metagenomic study of bacteria associated with different life stages of *L. sericata* and *Lucilia cuprina*, Singh et al (2015) reported that most fly-associated microbes were retained intragenerationally, and saw evidence for trans-generational inheritance and horizontal transmission of bacteria among flies. Additionally, Weatherbee et al. (2017) found evidence to suggest that carcass microbiomes are influenced by larval mass microbiomes, describing a sudden shift in bacteria relative abundances that correlated with maggot mass presence. This evidence supports our findings of the significant impacts of adult blow fly internal microbiomes on carcass microbiomes and may implicate larval stages and maggot mass dynamics as a potential driving force in microbial community succession in carrion ecology.

This study presents the first comprehensive look at blow fly-microbe interactions in vertebrate decomposition in two highly contrasting seasons Michigan. This seasonal context is of particular importance due to the significance of temperature as a primary driver of nearly all biological processes (Brown et al., 2004). Because temperature is directly proportional to a substance's kinetic energy, temperature governs chemical and metabolic rates for most organismal life. This principle is a cornerstone of the fields of forensic entomology and carrion ecology, as rates of insect development and decomposition are highly temperature dependent and are frequently measured in ADH, a convenient unit of heat and time. Microbes have also exhibited temperature dependence, with higher temperatures increasing microbial diversity and taxon richness (Zhou et al., 2016). These relationships suggest that, based on our results, microbe-insect interactions may have broad implications for ecosystem ecology and necrobiome dynamics such as rates of carrion removal and nutrient recycling. The study of decomposition within different temperature ranges may also become of particular importance as the effects of global climate change are felt, leading to potential shifts in species ranges, changes in community structure, and ecosystem disruption (Maxwell et al., 2019; Thuiller, 2004). These changes could have unforeseen consequences for decomposer communities and their ability to utilize and break down carrion. Additionally, understanding the effects of contrasting temperatures on the interdomain relationships of primary decomposers could also be a valuable tool for forensic investigators to estimate PMI more accurately, or positively link insect evidence to a set of remains.

This study aimed to investigate and characterize potential inter-kingdom interactions associated with insects and necrotic microbial communities and found support for the potential exchange or introduction of exogenous microbiota into carcass microbiomes by blow flies. This

interaction appears to be the precursor to significant temporal shifts observed in carcass microbiota, particularly the depletion of Moraxellaceae and increase in community diversity as decomposition progresses. More extensive and in-depth analyses of blow fly life stages during carrion decomposition could be useful to more conclusively identify microbes responsible for driving these changes, as well as if or how these introduced bacteria vary between dipteran species.

Tomberlin et al. (2011), in advocating for a unified, standardized framework for forensic science and decomposition research, specifically cited the need for further exploration of the role of microbiota in decomposition to better understand how they mediate arthropod activity and facilitate critical ecosystem services. One rationale for this is to improve guidelines and standardized practices for forensic entomological evidence in order to meet criteria outlined by the Daubert standard, which states that scientific evidence admitted into a court of law must be testable, have known error rates, and be peer-reviewed and accepted by that scientific community (Solomon & Hackett, 1996). While there are still many complex facets of the necrobiome that need to be examined in greater detail to inform our understanding of forensic entomology and carrion ecology, the findings of this study help address the issues outlined by Tomberlin et al. (2011), and also contribute to a working foundation for future, more specialized forays into microbe-insect interactions that can link basic and applied sciences. Building up this body of knowledge and more clearly defining the mechanisms that dictate carrion decomposition will not only strengthen our understanding of the broad ecological impacts of nutrient cycling across trophic levels, but also align these fields with the Daubert standard, allowing for more meaningful application and utility of entomological evidence in the legal system.

CHAPTER 2: POTENTIAL POSTMORTEM MICROBIAL BIOMARKERS OF INFANT DEATH INVESTIGATION

Abstract

Through life and after death, the microbiome is rapidly becoming a powerful tool to provide insight into the human health condition. Microbial communities on the human body are highly dynamic, adapting to reflect their host's environment and lifestyle over time. Studies have shown that the event of death is no exception, with microbiome data echoing antemortem health up to 48 hours following death. These predictable microbial biomarkers can critically inform death investigations by helping to estimate the postmortem interval and build models to identify cause and manner of death more accurately. However, no attempts have been made to survey and model potential microbial biomarkers in cases of infant (≤ 2 years) death. This study provided a cross-sectional survey of microbiota of 53 infant cases received to the Wayne County Medical Examiner's Office, Detroit, Michigan, and demonstrates support for the differentiation of microbial communities across anatomical sites previously documented in adult cases. To build a robust database, microbiota were collected from black and white infants from both sexes that died by accident, homicide, or natural causes, by swabbing the eyes, ears, nose, mouth, umbilicus, brain, rectum, and cardiac blood. 16SrRNA sequence analyses showed that sex, race, age, body site and manner of death (MOD) had a statistically significant effect on microbiome composition, with a significant interaction between MOD, race, and age. *Sneathia*, a potential biomarker associated with spontaneous preterm birth and preterm prelabor rupture of membranes was discovered.

Introduction

While speculations have been made about the importance of human microbiota as far back as the 1900s, the potential of the human microbiome as a tool to provide insight into the human health condition has become a subject of particular interest within the last decade or so (Blaser, 2006; Cho & Blaser, 2012; Knight et al., 2017; Metchnikoff, 1907). Due to remarkable advancements in DNA sequencing and bioinformatic technologies, studies have demonstrated that from birth microbes are a substantial presence on and in the human body, which may harbor an estimated 500-1,000 bacterial species and up to 20 million microbial genes at any time (Gilbert et al., 2018; Turnbaugh et al., 2007). This microbial diversity far exceeds the genetic diversity of the human genome, and also varies by anatomical site on the body, with distinct microbial communities observed in areas such as the eyes, ears, nose, mouth, gut, rectum, and on the hair and skin (Costello et al., 2009; Gilbert et al., 2018; Pechal et al., 2018). These microbial communities are typically specific to an individual like a fingerprint, but are also highly dynamic and variable through human development; adapting to their host's environment, physiology, and lifestyle over time (Lax et al., 2014; Meadow et al., 2015; Relman, 2012). Studies have shown this pattern continues even after death, with postmortem microbiomes resembling antemortem microbiota in a predictable succession up to 48 hours later (Pechal et al., 2018), and in some cases as late as 72 hours (Metcalf et al., 2013, 2016). In this way, human postmortem microbiota have a unique potential to inform our understanding of human health and death investigation. However, studies of the human microbiome are predominantly antemortem, have been limited primarily to adults, and rarely examine cases of infant death.

The long-term impacts, importance, and community structure of the microbiome in living human adult hosts have been documented in many contexts. Lifestyle traits like cohabitation

with pets, exercise and sleep habits, diet, and even stress levels have associations with microbiome composition (Gilbert et al., 2018). For example, the microbiome can mediate glycemic responses to diet and impact blood glucose levels differently from person to person, while stress and sleep deprivation are associated with shifts of bacterial ratios in the gut that can impact nutrient absorption, metabolism, and immune responses (Benedict et al., 2016; Karl et al., 2017; Zeevi et al., 2015). Research has also shown that human microbiomes are impacted by our environment, with evidence suggesting features of urban environments like abandoned buildings contribute to exposure to potential pathogens in sites like eyes, mouth, and nose, while green spaces are positively correlated with microbial biodiversity in the rectum and the nose (Pearson et al., 2019, 2020)

With so much information available within an individual's microbiome, this growing body of evidence has also revealed novel microbial biomarkers that can indicate the presence of certain immune, metabolic, and cognitive diseases, which may in turn be used to inform their diagnosis, treatment, and prevention strategies, as well as potential links to manner or cause of death (Gilbert et al., 2018; Kaszubinski et al., 2020; Pechal et al., 2018; Zhang et al., 2019). For example, genomic and metabolomic analyses found that *Fusobacterium* species are a significant biomarker of colorectal cancer, the third most common cancer worldwide, as well as a relationship between gut microbiota-dependent metabolism of phosphatidylcholine and cardiovascular disease, the leading cause of death globally (Balakumar et al., 2016; Ferlay et al., 2015; Kostic et al., 2012). Multiple potential biomarkers for inflammatory bowel disease have also been proposed such as increased ratios of Firmicutes and Actinobacteria, as well as Gammaproteobacteria, Enterococcus, and Enterococcaceae (Cho & Blaser, 2012; Lo Presti et al., 2019). While additional analyses are still needed to better understand many of these microbiome

configurations and their relationships with various diseases, great potential has been established for the microbiome as a practical tool to survey human health. However, a majority of work has examined the living host only, and less emphasis has been placed on the study of postmortem microbiota with the exception of a few studies such as Pearson et al. (2019, 2020) and Pechal et al (2018).

Though comparably lacking in study, temporal and localized anatomical changes in bacterial community structure have been observed during mammalian decomposition. Because microbes are significant drivers of decomposition due to their pivotal role in putrefaction as cellular integrity is compromised, most studies have viewed the postmortem microbiome through a forensic or ecological lens as a means to develop a postmortem interval (PMI), or time elapsed since death, for use within the criminal justice system or to investigate complex decomposition dynamics (Evans, 1963; Janaway et al., 2009; Metcalf et al., 2013; Pechal, Crippen, et al., 2014). This is often accomplished using high-throughput DNA sequencing due to its increasing affordability and reliability as a forensic tool. These investigations may utilize adult deceased human bodies or swine carcasses (*Sus scrofa* L.), which have been established as appropriate, accessible proxies to model human decomposition when human bodies are unavailable (Catts & Goff, 1992).

Like the antemortem microbiome, bacterial communities differ between body sites such as the skin, mouth, and gut, and change in a predictable succession over decomposition, with certain bacterial taxa associated with different taphonomic stages (Adserias-Garriga et al., 2017; Hyde et al., 2015; Metcalf et al., 2013; Pechal, Crippen, et al., 2014) and associated with manner of death (see citations in comments). Investigations of postmortem microbiota vary in focus however, with some examining only a single body site at a time or multiple at once, and nearly

all data are limited by the availability of human research subjects representative of real-world community demographics. Additionally, little to no comprehensive data is available for postmortem microbiota of children and infants, with the exception of a study from Pechal et al. (2017) examining the frozen and thawed remains of a 9-year-old and 13-year-old, and an audit by Pryce et al (2011) evaluating microbial cultures from routine postmortem sampling of sudden unexplained death in infants (SUDI) taken in the hospital to those taken at the time of autopsy. As evidenced by the significant variability of the antemortem microbiome from person to person, more robust data across different age ranges and demographics are needed of postmortem microbiota in order to provide a more cohesive understanding of these communities after death, but they are especially needed in infants.

Table 9. A summary of infant mortality rates (per 1,000 live births) for the United States, Michigan, and Wayne, Co., MI. ((Centers for Disease Control and Prevention, National Center for Health Statistics: Linked Birth / Infant Death Records, 2007-2020 Results, n.d.).

Geographic Region	Infant Mortality Rate (per 1,000 live births)
United States	6
Michigan	6.8
Wayne Co., MI	9.8

Infant mortality rates in the United States exceeded 19,000 deaths from 2007-2020, or 6 per 1,000 live births. This rate in Wayne County, Michigan is just over 1.5 times that of the United States (*Centers for Disease Control and Prevention, National Center for Health Statistics: Linked Birth / Infant Death Records, 2007-2020 Results, n.d.*). A prevalent cause of

death in infants is sudden unexplained infant death (SUID), also referred to as sudden infant death syndrome (SIDS), though the latter term is considered misleading by some pathologists and there remains an ongoing debate on how to appropriately define and diagnose this condition (Beckwith, 2003; Byard, 2018; Limerick & Bacon, 2004). Described as the “diagnosis without a disease”, SIDS is a term used to describe the sudden, unexpected death of an otherwise healthy infant while sleeping, and to date no tangible cause has been identified to explain these deaths (Byard, 2018). Another significant cause of death in infants is also co-sleeping, wherein an infant sleeps with a parent, sibling, or other caretaker in an adult bed, on a couch, or any area other than an infant crib by themselves. Studies have shown that this can create an unsafe sleeping situation for infants, as they are obligate nasal breathers and their airways may be easily blocked by the body of another person, a cushioned surface, or blankets, leading to asphyxiation (Byard, 2015; Mitchell, 2015). Complications thus arise when an unexplained infant death occurs, as SIDS and co-sleeping deaths present very similarly, and autopsy findings can rarely distinguish between them. This problem of determining the manner of death in suspected SUID cases, framed within the context of the postmortem microbiome, was the aim of this study.

The potential of the postmortem microbiome to reveal information about antemortem health has already been demonstrated in adults by Pechal et al. (2018), who observed evidence for decreased microbial diversity in individuals with heart disease. Using machine learning algorithms, Zhang et al. (2019) showed that microbial samples from the eyes were the most informative anatomical site overall to predict manner of death, though rectal samples independently were highly accurate models, and that different combinations of body site microbes increased each algorithm’s accuracy. These results show the potential of the postmortem microbiome as a predictive tool to not only survey the living health condition, but to

inform forensic investigations. Methods described by Pechal et al. (2018) to sample the postmortem microbiome could be integrated into routine autopsy procedure, and analyses for biomarkers could be developed into analytical workflow recommendations to aid in forensic investigation as proposed by Kaszubinski et al (2020). Further analyses, standardization, and robust datasets are needed before tools such as this can be feasibly integrated into real world scenarios and accepted into a court of law (*Daubert v. Merrell Dow Pharmaceuticals, Inc.*, 509 U.S. 579 (1993), n.d.; Tomberlin et al., 2011).

As the microbiome rapidly changes during the first three years of life, this could be a critical time to sample and investigate microbial community dynamics in infants (Knight et al., 2017). To investigate these potential interactions, we conducted a cross-sectional survey of 53 infant cases using 16SrRNA with the goals of 1) characterizing the composition of the infant bacterial postmortem microbiome for the first time; and 2) identifying potential bacterial biomarkers that could predict manner of death. We hypothesized that: 1) bacterial community composition will be structured by body site and by manner of death; and 2) that microbes from co-sleeping (control) deaths would be more similar in bacterial composition and structure than other manners of death, as these unexpected deaths are due to asphyxia of otherwise healthy infants.

Materials and Methods

Microbiome samples were acquired from the Wayne County Medical Examiner's Office (MEO) located in Detroit, MI, USA, through routine death investigations carried out since 2014. Only samples from cases of death in black or white individuals aged 2 years or younger were analyzed within this study. The following information for each decedent was compiled from available case reports: sex, ethnicity, date of birth, estimated age (days, months, and years), event location (indoors, outdoors, vehicular, or hospital), time of death, and season (winter, summer, etc.). In addition, the following information was collected from autopsy reports: autopsy date, height (crown-heel length, crown-rump length, foot length) and height percentile, weight and weight percentile, manner of death, cause of death, and state of decomposition at the time of autopsy, as well as any other significant pre-existing conditions or medical history. All cause and manner of death (MOD), and postmortem interval (PMI) estimates were determined by a board-certified forensic pathologist.

Manner of death classification

For the purposes of this study, MOD for each case was categorized as one of the following based on mechanism and cause of death: natural, accidental, non-accidental, or control. Natural death was assigned to cases where the circumstances of death were attributed to natural, pre-determined causes, such as a pre-existing genetic condition. Accidental death was assigned to cases involving chance circumstances such as accidental drownings, or airway obstruction unrelated to co-sleeping with an adult. In contrast, non-accidental death was assigned to cases involving intentional harm caused by blunt force injury, drug toxicity, or other non-accidental injury. Finally, control cases were those where circumstances of death were due to

asphyxia, airway obstruction, or over-lay specifically attributed to co-sleeping. Studies have shown that the act of co-sleeping with a sibling or adult caretaker can create an unsafe sleeping environment for infants, as their airways may be easily blocked by the body of another person, cushioned surfaces, or blankets, leading to asphyxiation (Byard 2015). Co-sleeping deaths were chosen as a control in this study since this MOD did not represent any compounding variables such as disease or bodily trauma.

Sample Collection

Sampling kits consisting of sterile, DNA-free, cotton-tipped applicators (25-806 2WC, FDNA, Puritan, Guilford, MA, USA), and sterile 1.5 ml microcentrifuge tubes (20170-038 VWR International, Radnor, PA, USA) filled with 100% molecular biology grade ethanol (BP2818-500, Fisher Scientific, Waltham, MA, USA) were provided to trained autopsy personnel within the Wayne County MEO to collect individual microbial communities from each decedent. Each swab kit was assigned a unique kit number by our lab and returned by MEO personnel with its corresponding case number for processing. A total of nine anatomical locations were sampled and assigned L1-L9 as follows: ears, eyes, nose, mouth, umbilicus, rectum, trabecular space, interhemispheric fissure, and cardiac blood. Sites were sampled by manually rubbing a single swab over the area for at least 30 seconds and breaking off the cotton tip of each swab into an individual 1.5 ml tube. Bacterial samples were taken from decedents within 24-48 hours of admission to the Wayne County ME, and all samples were transported in cooler storage from the MEO and immediately placed in -20 °C storage until DNA isolation. Sampling followed regulations outlined by the Institutional Review Board (IRB), which states that research utilizing

human remains from deceased autopsy subjects does not require the same consideration given human subjects.

DNA Isolation and Quantification

DNA was extracted from cotton swabs in a biological safety cabinet using the QIAGEN DNeasy Blood & Tissue Kit (QIAGEN, Hilden, Germany). Swabs were first prepared for lysis on Parafilm sheets (Bemis Company, Inc, Neenah, WI, USA) by using sterilized dissecting forceps and scalpels (12-000-164, Thermo Fisher Scientific, Waltham, MA, USA) with sterile, single-use carbon steel blades (22-079-697, Surgical Design Inc. Lorton, VA, USA) to carefully remove cotton from the wooden handle. The cotton was then placed back into its respective 1.5ml tube, and the wooden handle and Parafilm were discarded. To preserve the individual microbial communities, new Parafilm sheets and sterile instruments were used to prepare each sample. The manufacturer's protocol was then followed accordingly with the addition of 10ul of 15 mg/ml lysozyme to promote increased microbial cell lysis. Samples were also treated with 4ul 100mg/ml RNase A following incubation per the MSU Genomics Core Illumina sample sequencing requirements, and final DNA elution volume was modified from 200ul to 50ul. DNA was then quantified using a Qubit 2.0 and a 1x dsDNA High Sensitivity Assay (Thermo Fisher Scientific, Waltham, MA, USA). DNA was stored at -20°C to await further processing.

16S rRNA Confirmation

The microbial gene amplicon V4 region was amplified using conventional PCR in triplicate with Invitrogen Platinum Green Hot Start Master Mix (2x) (Thermo Fisher Scientific, Waltham, MA, USA), PCR-grade nuclease free water, and region-specific primers 515f/806r (5'

GTGCCAGCMGCCGCGGTAA, 5' GGACTACHVGGGTWTCTAAT). PCR samples were each prepared with 24ul mastermix and 1ul template DNA, loaded into 96-well plates (82006-636 VWR International, Radnor, PA, USA), and sealed with qPCR film (6091-078, VWR International, Radnor, PA, USA) in a biological safety cabinet. The positive and negative controls run in each plate were *E. coli* and PCR-grade nuclease-free water, respectively. PCR samples were spun down in a Sorvall ST 8 centrifuge (Thermo Fisher Scientific, Waltham, MA, USA), placed into a Veriti 96-well thermal cycler (Thermo Fisher Scientific, Waltham, MA, USA) and amplified according to previously described methods (Caporaso et al., 2011). The resulting PCR product was stored at -20°C.

Visual 16S rRNA confirmation was then performed via gel electrophoresis. 3% agarose gels (3.6 g agarose in 120 ml 1X TAE) (N605-500G, VWR International, Radnor, PA, USA) were cast in a Thermo EC Midicell Primo EC-330 Horizontal Gel System. 5ul each of GeneRuler 1kb ladder (Thermo Fisher Scientific, Waltham, MA, USA), PCR product, and controls were loaded and run at 90 V for 40 minutes. Gels were then agitated in GelRed solution (60 ul GelRed in 200 ml DI water) (Thermo Fisher Scientific, Waltham, MA, USA) for 30 minutes on a 3D platform rotator. Gels were imaged using the Axygen Gel Documentation System (Corning Incorporated, Corning, NY, USA) at UV 302.

Table 10. An overview of sample size and demographics for sequenced cases. TS = trabecular space, IF = interhemispheric fissure, CB = cardiac blood.

Sample Size (Cases)	Median Age	Age Range	Ethnicity	Sex	Years Collected	Body Sites Collected
53	109 Days 3.6 Months 0.3 Years	0-817 Days 0-27 Months 0-2.22 Years	40 Black, 13 White	26 Male, 27 Female	2015-2022	Ears, Eyes, Nose, Mouth, Umbilicus, Rectum, TS, IF, CB

Table 11. A summary of MOD categories for sequenced cases broken down by sex and race. ND indicates cases with an unknown or indeterminate MOD based on available case information.

Manner of Death	Black			White			Total
	Female	Male	Total	Female	Male	Total	
Accidental	4	2	6	2	1	3	9
Non-accidental	4	6	10	2	0	2	12
Natural	1	4	5	2	1	3	8
Control	5	3	8	1	3	4	12
Indeterminate	3	3	6	0	0	0	6
ND	2	3	5	1	0	1	6
Total	19	21	40	8	5	13	53

Table 12. Manners and causes of death for sequenced cases of infant death. Cause of death was determined by a board-certified forensic pathologist.

Manner of Death	Cause of Death
Accidental	Airway obstruction, asphyxia, drug toxicity, drowning
Non-accidental	Abusive head trauma, asphyxia, blunt force trauma, cranio-cerebral injuries, drug toxicity, multiple blunt force injuries, multiple blunt trauma, multiple stab wounds, premature birth
Natural	Acute bronchitis, complications of edwards syndrome, congenital heart disease, pneumonia, RSV bronchiolitis, prematurity complications, sepsis due to urinary tract infection, status asthmaticus
Control	Airway obstruction or asphyxia due to co-sleeping
Indeterminate	Anoxic encephelopathy, fentanyl toxicity, fentanyl toxicity with complications, sudden death, suffocation, unknown

Table 13. Totals of each body site processed and sequenced with 16S rRNA gene amplicon high-throughput sequencing.

Body Site	Number Sequenced
Eyes	16
Ears	38
Nose	49
Mouth	46
Umbilicus	3
Rectum	45
Trabcular space (TS)	40
Interhemispheric fissure (IF)	36
Cardiac blood (CB)	24
Total	298

16S rRNA Gene Amplicon Sequencing

DNA sequencing and library construction for 298 individual microbial body site samples was performed at the Michigan State University Genomics Core facility (East Lansing, MI, USA) on the Illumina MiSeq (2 x 250 bp paired-end reads). The V4 region of the 16S rRNA gene was amplified using dual indexed 515F/806R Illumina primers (5'-GTGCCAGCMGCCGCGG-3', 5'-TACNVGGGTATCTAATCC-3') following the protocol described in Kozich, JJ, et al. (2013). PCR products were batch normalized using an Invitrogen SequalPrep DNA Normalization plate, and products were pooled and cleaned up using a QIAquick Spin column and AMPure XP magnetic beads. Library pools were quality controlled and quantified using a combination of Qubit dsDNA HS, Agilent 4200 TapeStation HS DNA1000, and Invitrogen Collibri Illumina Library Quantification qPCR assays. Amplicon

pools were then loaded onto a MiSeq v2 standard flow cell and sequencing was carried out in a 2 x 250 bp paired-end format using a MiSeq v2 500 cycle reagent cartridge. Custom sequencing and index primers complementary to the 515f/806r oligomers were added to appropriate wells of the reagent cartridge. Base calling was performed by Illumina Real Time Analysis (RTA) v1.18.54 and output of RTA was demultiplexed and converted to FastQ format with Illumina Bcl2fastq v2.20.0.

16S rRNA Sequence Analyses

QIIME2 (Quantitative Insights Into Microbial Ecology) (v2023.2) was used to filter and analyze raw 16S microbial sequencing data. Demultiplexed reads were assembled and quality filtered for chimeric reads and artifacts using DADA2. A Naïve Bayes classifier (V4, SILVA database v138-99) trained against the 16S rRNA region was used to classify filtered reads into taxonomic groups and assign taxonomy (Quast et al., 2013; Yilmaz et al., 2014). Sequences were aligned with a De novo multiple sequence alignment program in QIIME2 (Mafft v7) and contingency filtered to remove singletons and reads corresponding with mitochondria or chloroplasts (Kato & Standley, 2013). 16SrRNA relative abundances of bacterial communities at the phylum (>1%) and family level among body sites and manners of death were analyzed with the phyloseq, MicrobeR, microbiome, qiime2R, microbiomeSeq, and microbiomeutilities packages in Rstudio (v4.3.1).

Statistical Analyses

Permutational Multivariate Analysis of Variance (PERMANOVA, 999 iterations) and pairwise PERMANOVA (FDR corrections) tests using weighted UniFrac distances using the

vegan R package (Oksanen et al., 2015) were conducted evaluate the effect of body site, manner of death, and additional covariates (age, sex, race) on overall microbiome composition. Pairwise Wilcoxon rank-sum tests of observed and Shannon diversity (False Discovery Rate (FDR) correction) were also performed to determine significant differences in bacterial alpha diversity among body sites and manners of death (Benjamini & Hochberg, 1995). Weighted UniFrac distances were used to visualize covariate relationships and microbiome structure with principal coordinates analysis (PCoA) and 95% confidence intervals (CI) for multivariate t-distributions. Weighted UniFrac metrics were used for these ordinations because they account for phylogenetic distances and relative abundances among microbes (Lozupone & Knight, 2005).

To identify potential biomarkers most likely to explain differences among significantly distinct microbiota, covariates were tested using the linear discriminant analysis (LDA) effect size (LEfSe) using default settings in the microbiomeMarker package (Rstudio) (Cao et al., 2022; Segata et al., 2011). LEfSe is an algorithm that uses Kruskal-Wallis tests to discover high-dimensional biomarkers that can statistically significantly differentiate between biological groups (Fang et al., 2018; Segata et al., 2011). All statistical analyses were conducted in Rstudio (v4.3.1) and all p-values were considered significant with $\alpha \leq 0.05$.

Results

16S rRNA sequences from a total of 298 body site samples (eyes, ears, nose, mouth, umbilicus, rectum, TS, IF, and CB) (Table 13) from 53 cases of routine infant autopsy collected from 2015 to 2022 (Table 10) in Wayne County, Michigan, were analyzed to characterize infant postmortem microbiota and identify potential microbial correlations linked to manner of death. Of the 53 cases there were 26 males and 27 females, 40 black and 13 white, with case ages ranging from 0-27 months old. 12 cases each were identified as non-accidental and controls, with nine accidental deaths and eight natural deaths. A more detailed breakdown of sequencing and demographic totals can be seen in Tables 10, 11, and 13. Manner and causes of death observed in this dataset are summarized in Table 12 and were categorized based on individual evaluation of circumstances described in autopsy and case reports. There were also six cases wherein MOD could not be conclusively determined through routine autopsy, referred to hereafter as indeterminate deaths, as well as six cases with no available data for cause or manner of death (ND). Due to the limited availability of samples from cases of infant death, these cases were still included in analyses to build a more robust database of postmortem infant microbiota, especially since there are no comprehensive published findings of postmortem microbiome profiles of humans in this age range. While microbiome composition and phylum and family-level relative abundances of all samples were investigated, samples from cases with an MOD classified as Indeterminate and ND were filtered from the dataset for the purpose of statistical analysis.

Bacterial community structure

Infant postmortem microbiota were represented by four primary phyla: Actinobacteria, Bacteroidota, Firmicutes, and Proteobacteria (Figure 20) Among all body sites the most

dominant phylum was Firmicutes, ranging from 34.3% relative abundance in umbilicus samples to 62% relative abundance in ear samples. The second most relatively abundant phylum was Proteobacteria among cardiac blood samples (31.5%), eyes (38.8%), nose (36.2%), trabecular space (31.7%), interhemispheric fissure (32.9%), and mouth (22.1%). Bacteroidota was second most abundant in rectum samples (24.2%), and 28.3% relative abundance of umbilicus samples was represented by “Other” phyla. Among manners of death the most dominant phylum was again Firmicutes (30-60% relative abundance), followed by Proteobacteria (18-42% relative abundance). Relative abundances for the top 13 family-level taxa were also plotted (figure []), and varied among body sites, with the most prevalent being Streptococcaceae (1.3% in rectum samples to 30% in mouth samples), Enterobacteriaceae (2.5% in umbilicus samples to 19% in eye samples).

Ear samples were represented by Staphylococcaceae (44.5% relative abundance) more than any other site, and rectum samples had the highest abundance of Lachnospiraceae (12.7%) and Peptostreptococcales-Tissierellales (5.6%), but lacked Moraxellaceae, a family present at low relative abundance (0.6-7.2%) in all other sites. Bifidobacteriaceae was also more abundant in the rectum (10.7%) and umbilicus (10.1%) than other body sites (<5%). Among manners of death “Other” family-level taxa represented the most relative abundance (24-36%) overall. Enterobacteriaceae was most abundant in accidental deaths (25% relative abundance), and Streptococcaceae was present at 12-26% relative abundance among all MODs. Indeterminate deaths were represented by Prevotellaceae (18.5% relative abundance) more than other MODs.

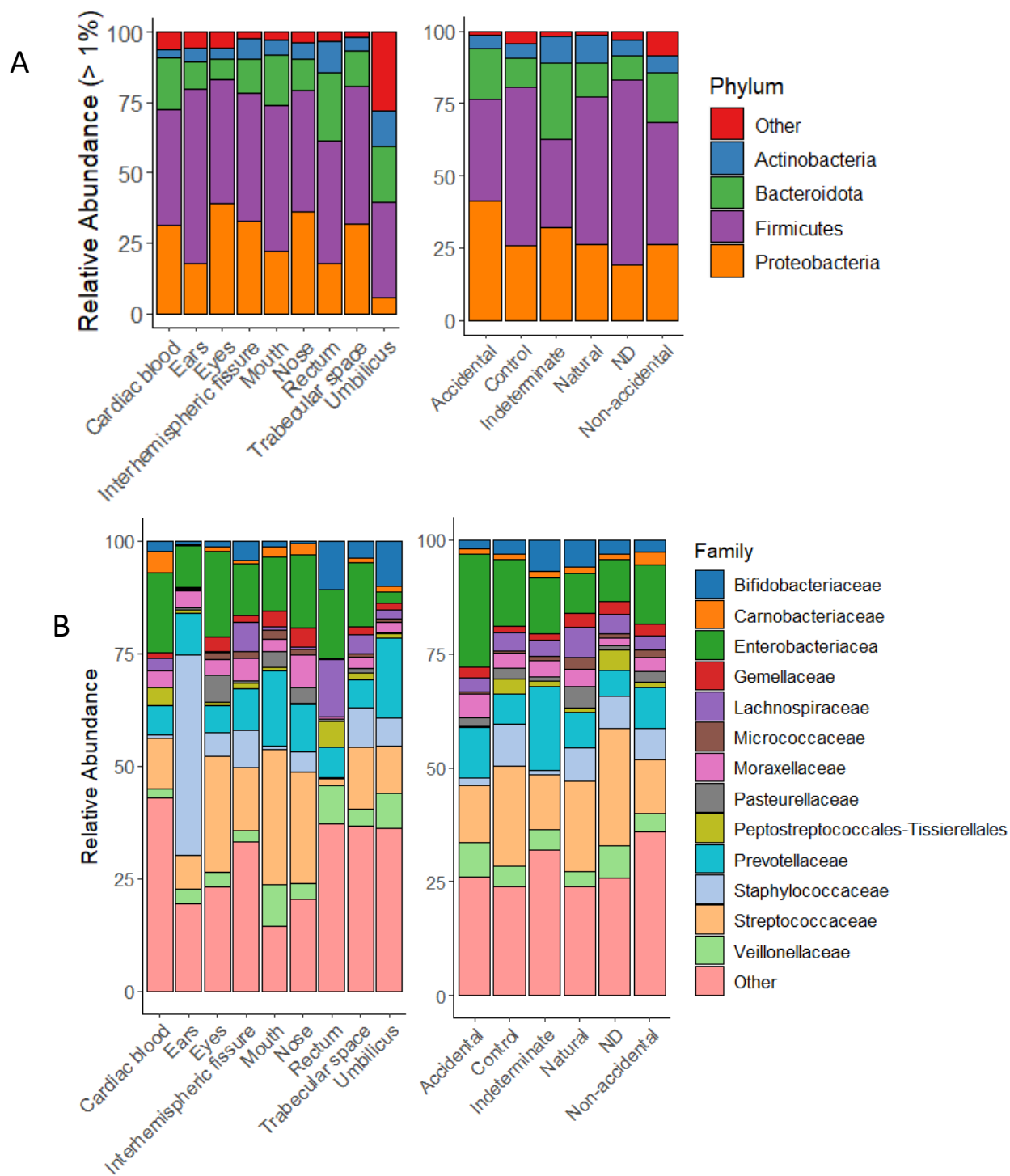


Figure 20. A) Phylum and B) family level bacterial relative abundance by body site (left) and manner of death (right). Only phylum-level taxa which comprised greater than 1% of total abundance are shown.

Pairwise tests of Shannon and Observed diversity (Wilcoxon rank-sum test, FDR correction) among body sites indicated many significant differences in alpha diversity (Figure 21). Shannon diversity showed distinct microbiota for comparisons of cardiac blood-mouth ($P = 0.002$), cardiac blood-nose ($P = 0.015$), and cardiac blood-rectum ($P = 0.0002$), for ears-mouth ($P = 0.030$) and ears-rectum ($P = 0.011$), for eyes-mouth ($P = 0.019$) and eyes-rectum ($P = 0.002$), for interhemispheric fissure-mouth ($P = 0.040$) and rectum ($P = 0.008$), for rectum-nose ($P = 0.019$) and trabecular space-rectum ($P = 0.047$). More distinct differences among body sites in pairwise tests of Observed diversity were found than Shannon, with very high significance ($P < 0.0001$) between cardiac blood and the mouth, nose, and rectum, between eyes and the mouth and rectum, between the interhemispheric fissure and the mouth, nose, and rectum, and between the trabecular space and mouth, and rectum. Less highly significant differences were found for cardiac blood-ears ($P = 0.043$) and cardiac blood-umbilicus ($P = 0.021$), for ears-rectum ($P = 0.043$), for interhemispheric fissure-eyes ($P = 0.038$) and interhemispheric fissure-umbilicus ($P = 0.027$), and for the rectum-nose ($P = 0.027$). Tests were run of all sequences and filtered sequences (with and without ND and Indeterminate MOD cases) to investigate significant pairwise differences in alpha diversity for manner of death, but no significantly distinct microbiota for either measure were detected for either test among MODs.

Results of permutational analysis of variance of body site and MOD showed that body site ($F = 3.968$, $P = 0.001$) and MOD ($F = 2.626$, $P = 0.001$) had statistically significant effects on microbiome composition (Table 13). However, the interaction between body site and MOD ($F = 0.952$, $P = 0.632$) did not have a statistically significant effects on microbiome composition. Further investigation of other study covariates however showed that race (black or white) had a significant effect on bacterial communities when tested for interaction with body site ($F = 2.47$, P

= 0.018) and MOD (F = 2.942, P = 0.014)), as well as a significant interaction with MOD (F = 2.971, P = 0.001) (Table 14-15). Sex (male or female) was also shown to have a significant interaction with MOD (F = 1.765, P = 0.026), but alone did not have a significant effect (Table 14). Finally, age also had a significant structuring effect on microbiomes, but had no interactions with body site or MOD. Principal coordinates analyses were plotted to visualize these interactions within microbial communities (Figure 21)

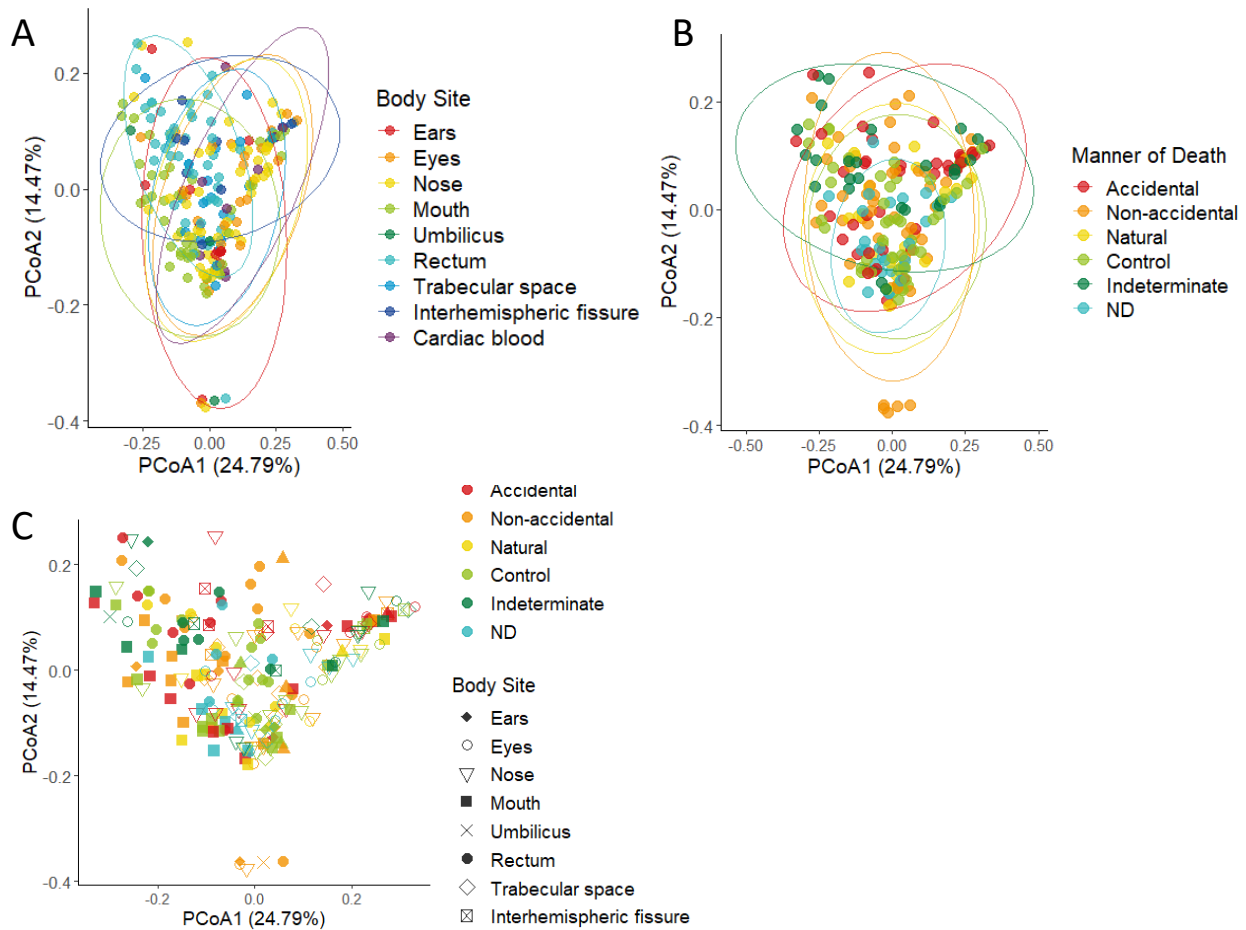


Figure 21. Principal coordinates analyses (PCoA) of weighted UniFrac distances expressed as A) body site, B) manner of death, and C) manner of death and body site. Ellipses indicate 95% confidence intervals.

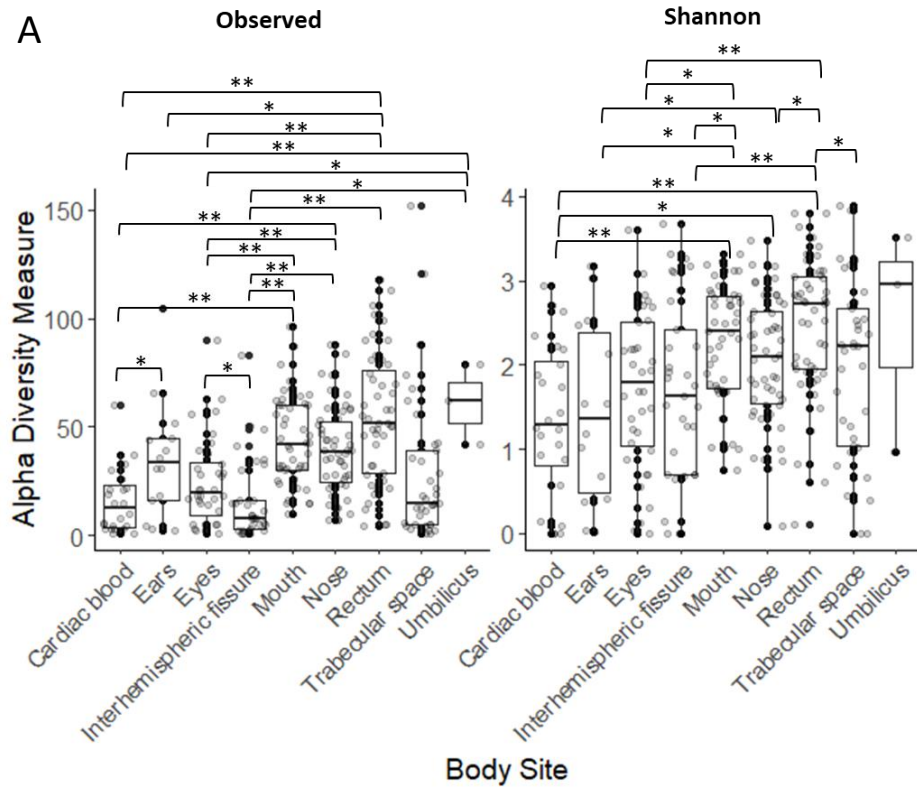


Figure 22. Pairwise tests of Observed and Shannon diversity (Wilcoxon rank-sum test, FDR correction) between A) body sites and B) manners of death. Significant differences are denoted by brackets. * = $P\text{-adj} < 0.05$, ** = $P\text{-adj} < 0.01$.

Table 14. Impact of body site and MOD on bacterial beta diversity. Significant values (<0.05) are indicated in bold. PERMANOVA test (weighted UniFrac distance) was conducted with 999 permutations. DF = Degrees of Freedom, SS = Sum of Squares.

Factor	DF	SS	R²	F	Pr(>F)
Manner of Death	3	0.6856	0.03094	2.626	0.001
Body Site	8	2.7629	0.1247	3.968	0.001
Manner of Death:Body Site	22	1.8224	0.08225	0.952	0.632
Residual	194	16.8862	0.76211		
Total	227	22.1571	1		

Table 15. Impact of MOD, race, sex, and age on bacterial beta diversity. Significant values (<0.05) are indicated in bold. PERMANOVA test (weighted UniFrac distance) was conducted with 999 permutations. DF = Degrees of Freedom, SS = Sum of Squares.

Factor	DF	SS	R²	F	Pr(>F)
Manner of Death	3	0.6856	0.0309	2.468	0.003
Race	1	0.2724	0.0123	2.942	0.014
Manner of Death:Race	3	0.8255	0.0373	2.971	0.001
Residual	220	20.3735	0.9195		
Total	227	22.1571	1		
Manner of Death	3	0.6856	0.0309	2.405	0.003
Sex	1	0.0617	0.0028	0.65	0.746
Manner of Death:Sex	3	0.5033	0.0227	1.765	0.026
Residual	220	20.9064	0.9436		
Total	227	22.1571	1		
Manner of Death	3	0.6856	0.0309	2.897	0.001
Age	38	6.7701	0.3056	2.258	0.001
Manner of Death:Age	1	0.107	0.0048	1.356	0.202
Residual	185	14.5944	0.6587		
Total	227	22.1571	1		

Table 16. Impact of body site, race, sex, and age on bacterial beta diversity. Significant values (<0.05) are indicated in bold. PERMANOVA test (weighted UniFrac distance) was conducted with 999 permutations. DF = Degrees of Freedom, SS = Sum of Squares.

Factor	DF	SS	R²	F	Pr(>F)
Body Site	8	2.7491	0.12407	3.9194	0.001
Race	1	0.2168	0.00978	2.4727	0.018
Body Site:Race	8	0.7791	0.03516	1.1108	0.26
Residual	210	18.412	0.83098		
Total	227	22.1571	1		
Body Site	8	2.7491	0.12407	3.8828	0.001
Sex	1	0.0867	0.00391	0.9791	0.398
Body Site:Sex	8	0.7357	0.0332	1.039	0.409
Residual	210	18.5856	0.83881		
Total	227	22.1571	1		
Body Site	8	2.7491	0.12407	3.8306	0.001
Age	38	6.8265	0.30809	2.0025	0.001
Body Site:Age	162	10.877	0.4909	0.7484	0.986
Residual	19	1.7045	0.07693		
Total	227	22.1571	1		

Table 17. Pairwise PERMANOVA calculated from weighted UniFrac distances among manners of death. Values indicating significantly distinct microbiota (<0.05) are shown in bold.

Comparison (MOD)		P adj.
Non-accidental	Natural	0.294
Non-accidental	Accidental	0.024
Non-accidental	Control	0.1185
Natural	Accidental	0.026
Natural	Control	0.2568
Accidental	Control	0.026

Table 18. Pairwise PERMANOVA calculated from weighted UniFrac distances among body sites. Values indicating significantly distinct microbiota (<0.05) are shown in bold.

Comparison (Body site)		P adj.
Ears	Eyes	0.058
Ears	Nose	0.029
Ears	Umbilicus	0.207
Ears	Rectum	0.005
Ears	TS	0.107
Ears	Mouth	0.036
Ears	IF	0.089
Ears	Cardiac blood	0.059
Eyes	Nose	0.353
Eyes	Umbilicus	0.107
Eyes	Rectum	0.005
Eyes	TS	0.125
Eyes	Mouth	0.036
Eyes	IF	0.107
Eyes	Cardiac blood	0.058
Nose	Umbilicus	0.107
Nose	Rectum	0.005
Nose	TS	0.107
Nose	Mouth	0.107
Nose	IF	0.099
Nose	Cardiac blood	0.016
Umbilicus	Rectum	0.078
Umbilicus	TS	0.107
Umbilicus	Mouth	0.099
Umbilicus	IF	0.133
Umbilicus	Cardiac blood	0.141
Rectum	TS	0.005
Rectum	Mouth	0.005
Rectum	IF	0.005
Rectum	Cardiac blood	0.005
TS	Mouth	0.059
TS	IF	0.906
TS	Cardiac blood	0.323
Mouth	IF	0.036
Mouth	Cardiac blood	0.014
IF	Cardiac blood	0.650

Pairwise PERMANOVA was used to further identify significant interactions for body site and manner of death (Table 16-17). Comparisons of non-accidental and accidental ($P = 0.024$), natural and accidental ($P = 0.026$), and accidental and control ($P = 0.026$) were significantly distinct, while ears-nose ($P = 0.029$), ears-rectum ($P = 0.005$), ears-mouth ($P = 0.036$), eyes-mouth ($P = 0.036$), nose-rectum ($P = 0.005$), nose-cardiac blood ($P = 0.016$), all rectum comparisons ($P = 0.005$), mouth-interhemispheric fissure ($P = 0.036$), and mouth-cardiac blood ($P = 0.014$) were significant among body sites.

To better understand how race, sex, and age influence microbiome structure, additional pairwise tests of Shannon and Observed diversity (Wilcoxon rank-sum test, FDR correction) were conducted (Figure 23). No significant differences were observed in alpha diversity measures between males and females, or black and white infants (Figure 23B). There were however significant distinctions observed for ranges of age in days, with microbiota originating from cases aged 1-30 days and 66-92 days differing from cases aged 383-820 days in Observed diversity (Figure 23A). Microbiota from cases aged 165-380 days old were also significantly different from age ranges of 1-30 days, 31-60 days, and 66-92 days, as well as between age range 383-570 and ranges 1-30 and 31-60 for Shannon diversity measures. Additionally, infant age appears to be positively correlated with alpha diversity measures, which is particularly evident for Shannon diversity (Figure 23A).

Identification of potential biomarkers

To attempt to identify potential biomarkers most likely to explain differences in microbiome structure caused by covariates, linear discriminant analysis effect size (LEFSe) analyses were attempted for all covariates, and significant results were visualized as a heatmap

(Figure 24). Only analyses of sex and race were able to identify potential biomarkers. Features most likely to explain differences based on race were Leptotrichiaceae ($P = 0.0098$), Sneathia ($P = 0.0064$), and an uncultured Sneathia species ($P = 0.001$). These features were associated with microbiota from white cases and based on the heatmap (Figure 24B) also appear to correlate with a male and non-accidental death most closely. However much lower prevalence of Sneathia is also seen in alignment with black, male, and non-accidental covariates. Results of LEFSe analysis based on sex resulted in one identified feature, Escherichia-Shigella ($P = 0.0100$), which enriched microbiota associated with the female sex, and based on the heatmap also appear to correlate most distinctly with white, accidental death.

The criteria for association with Sneathia were used to filter through sample metadata and identify potential candidates that may be the origin of this biomarker. One case, 2017-S077 is the only case that matches these criteria. This case is represented by six samples (ears, eyes, nose, umbilicus, rectum, and trabecular space), and is also the youngest case overall (< 1 day). The cause and manner of death assigned by the medical examiner were asphyxia and homicide, respectively.

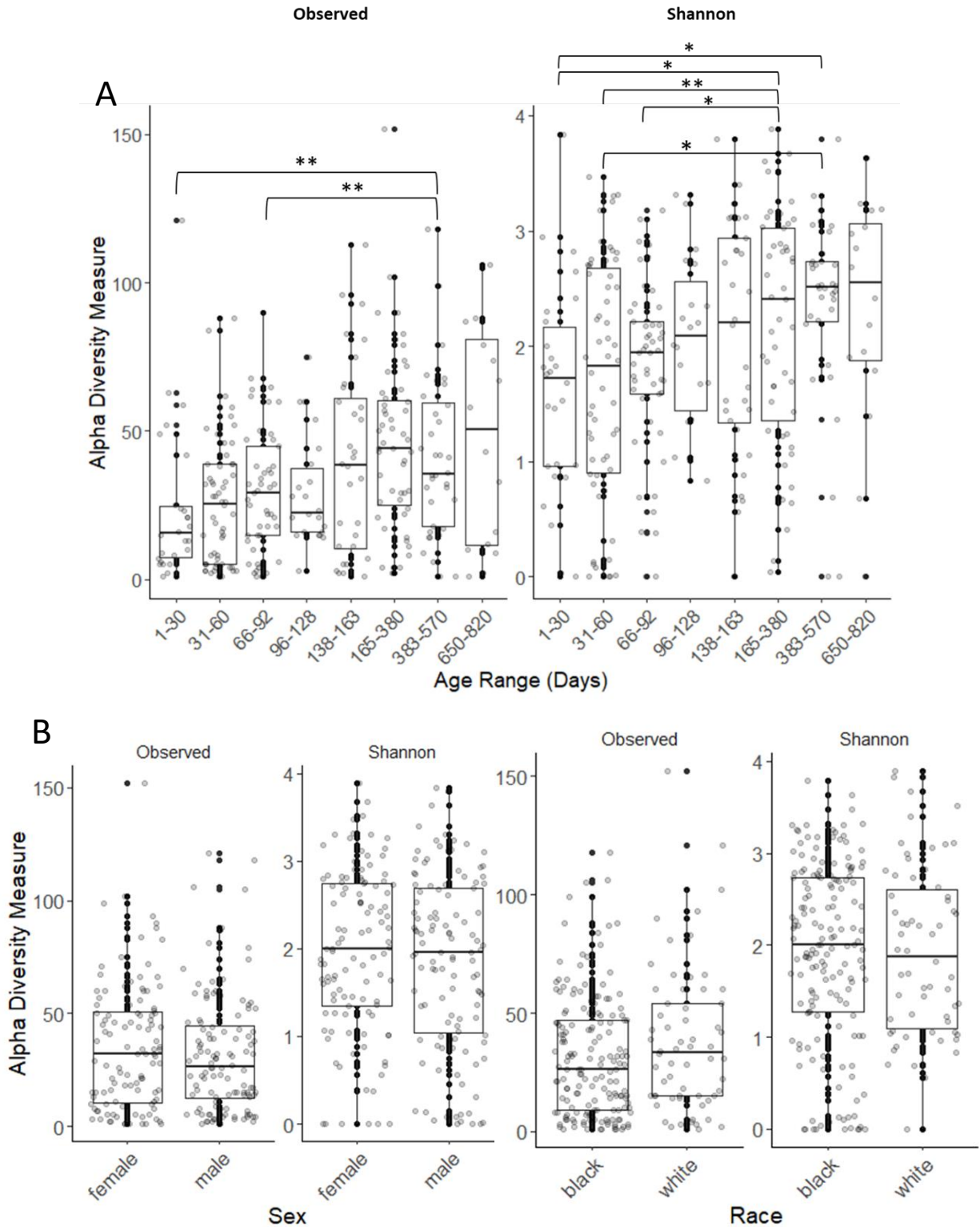


Figure 23. Differences in alpha diversity among sex, race, and age ranges in days. Pairwise tests of Observed and Shannon diversity (Wilcoxon rank-sum test, FDR correction). Alpha diversity for A) age ranges in days and B) sex and race. Significant differences are denoted by brackets. * = $P\text{-adj} < 0.05$, ** = $P\text{-adj} < 0.01$.

A

Class	Feature	Enriched Group	LDA Score	P.adj.
Race	Leptotrichiaceae	White	4.815935	0.0098
	Sneathia	White	4.809275	0.0064
	Sneathia_uncultured bacterium	White	4.806226	0.0001
Sex	Escherichia-Shigella	Female	4.501279	0.0100

B

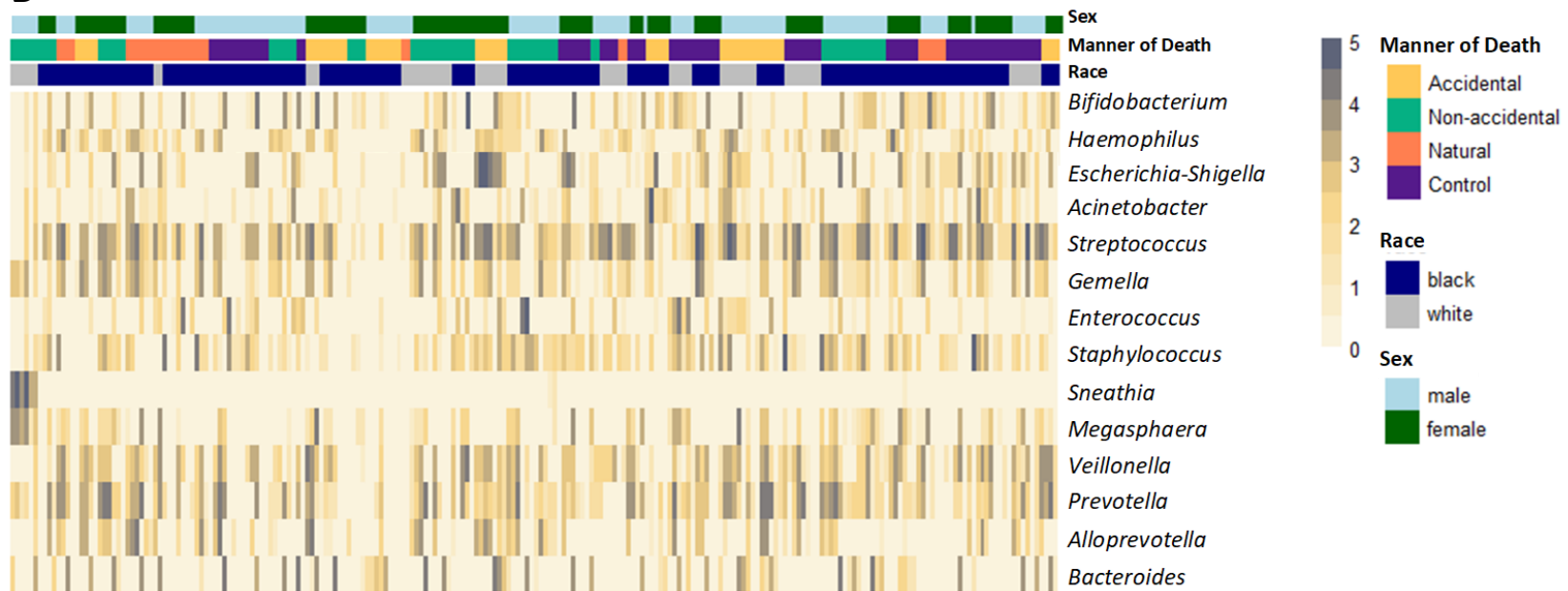


Figure 24. Potential biomarkers associated with manner of death in analyzed infant postmortem microbiota. A) LEFSse analysis results (Wilcoxon cutoff = 0.01, kw cutoff = 0.01, LDA cutoff = 4, CPM (counts per million) pre sample normalization). B) Heatmap visualization at the genus-level of covariates associated with identified biomarkers and their interaction with manner of death.

Discussion

Interest in the human microbiome as a powerful tool with great potential to improve our understanding of the human health condition has grown significantly in recent years. Studies of microbiome structure and function can reveal a wealth of information about individual health and lifestyle, and as this body of evidence grows it informs the way diseases may be treated, diagnosed, and prevented (Gilbert et al., 2018). With the advances being made in applications for antemortem health, the resilience and utility of human postmortem microbiota are frequently overlooked. Even so, studies have established that postmortem microbiota play a significant role in decomposition, with temporal patterns of microbial succession and distinct microbial communities observed at anatomical sites on human remains and other mammalian proxies (Hyde et al., 2015; Metcalf et al., 2016; Pechal, Crippen, et al., 2014), including manner of death (Pechal et al 2018; Zhang et al 2019; Kaszubinski et al 2020). With much to be learned from the postmortem microbiome before it can be standardized as a practical tool for use in forensic investigation or public health, there is a real need for robust, cross-sectional data representative of human microbiota of all ages and demographics. To address this need, this study presents the first comprehensive survey of the infant postmortem microbiome that contributes to a larger effort to understand the postmortem microbiome of all age, race and ethnic groups more comprehensively.

While body site and manner of death each had a significant effect on infant postmortem microbiome composition as predicted, there was no evidence discovered here to suggest yet that circumstances of death in infants are correlated with bacterial community structure in specific anatomical sites. Instead, of all covariates our results indicated significant interactions between MOD and sex and race. This was not an anticipated result, and contradicts findings by Pechal et

al (2018) which demonstrated a lack of significance ($P > 0.6$) of race/ethnicity in structuring the postmortem microbiome. Fortenberry (2013) urges caution in examining racial and ethnic categories due to their lack of biological significance and reliability in determining human genomic diversity, while results from Huttenhower et al. (2012) indicate a strong relationship exists between race/ethnicity and microbial community composition. Other studies have demonstrated consistent associations with ethnicity and bacterial abundance in body sites like the mouth, gut, and vagina, with the aim of understanding differential disease susceptibility and addressing health conditions such as bacterial vaginosis that disproportionately affect minorities (Brooks et al., 2018; Fettweis et al., 2014; Mallott et al., 2023; Mason et al., 2013).

Overlap of sex, race, and MOD (Figure 24) implicated a white, male, non-accidental (homicide) case of infant death as the origin of the *Sneathia* marker. *Sneathia* is a genus belonging to Leptotrichiaceae, a family of obligate or facultative anaerobes (Theis et al., 2021). This genus has been found in the mouth, gut, and cervix and vagina, and is thought to correlate with spontaneous preterm birth and labor, and preterm prelabor rupture of membranes (PPROM) (Theis et al., 2021). Additionally, *Sneathia* is associated with bacterial vaginosis, may be capable of infecting the upper respiratory tract during pregnancy, and one species, *Sneathia amnii* is even documented invading fetal membranes and jeopardizing tissue viability (Theis et al., 2021). Preterm birth (PTB) has been declared the second leading cause of neonate death worldwide, and *Sneathia* species detected in early-mid pregnancy may be associated with spontaneous PTB (Fettweis et al., 2019; Nelson et al., 2014). Based on the information available about manner and cause of death (non-accidental, asphyxia) in the infant case clearly associated with this genus, it is unclear exactly how this biomarker became a part of this infant microbiome, as well as how many and which body sites it is detected in.

Another observation of note presented here is the significant effect of age on microbiome composition, more specifically the increase in alpha diversity associated with increasing age (Figure 23A). The development of the living infant microbiome has been studied at length, and this early life process is a critical window for proper immunological development, but not all sources and exact mechanisms of transmission are understood (Moore & Townsend, 2019). Infants most likely obtain microbes vertically and horizontally, receiving their first microbes from their mother via maternal seeding, and from the surrounding community post-birth (Moore & Townsend, 2019). This community or environmental effect has also been described by Pearson et al. (2020) who observed the relationship between neighborhood environmental conditions and the human microbiome. Findings from Mallott et al (2023) also demonstrate the diversification of infant microbes over time, with a significant shift observed at or just after three months of age associated with race and ethnicity. This is likely due to many factors such as varying diets (breastfeeding versus starting solid food), association with green spaces, and social exposure from other children or caretakers (Mallott et al., 2023). While we did not observe a similar shift at three months, samples in the age range of 165-380 days old (5.5 to 12.7 months) had more significantly distinct pairwise differences in Shannon diversity.

This study presents the first comprehensive survey of the postmortem infant microbiome and shows support for the significant effect of anatomical site and MOD on microbial community structure, as well as a potential biomarker of infant death related to PTB. These findings represent only one more step towards our understanding of the complex dynamics that make up the human microbiome, and greater sample sizes and variability are needed to develop a truly representative database that can proactively inform human health in the way antemortem microbiome studies have. Characterizing these microbiota and postmortem interactions is critical

to build our knowledge base regarding human microbiome composition across a broad range of ages, lifestyles, demographics, and socio-economic status. Additionally, based on the significant effect of MOD on postmortem microbiota presented here, additional surveys and analyses may also uncover more specific biomarkers that more clearly indicate correlation with circumstances of death. These data have already been explored as such from the human postmortem microbiome, and when analyzed using machine learning algorithms showed increasing predictive power and accuracy with the incorporation of microbiota from more anatomical sites (Zhang et al., 2019). Pechal et al (2014) also used a similar approach, utilizing bacterial communities and general additive models to estimate physiological time as a measure of carrion decomposition. These modelling strategies exhibit marked potential to improve accuracy rates in the classification of infant manner of death when traditional autopsy examination fails to ascertain why an infant death occurred due to a lack of bodily evidence or injury. Our methodology presented here already provides support for the routine collection of postmortem microbiota from a variety of anatomical sites as an addition to standard autopsy protocol. With further data collection, analysis, and systematic modelling via machine learning algorithms, standardized workflows and recommendations could be developed for practical applications during death investigation.

LITERATURE CITED

- Adserias-Garriga, J., Quijada, N. m., Hernandez, M., Rodríguez Lázaro, D., Steadman, D., & Garcia-Gil, L. j. (2017). Dynamics of the oral microbiota as a tool to estimate time since death. *Molecular Oral Microbiology*, 32(6), 511–516. <https://doi.org/10.1111/omi.12191>
- Ahmad, A., Broce, A., & Zurek, L. (2006). Evaluation of Significance of Bacteria in Larval Development of *Cochliomyia macellaria* (Diptera: Calliphoridae). *Journal of Medical Entomology*, 43(6), 1129–1133. <https://doi.org/10.1093/jmedent/43.6.1129>
- Anderson, G. S. (2011). Comparison of Decomposition Rates and Faunal Colonization of Carrion in Indoor and Outdoor Environments. *Journal of Forensic Sciences*, 56(1), 136–142. <https://doi.org/10.1111/j.1556-4029.2010.01539.x>
- Archer, M. S. (2004). Annual variation in arrival and departure times of carrion insects at carcasses: Implications for succession studies in forensic entomology. *Australian Journal of Zoology*, 51(6), 569–576. <https://doi.org/10.1071/zo03053>
- Armstrong, G. L., Hollingsworth, J., & Morris, J. G., Jr. (1996). Emerging Foodborne Pathogens: *Escherichia coli* O157:H7 as a Model of Entry of a New Pathogen into the Food Supply of the Developed World. *Epidemiologic Reviews*, 18(1), 29–51. <https://doi.org/10.1093/oxfordjournals.epirev.a017914>
- Babcock, N. J., Pechal, J. L., & Benbow, M. E. (2020). Adult Blow Fly (Diptera: Calliphoridae) Community Structure across Urban-Rural Landscapes in Michigan, United States. *Journal of Medical Entomology*, 57(3), 705–714. <https://doi.org/10.1093/jme/tjz246>
- Balakumar, P., Maung-U, K., & Jagadeesh, G. (2016). Prevalence and prevention of cardiovascular disease and diabetes mellitus. *Pharmacological Research*, 113, 600–609. <https://doi.org/10.1016/j.phrs.2016.09.040>
- Barton, P. S., Cunningham, S. A., Lindenmayer, D. B., & Manning, A. D. (2013). The role of carrion in maintaining biodiversity and ecological processes in terrestrial ecosystems. *Oecologia*, 171(4), 761–772. <https://doi.org/10.1007/s00442-012-2460-3>
- Barton, P. S., Cunningham, S. A., Macdonald, B. C. T., McIntyre, S., Lindenmayer, D. B., & Manning, A. D. (2013). Species Traits Predict Assemblage Dynamics at Ephemeral Resource Patches Created by Carrion. *PLOS ONE*, 8(1), e53961. <https://doi.org/10.1371/journal.pone.0053961>
- Barton, P. S., Evans, M. J., Foster, C. N., Pechal, J. L., Bump, J. K., Quaggiotto, M.-M., & Benbow, M. E. (2019). Towards Quantifying Carrion Biomass in Ecosystems. *Trends in Ecology & Evolution*, 34(10), 950–961. <https://doi.org/10.1016/j.tree.2019.06.001>

- Beckwith, J. B. (2003). Defining the Sudden Infant Death Syndrome. *Archives of Pediatrics & Adolescent Medicine*, 157(3), 286–290. <https://doi.org/10.1001/archpedi.157.3.286>
- Benbow, M. E., Barton, P. S., Ulyshen, M. D., Beasley, J. C., DeVault, T. L., Strickland, M. S., Tomberlin, J. K., Jordan, H. R., & Pechal, J. L. (2019). Necrobiome framework for bridging decomposition ecology of autotrophically and heterotrophically derived organic matter. *Ecological Monographs*, 89(1). <https://doi.org/10.1002/ecm.1331>
- Benbow, M. E., Lewis, A. J., Tomberlin, J. K., & Pechal, J. L. (2013). Seasonal necrophagous insect community assembly during vertebrate carrion decomposition. *Journal of Medical Entomology*, 50(2), 440–450. <https://doi.org/10.1603/ME12194>
- Benedict, C., Vogel, H., Jonas, W., Woting, A., Blaut, M., Schurmann, A., & Cedernaes, J. (2016). Gut microbiota and glucometabolic alterations in response to recurrent partial sleep deprivation in normal-weight young individuals. *Molecular Metabolism*, 5(12), 1175–1186. <http://dx.doi.org/10.1016/j.molmet.2016.10.003>
- Benjamini, Y., & Hochberg, Y. (1995). Controlling the False Discovery Rate: A Practical and Powerful Approach to Multiple Testing. *Journal of the Royal Statistical Society. Series B (Methodological)*, 57(1), 289–300.
- Blaser, M. J. (2006). Who are we? Indigenous microbes and the ecology of human diseases. *EMBO Reports*, 7(10), 956–960. <https://doi.org/10.1038/sj.embor.7400812>
- Brooks, A. W., Priya, S., Blekhman, R., & Bordenstein, S. R. (2018). Gut microbiota diversity across ethnicities in the United States. *PLOS Biology*, 16(12), e2006842. <https://doi.org/10.1371/journal.pbio.2006842>
- Brown, J. H., Gillooly, J. F., Allen, A. P., Savage, V. M., & West, G. B. (2004). Toward a Metabolic Theory of Ecology. *Ecology*, 85(7), 1771–1789. <https://doi.org/10.1890/03-9000>
- Byard, R. W. (2015). Overlaying, co-sleeping, suffocation, and sudden infant death syndrome: The elephant in the room. *Forensic Science, Medicine, and Pathology*, 11(2), 273–274. <https://doi.org/10.1007/s12024-014-9600-5>
- Byard, R. W. (2018). Sudden Infant Death Syndrome: Definitions. In J. R. Duncan & R. W. Byard (Eds.), *SIDS Sudden Infant and Early Childhood Death: The Past, the Present and the Future*. University of Adelaide Press. <http://www.ncbi.nlm.nih.gov/books/NBK513393/>
- Byrd, J. H., & Caster, J. L. (Eds.). (2009). *Forensic Entomology: The Utility of Arthropods in Legal Investigations, Second Edition* (2nd ed.). CRC Press. <https://doi.org/10.1201/NOE0849392153>

- Cao, Y., Dong, Q., Wang, D., Zhang, P., Liu, Y., & Niu, C. (2022). microbiomeMarker: An R/Bioconductor package for microbiome marker identification and visualization. *Bioinformatics*, 38(16), 4027–4029. <https://doi.org/10.1093/bioinformatics/btac438>
- Caporaso, J. G., Lauber, C. L., Walters, W. A., Berg-Lyons, D., Lozupone, C. A., Turnbaugh, P. J., Fierer, N., & Knight, R. (2011). Global patterns of 16S rRNA diversity at a depth of millions of sequences per sample. *Proceedings of the National Academy of Sciences*, 108(supplement_1), 4516–4522. <https://doi.org/10.1073/pnas.1000080107>
- Catts, E. P., & Goff, M. L. (1992). Forensic Entomology in Criminal Investigations. *Annual Review of Entomology*, 37(1), 253–272. <https://doi.org/10.1146/annurev.en.37.010192.001345>
- Centers for Disease Control and Prevention, National Center for Health Statistics: Linked Birth / Infant Death Records, 2007-2020 Results. (n.d.). Retrieved July 11, 2023, from <https://wonder.cdc.gov/controller/datarequest/D69;jsessionid=6C6BB0D144629AA3BF9730790729>
- Cho, I., & Blaser, M. J. (2012). The human microbiome: At the interface of health and disease. *Nature Reviews Genetics*, 13(4), Article 4. <https://doi.org/10.1038/nrg3182>
- Costello, E. K., Lauber, C. L., Hamady, M., Fierer, N., Gordon, J. I., & Knight, R. (2009). Bacterial community variation in human body habitats across space and time. *Science*, 326(5960), 1694–1697. <https://doi.org/10.1126/science.1177486>
- Daubert v. Merrell Dow Pharmaceuticals, Inc.*, 509 U.S. 579 (1993). (n.d.). Justia Law. Retrieved March 30, 2023, from <https://supreme.justia.com/cases/federal/us/509/579/>
- De Jong, G. D., & Merritt, R. W. (2015). Arthropod Communities in Terrestrial Environments. In *Carrion Ecology, Evolution, and Their Applications*. CRC Press.
- Díaz-Aranda, L. M., Martín-Vega, D., Gómez-Gómez, A., Cifrián, B., & Baz, A. (2018). Annual variation in decomposition and insect succession at a periurban area of central Iberian Peninsula. *Journal of Forensic and Legal Medicine*, 56, 21–31. <https://doi.org/10.1016/j.jflm.2018.03.005>
- Early, M., & Goff, M. L. (1986). ARTHROPOD SUCCESSION PATTERNS IN EXPOSED CARRION ON THE ISLAND OF O'AHU, HAWAIIAN ISLANDS, USA 1. In *J. Med. Entomol* (Vol. 23, Issue 5, pp. 520–531). <https://academic.oup.com/jme/article/23/5/520/2220527>
- Evans, W. E. D. (1963). *The chemistry of death*. Thomas. <https://catalog.hathitrust.org/Record/000858400>
- Fang, D., Zhao, G., Xu, X., Zhang, Q., Shen, Q., Fang, Z., Huang, L., & Ji, F. (2018). Microbial community structures and functions of wastewater treatment systems in plateau and cold

- regions. *Bioresource Technology*, 249, 684–693.
<https://doi.org/10.1016/j.biortech.2017.10.063>
- Ferlay, J., Soerjomataram, I., Dikshit, R., Eser, S., Mathers, C., Rebelo, M., Parkin, D. M., Forman, D., & Bray, F. (2015). Cancer incidence and mortality worldwide: Sources, methods and major patterns in GLOBOCAN 2012. *International Journal of Cancer*, 136(5), E359–E386. <https://doi.org/10.1002/ijc.29210>
- Fettweis, J. M., Brooks, J. P., Serrano, M. G., Sheth, N. U., Girerd, P. H., Edwards, D. J., Strauss, J. F., the Vaginal Microbiome Consortium, Jefferson, K. K., & Buck, G. A. (2014). Differences in vaginal microbiome in African American women versus women of European ancestry. *Microbiology*, 160(10), 2272–2282.
<https://doi.org/10.1099/mic.0.081034-0>
- Fettweis, J. M., Serrano, M. G., Brooks, J. P., Edwards, D. J., Girerd, P. H., Parikh, H. I., Huang, B., Arodz, T. J., Edupuganti, L., Glascock, A. L., Xu, J., Jimenez, N. R., Vivadelli, S. C., Fong, S. S., Sheth, N. U., Jean, S., Lee, V., Bokhari, Y. A., Lara, A. M., ... Buck, G. A. (2019). The vaginal microbiome and preterm birth. *Nature Medicine*, 25(6), Article 6.
<https://doi.org/10.1038/s41591-019-0450-2>
- Fortenberry, J. D. (2013). The uses of race and ethnicity in human microbiome research. *Trends in Microbiology*, 21(4), 165–166. <https://doi.org/10.1016/j.tim.2013.01.001>
- Gilbert, J. A., Blaser, M. J., Caporaso, J. G., Jansson, J. K., Lynch, S. V., & Knight, R. (2018). Current understanding of the human microbiome. *Nature Medicine*, 24(4), Article 4.
<https://doi.org/10.1038/nm.4517>
- Graczyk, T. K., Knight, R., Gilman, R. H., & Cranfield, M. R. (2001). The role of non-biting flies in the epidemiology of human infectious diseases. *Microbes and Infection*, 3(3), 231–235. [https://doi.org/10.1016/S1286-4579\(01\)01371-5](https://doi.org/10.1016/S1286-4579(01)01371-5)
- Greenberg, B. (1991). Flies as Forensic Indicators. *Journal of Medical Entomology*, 28(5), 565–577. <https://doi.org/10.1093/jmedent/28.5.565>
- Guo, J., Fu, X., Liao, H., Hu, Z., Long, L., Yan, W., Ding, Y., Zha, L., Guo, Y., Yan, J., Chang, Y., & Cai, J. (2016). Potential use of bacterial community succession for estimating post-mortem interval as revealed by high-throughput sequencing. *Scientific Reports*, 6(1), Article 1. <https://doi.org/10.1038/srep24197>
- Huttenhower, C., Gevers, D., Knight, R., Abubucker, S., Badger, J. H., Chinwalla, A. T., Creasy, H. H., Earl, A. M., FitzGerald, M. G., Fulton, R. S., Giglio, M. G., Hallsworth-Pepin, K., Lobos, E. A., Madupu, R., Magrini, V., Martin, J. C., Mitreva, M., Muzny, D. M., Sodergren, E. J., ... The Human Microbiome Project Consortium. (2012). Structure, function and diversity of the healthy human microbiome. *Nature*, 486(7402), Article 7402. <https://doi.org/10.1038/nature11234>

- Hyde, E. R., Haarmann, D. P., Petrosino, J. F., Lynne, A. M., & Bucheli, S. R. (2015). Initial insights into bacterial succession during human decomposition. *International Journal of Legal Medicine*, 129(3), 661–671. <https://doi.org/10.1007/s00414-014-1128-4>
- Iancu, L., Carter, D. O., Junkins, E. N., & Purcarea, C. (2015). Using bacterial and necrophagous insect dynamics for post-mortem interval estimation during cold season: Novel case study in Romania. *Forensic Science International*, 254, 106–117. <https://doi.org/10.1016/j.forsciint.2015.07.024>
- Janaway, R. C., Percival, S. L., & Wilson, A. S. (2009). Decomposition of Human Remains. In S. L. Percival (Ed.), *Microbiology and Aging: Clinical Manifestations* (pp. 313–334). Humana Press. https://doi.org/10.1007/978-1-59745-327-1_14
- Jones, N., Whitworth, T., & Marshal, S. A. (2019). Blow flies of North America: Keys to the subfamilies and genera of Calliphoridae, and to the species of the subfamilies Calliphorinae, Luciliinae and Chrysomyinae. *Canadian Journal of Arthropod Identification*, 39(191). <https://doi.org/10.3752/cjai.2019.39>
- Karl, P. J., Margolis, L. M., Madslie, E. H., Murphy, N. E., Castellani, J. W., Gunderson, Y., Hoke, A. V., Levangie, M. W., Kumar, R., Chakraborty, N., Gautam, A., Hammamieh, R., Martini, S., Montain, S. J., & Pasiakos, S. M. (2017). Changes in intestinal microbiota composition and metabolism coincide with increased intestinal permeability in young adults under prolonged physiological stress. *American Journal of Physiology*, 312(6), G559–G571. <https://doi.org/doi:10.1152/ajpgi.00066.2017>
- Kaszubinski, S. F., Pechal, J. L., Schmidt, C. J., Jordan, H. R., Benbow, M. E., & Meek, M. H. (2020). Evaluating Bioinformatic Pipeline Performance for Forensic Microbiome Analysis*,†,‡. *Journal of Forensic Sciences*, 65(2), 513–525. <https://doi.org/10.1111/1556-4029.14213>
- Katoh, K., & Standley, D. M. (2013). MAFFT Multiple Sequence Alignment Software Version 7: Improvements in Performance and Usability. *Molecular Biology and Evolution*, 30(4), 772–780. <https://doi.org/10.1093/molbev/mst010>
- Knight, R., Callewaert, C., Marotz, C., Hyde, E. R., Debelius, J. W., McDonald, D., & Sogin, M. L. (2017). The Microbiome and Human Biology. *Annual Review of Genomics and Human Genetics*, 18(1), 65–86. <https://doi.org/10.1146/annurev-genom-083115-022438>
- Kostic, A. D., Gevers, D., Pedamallu, C. S., Michaud, M., Duke, F., Earl, A. M., Ojesina, A. I., Jung, J., Bass, A. J., Taberner, J., Baselga, J., Liu, C., Shivdasani, R. A., Ogino, S., Birren, B. W., Huttenhower, C., Garrett, W. S., & Meyerson, M. (2012). Genomic analysis identifies association of *Fusobacterium* with colorectal carcinoma. *Genome Research*, 22(2), 292–298. <https://doi.org/10.1101/gr.126573.111>
- Kozich, J. J., Westcott, S. L., Baxter, N. T., Highlander, S. K., & Schloss, P. D. (2013). Development of a dual-index sequencing strategy and curation pipeline for analyzing

- amplicon sequence data on the MiSeq Illumina sequencing platform. *Applied and Environmental Microbiology*, 79(17), 5112–5120. <https://doi.org/10.1128/AEM.01043-13>
- Kulshrestha, P., & Satpathy, D. K. (2001). Use of beetles in forensic entomology. *Forensic Science International*, 120(1), 15–17. [https://doi.org/10.1016/S0379-0738\(01\)00410-8](https://doi.org/10.1016/S0379-0738(01)00410-8)
- Lax, S., Smith, D. P., Hampton-Marcell, J., Owens, S. M., Handley, K. M., Scott, N. M., Gibbons, S. M., Larsen, P., Shogan, B. D., Weiss, S., Metcalf, J. L., Ursell, L. K., Vázquez-Baeza, Y., Van Treuren, W., Hasan, N. A., Gibson, M. K., Colwell, R., Dantas, G., Knight, R., & Gilbert, J. A. (2014). Longitudinal analysis of microbial interaction between humans and the indoor environment. *Science*, 345(6200), 1048–1052. <https://doi.org/10.1126/science.1254529>
- Limerick, S. R., & Bacon, C. J. (2004). Terminology used by pathologists in reporting on sudden infant deaths. *Journal of Clinical Pathology*, 57(3), 309–311. <https://doi.org/10.1136/jcp.2003.013052>
- Lo Presti, A., Zorzi, F., Del Chierico, F., Altomare, A., Cocca, S., Avola, A., De Biasio, F., Russo, A., Cella, E., Reddel, S., Calabrese, E., Biancone, L., Monteleone, G., Cicala, M., Angeletti, S., Ciccozzi, M., Putignani, L., & Guarino, M. P. L. (2019). Fecal and Mucosal Microbiota Profiling in Irritable Bowel Syndrome and Inflammatory Bowel Disease. *Frontiers in Microbiology*, 10. <https://www.frontiersin.org/articles/10.3389/fmicb.2019.01655>
- Lozupone, C., & Knight, R. (2005). UniFrac: A New Phylogenetic Method for Comparing Microbial Communities. *Applied and Environmental Microbiology*, 71(12), 8228–8235. <https://doi.org/10.1128/AEM.71.12.8228-8235.2005>
- Majumder, R., Sutcliffe, B., Taylor, P. W., & Chapman, T. A. (2020). Microbiome of the Queensland Fruit Fly through Metamorphosis. *Microorganisms*, 8(6), Article 6. <https://doi.org/10.3390/microorganisms8060795>
- Mallott, E. K., Sitarik, A. R., Leve, L. D., Cioffi, C., Camargo, C. A., Hasegawa, K., & Bordenstein, S. R. (2023). Human microbiome variation associated with race and ethnicity emerges as early as 3 months of age. *PLOS Biology*, 21(8), e3002230. <https://doi.org/10.1371/journal.pbio.3002230>
- Mason, M. R., Nagaraja, H. N., Camerlengo, T., Joshi, V., & Kumar, P. S. (2013). Deep Sequencing Identifies Ethnicity-Specific Bacterial Signatures in the Oral Microbiome. *PLOS ONE*, 8(10), e77287. <https://doi.org/10.1371/journal.pone.0077287>
- Matuszewski, S., Bajerlein, D., Konwerski, S., & Szpila, K. (2008). An initial study of insect succession and carrion decomposition in various forest habitats of Central Europe. *Forensic Science International*, 180(2), 61–69.

<https://doi.org/10.1016/j.forsciint.2008.06.015>

- Maxwell, S. L., Butt, N., Maron, M., McAlpine, C. A., Chapman, S., Ullmann, A., Segan, D. B., & Watson, J. E. M. (2019). Conservation implications of ecological responses to extreme weather and climate events. *Diversity and Distributions*, 25(4), 613–625. <https://doi.org/10.1111/ddi.12878>
- Meadow, J. F., Altrichter, A. E., Bateman, A. C., Stenson, J., Brown, G. Z., Green, J. L., & Bohannan, B. J. M. (2015). Humans differ in their personal microbial cloud. *PeerJ*, 3, e1258. <https://doi.org/10.7717/peerj.1258>
- Merritt, R. W., Courtney, G. W., & Keiper, J. B. (2009). Chapter 76 - Diptera: (Flies, Mosquitoes, Midges, Gnats). In V. H. Resh & R. T. Cardé (Eds.), *Encyclopedia of Insects (Second Edition)* (pp. 284–297). Academic Press. <https://doi.org/10.1016/B978-0-12-374144-8.00085-0>
- Metcalf, J. L., Wegener Parfrey, L., Gonzalez, A., Lauber, C. L., Knights, D., Ackermann, G., Humphrey, G. C., Gebert, M. J., Van Treuren, W., Berg-Lyons, D., Keepers, K., Guo, Y., Bullard, J., Fierer, N., Carter, D. O., & Knight, R. (2013). A microbial clock provides an accurate estimate of the postmortem interval in a mouse model system. *eLife*, 2, e01104. <https://doi.org/10.7554/eLife.01104>
- Metcalf, J. L., Xu, Z. Z., Weiss, S., Lax, S., Van Treuren, W., Hyde, E. R., Song, S. J., Amir, A., Larsen, P., Sangwan, N., Haarmann, D., Humphrey, G. C., Ackermann, G., Thompson, L. R., Lauber, C., Bibat, A., Nicholas, C., Gebert, M. J., Petrosino, J. F., ... Knight, R. (2016). Microbial community assembly and metabolic function during mammalian corpse decomposition. *Science*, 351(6269), 158–162. <https://doi.org/10.1126/science.aad2646>
- Metchnikoff, E. (1907). *The Prolongation of life: Optimistic studies*. G. P. Putnam's Sons.
- Mitchell, E. A. (2015). Co-sleeping and suffocation. *Forensic Science, Medicine, and Pathology*, 11(2), 277–278. <https://doi.org/10.1007/s12024-014-9616-x>
- Moore, R. E., & Townsend, S. D. (2019). Temporal development of the infant gut microbiome. *Open Biology*, 9(9), 190128. <https://doi.org/10.1098/rsob.190128>
- Nartshuk, E. P. (2014). Grass-fly larvae (Diptera, Chloropidae): Diversity, habitats, and feeding specializations. *Entomological Review*, 94(4), 514–525. <https://doi.org/10.1134/S001387381404006X>
- Nelson, D. B., Hanlon, A., Nachamkin, I., Haggerty, C., Mastrogiannis, D. S., Liu, C., & Fredricks, D. N. (2014). Early Pregnancy Changes in Bacterial Vaginosis-Associated Bacteria and Preterm Delivery. *Paediatric and Perinatal Epidemiology*, 28(2), 88–96. <https://doi.org/10.1111/ppe.12106>

- Oksanen, J., Blanchet, F. G., Kindt, R., Legendre, P., Minchin, P. R., O'hara, R., Simpson, G. L., Solymos, P., Stevens, M. H. H., & Wagner, H. (2015). *Package "vegan". Community ecology package, version 2.*
- Parmenter, R. R., & Macmahon, J. A. (2009). Carrion decomposition and nutrient cycling in a semiarid shrub-steppe ecosystem. *Ecological Monographs*, 79(4), 637–661. <https://doi.org/10.1890/08-0972.1>
- Payne, J. A. (1965). *A Summer Carrion Study of the Baby Pig Sus Scrofa Linnaeus* (Vol. 46, Issue 5, pp. 592–602).
- Pearson, A. L., Pechal, J., Lin, Z., Benbow, M. E., Schmidt, C., & Mavoia, S. (2020). Associations detected between measures of neighborhood environmental conditions and human microbiome diversity. *Science of The Total Environment*, 745, 141029. <https://doi.org/10.1016/j.scitotenv.2020.141029>
- Pearson, A. L., Rzotkiewicz, A., Pechal, J. L., Schmidt, C. J., Jordan, H. R., Zwickle, A., & Benbow, M. E. (2019). Initial Evidence of the Relationships between the Human Postmortem Microbiome and Neighborhood Blight and Greening Efforts. *Annals of the American Association of Geographers*, 109(3), 958–978. <https://doi.org/10.1080/24694452.2018.1519407>
- Pechal, J. L., & Benbow, M. E. (2016). Microbial ecology of the salmon necrobiome: Evidence salmon carrion decomposition influences aquatic and terrestrial insect microbiomes: Salmon decomposition and insect microbiomes. *Environmental Microbiology*, 18(5), 1511–1522. <https://doi.org/10.1111/1462-2920.13187>
- Pechal, J. L., Benbow, M. E., Crippen, T. L., Tarone, A. M., & Tomberlin, J. K. (2014). Delayed insect access alters carrion decomposition and necrophagous insect community assembly. *Ecosphere*, 5(4). <https://doi.org/10.1890/ES14-00022.1>
- Pechal, J. L., Crippen, T. L., Benbow, M. E., Tarone, A. M., Dowd, S., & Tomberlin, J. K. (2014). The potential use of bacterial community succession in forensics as described by high throughput metagenomic sequencing. *International Journal of Legal Medicine*, 128(1), 193–205. <https://doi.org/10.1007/s00414-013-0872-1>
- Pechal, J. L., Schmidt, C. J., Jordan, H. R., & Benbow, M. E. (2017). Frozen: Thawing and Its Effect on the Postmortem Microbiome in Two Pediatric Cases. *Journal of Forensic Sciences*, 62(5), 1399–1405. <https://doi.org/10.1111/1556-4029.13419>
- Pechal, J. L., Schmidt, C. J., Jordan, H. R., & Benbow, M. E. (2018). A large-scale survey of the postmortem human microbiome, and its potential to provide insight into the living health condition. *Scientific Reports*, 8(1). <https://doi.org/10.1038/s41598-018-23989-w>
- Pryce, J. W., Roberts, S. E. A., Weber, M. A., Klein, N. J., Ashworth, M. T., & Sebire, N. J. (2011). Microbiological findings in sudden unexpected death in infancy: Comparison of

- immediate postmortem sampling in casualty departments and at autopsy. *Journal of Clinical Pathology*, 64(5), 421–425. <https://doi.org/10.1136/jcp.2011.089698>
- Quast, C., Pruesse, E., Yilmaz, P., Gerken, J., Schweer, T., Yarza, P., Peplies, J., & Glöckner, F. O. (2013). The SILVA ribosomal RNA gene database project: Improved data processing and web-based tools. *Nucleic Acids Research*, 41(D1), D590–D596. <https://doi.org/10.1093/nar/gks1219>
- Relman, D. A. (2012). The human microbiome: Ecosystem resilience and health. *Nutrition Reviews*, 70(suppl_1), S2–S9. <https://doi.org/10.1111/j.1753-4887.2012.00489.x>
- Segata, N., Izard, J., Waldron, L., Gevers, D., Miropolsky, L., Garrett, W. S., & Huttenhower, C. (2011). Metagenomic biomarker discovery and explanation. *Genome Biology*, 12(6), R60. <https://doi.org/10.1186/gb-2011-12-6-r60>
- Sharanowski, B. J., Walker, E. G., & Anderson, G. S. (2008). Insect succession and decomposition patterns on shaded and sunlit carrion in Saskatchewan in three different seasons. *Forensic Science International*, 179(2), 219–240. <https://doi.org/10.1016/j.forsciint.2008.05.019>
- Singh, B., Crippen, T. L., Zheng, L., Fields, A. T., Yu, Z., Ma, Q., Wood, T. K., Dowd, S. E., Flores, M., Tomberlin, J. K., & Tarone, A. M. (2015). A metagenomic assessment of the bacteria associated with *Lucilia sericata* and *Lucilia cuprina* (Diptera: Calliphoridae). *Applied Microbiology and Biotechnology*, 99(2), 869–883. <https://doi.org/10.1007/s00253-014-6115-7>
- Solomon, S. M., & Hackett, E. J. (1996). Setting Boundaries between Science and Law: Lessons from *Daubert v. Merrell Dow Pharmaceuticals, Inc.* *Science, Technology, & Human Values*, 21(2), 131–156. <https://doi.org/10.1177/016224399602100201>
- Talley, J. L., Wayadande, A. C., Wasala, L. P., Gerry, A. C., Fletcher, J., Desilva, U., & Gilliland, S. E. (2009). Association of *Escherichia coli* O157:H7 with Filth Flies (Muscidae and Calliphoridae) Captured in Leafy Greens Fields and Experimental Transmission of *E. coli* O157:H7 to Spinach Leaves by House Flies (Diptera: Muscidae). *Journal of Food Protection*, 72(7), 1547–1552. <https://doi.org/10.4315/0362-028X-72.7.1547>
- Tan, S. C., & Yiap, B. C. (2009). DNA, RNA, and Protein Extraction: The Past and The Present. *BioMed Research International*, 2009, e574398. <https://doi.org/10.1155/2009/574398>
- Theis, K. R., Florova, V., Romero, R., Borisov, A. B., Winters, A. D., Galaz, J., & Gomez-Lopez, N. (2021). *Sneathia*: An emerging pathogen in female reproductive disease and adverse perinatal outcomes. *Critical Reviews in Microbiology*, 47(4), 517–542. <https://doi.org/10.1080/1040841X.2021.1905606>

- Thuiller, W. (2004). Patterns and uncertainties of species' range shifts under climate change. *Global Change Biology*, *10*(12), 2020–2027. <https://doi.org/10.1111/j.1365-2486.2004.00859.x>
- Tomberlin, J. K., Mohr, R., Benbow, M. E., Tarone, A. M., & VanLaerhoven, S. (2011). A Roadmap for Bridging Basic and Applied Research in Forensic Entomology. *Annual Review of Entomology*, *56*(1), 401–421. <https://doi.org/10.1146/annurev-ento-051710-103143>
- Triplehorn, C. A., Johnson, N. F., & Borror, D. J. (2004). *Borror and DeLong's Introduction to the Study of Insects* (7th ed.). Cengage Learning.
- Turnbaugh, P. J., Ley, R. E., Hamady, M., Fraser-Liggett, C. M., Knight, R., & Gordon, J. I. (2007). The Human Microbiome Project. *Nature*, *449*(7164), Article 7164. <https://doi.org/10.1038/nature06244>
- VanLaerhoven, S. L. (2008). Blind validation of postmortem interval estimates using developmental rates of blow flies. *Forensic Science International*, *180*(2–3), 76–80. <https://doi.org/10.1016/j.forsciint.2008.07.002>
- Vass, A. A. (2001). *Beyond the grave—Understanding human decomposition*. 28, 190–190.
- Wall, R., French, N., & Morgan, K. L. (1992). Effects of temperature on the development and abundance of the sheep blowfly *Lucilia sericata* (Diptera: Calliphoridae). *Bulletin of Entomological Research*, *82*(1), 125–131. <https://doi.org/10.1017/S0007485300051531>
- Wang, Y., Iii, T. M. G., Kukutla, P., Yan, G., & Xu, J. (2011). Dynamic Gut Microbiome across Life History of the Malaria Mosquito *Anopheles gambiae* in Kenya. *PLOS ONE*, *6*(9), e24767. <https://doi.org/10.1371/journal.pone.0024767>
- Watson, E. J., & Carlton, C. E. (2005). Insect Succession and Decomposition of Wildlife Carcasses During Fall and Winter in Louisiana. *Journal of Medical Entomology*, *42*(2), 193–203. <https://doi.org/10.1093/jmedent/42.2.193>
- Weatherbee, C. R., Pechal, J. L., & Benbow, M. E. (2017). The dynamic maggot mass microbiome. *Annals of the Entomological Society of America*, *110*(1), 45–53. <https://doi.org/10.1093/aesa/saw088>
- Whitworth, T. (2006). *Keys to the Genera and Species of Blow Flies (Diptera: Calliphoridae) of America North of Mexico*. *108*(3), 689–725.
- Yilmaz, P., Parfrey, L. W., Yarza, P., Gerken, J., Pruesse, E., Quast, C., Schweer, T., Peplies, J., Ludwig, W., & Glöckner, F. O. (2014). The SILVA and “All-species Living Tree Project (LTP)” taxonomic frameworks. *Nucleic Acids Research*, *42*(D1), D643–D648. <https://doi.org/10.1093/nar/gkt1209>

- Zeevi, D., Korem, T., Zmora, N., Israeli, D., Rothschild, D., Weinberger, A., Ben-Yacov, O., Lador, D., Avnit-Sagi, T., Lotan-Pompan, M., Suez, J., Mahdi, J. A., Matot, E., Malka, G., Kosower, N., Rein, M., Zilberman-Schapira, G., Dohnalová, L., Pevsner-Fischer, M., ... Segal, E. (2015). Personalized Nutrition by Prediction of Glycemic Responses. *Cell*, *163*(5), 1079–1094. <https://doi.org/10.1016/j.cell.2015.11.001>
- Zhang, Y., Pechal, J. L., Schmidt, C. J., Jordan, H. R., Wang, W. W., Benbow, M. E., Sze, S. H., & Tarone, A. M. (2019). Machine learning performance in a microbial molecular autopsy context: A cross-sectional postmortem human population study. *PLoS ONE*, *14*(4). <https://doi.org/10.1371/journal.pone.0213829>
- Zheng, L., Crippen, T. L., Holmes, L., Singh, B., Pimsler, M. L., Benbow, M. E., Tarone, A. M., Dowd, S., Yu, Z., Vanlaerhoven, S. L., Wood, T. K., & Tomberlin, J. K. (2013). Bacteria Mediate Oviposition by the Black Soldier Fly, *Hermetia illucens* (L.), (Diptera: Stratiomyidae). *Scientific Reports*, *3*(1), Article 1. <https://doi.org/10.1038/srep02563>
- Zheng, L., Crippen, T. L., Singh, B., Tarone, A. M., Dowd, S., Yu, Z., Wood, T. K., & Tomberlin, J. K. (2013). A Survey of Bacterial Diversity From Successive Life Stages of Black Soldier Fly (Diptera: Stratiomyidae) by Using 16S rDNA Pyrosequencing. *Journal of Medical Entomology*, *50*(3), 647–658. <https://doi.org/10.1603/ME12199>
- Zhou, J., Deng, Y., Shen, L., Wen, C., Yan, Q., Ning, D., Qin, Y., Xue, K., Wu, L., He, Z., Voordeckers, J. W., Nostrand, J. D. V., Buzzard, V., Michaletz, S. T., Enquist, B. J., Weiser, M. D., Kaspari, M., Waide, R., Yang, Y., & Brown, J. H. (2016). Temperature mediates continental-scale diversity of microbes in forest soils. *Nature Communications*, *7*(1), Article 1. <https://doi.org/10.1038/ncomms12083>
- Zurek, L., Schal, C., & Watson, D. W. (2000). Diversity and Contribution of the Intestinal Bacterial Community to the Development of *Musca domestica* (Diptera: Muscidae) Larvae. *Journal of Medical Entomology*, *37*(6), 924–928. <https://doi.org/10.1603/0022-2585-37.6.924>

APPENDIX A: RECORD OF DEPOSITION OF VOUCHER SPECIMENS

The specimens listed below, or photos thereof (due to destructive sampling) have been deposited in the named museum as samples of those species or other taxa, which were used in this research.

Voucher Number: 2023-12

Author and Title of thesis:

Bethany G. Mikles - Seasonal Necrobiome Variation in Michigan and Potential Postmortem Microbial Biomarkers of Infant Death Investigation

Museum where deposited:

Albert J. Cook Arthropod Research Collection, Michigan State University (MSU)

Table 19. A list of deposited voucher specimens including their life stage, quantity deposited, and preservation method. Photographs of all destructively sampled blowflies were taken dorsally, laterally, and of the face to document morphological characteristics. Pinned specimens were caught supplementally using butterfly traps and are representative of sampled blowflies. Three pinned specimens of each sex of the most abundant species caught were provided.

Family	Genus-Species	Life Stage	Quantity	Preservation
Calliphoridae	<i>Lucilia coeruleiviridis</i>	Adult	6	Pinned
Calliphoridae	<i>Lucilia coeruleiviridis</i>	Adult	53	Photographs
Calliphoridae	<i>Lucilia silvarum</i>	Adult	6	Pinned
Calliphoridae	<i>Lucilia silvarum</i>	Adult	24	Photographs
Calliphoridae	<i>Lucilia sericata</i>	Adult	13	Photographs
Calliphoridae	<i>Lucilia illustris</i>	Adult	12	Photographs
Calliphoridae	<i>Calliphora vomitoria</i>	Adult	7	Photographs
Calliphoridae	<i>Cynomya cadaverina</i>	Adult	12	Photographs
Calliphoridae	<i>Phormia regina</i>	Adult	3	Photographs

APPENDIX B: SUPPLEMENTARY MATERIALS

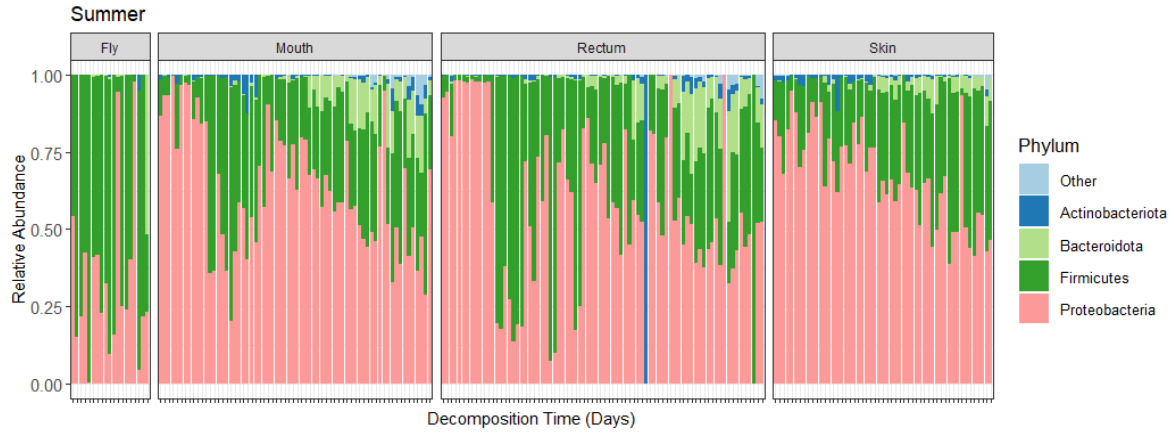


Figure 25. Phylum-level relative abundances grouped by sample type for the summer.



Figure 26. Phylum-level relative abundances grouped by sample type for the fall.

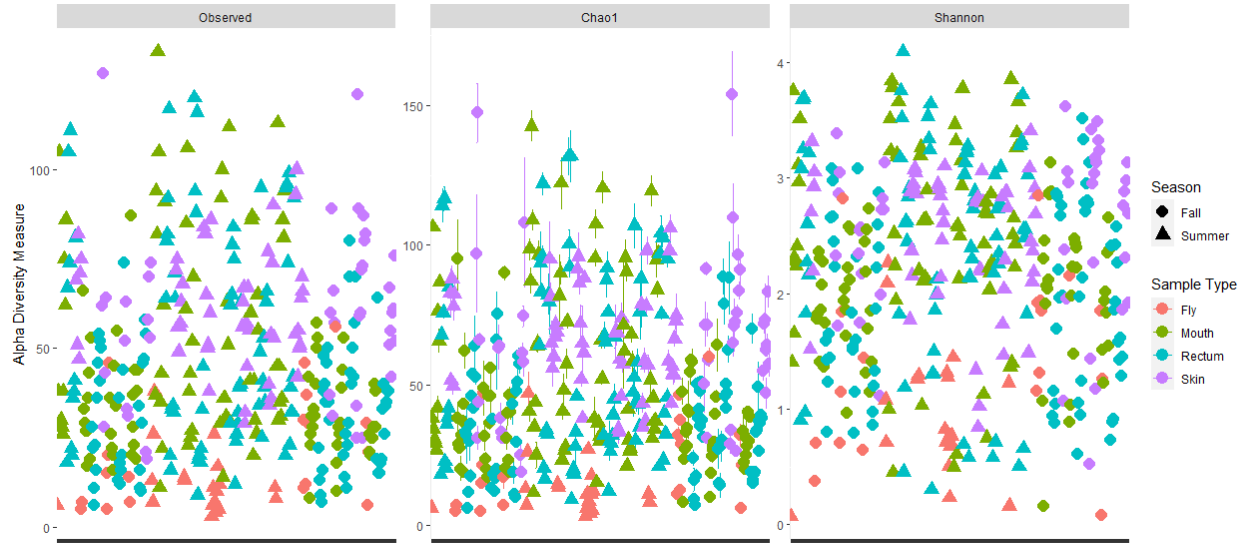


Figure 27. Observed, Chao, and Shannon diversity expressed as season and sample type.

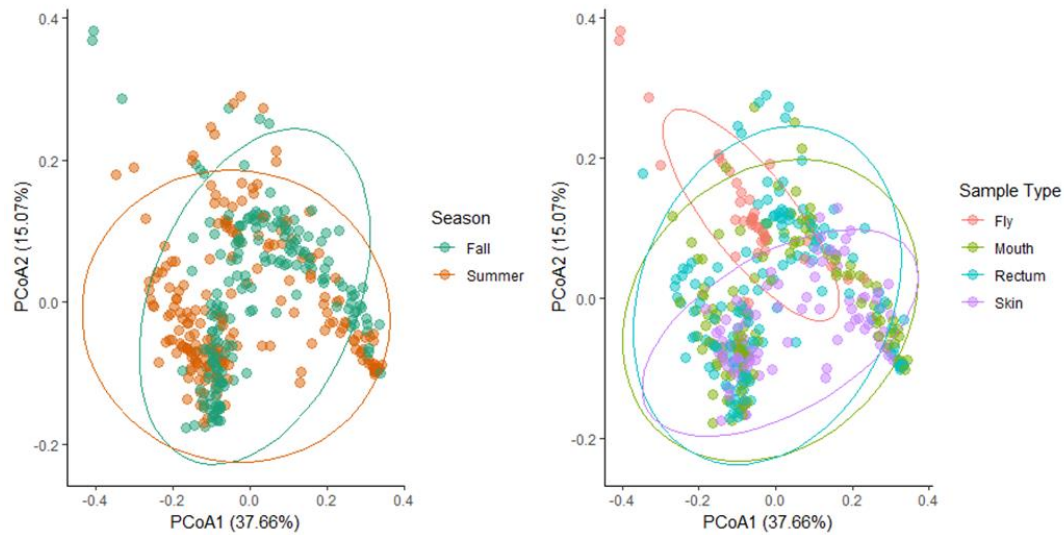


Figure 28. Principal coordinates analysis (PCoA) of weighted UniFrac distances for all samples (skin, mouth, rectum, and blowflies) from both seasons expressed as season (left), and all samples and both seasons expressed as sample type (right). Ellipses indicate 95% confidence intervals (CI) for multivariate t-distributions.

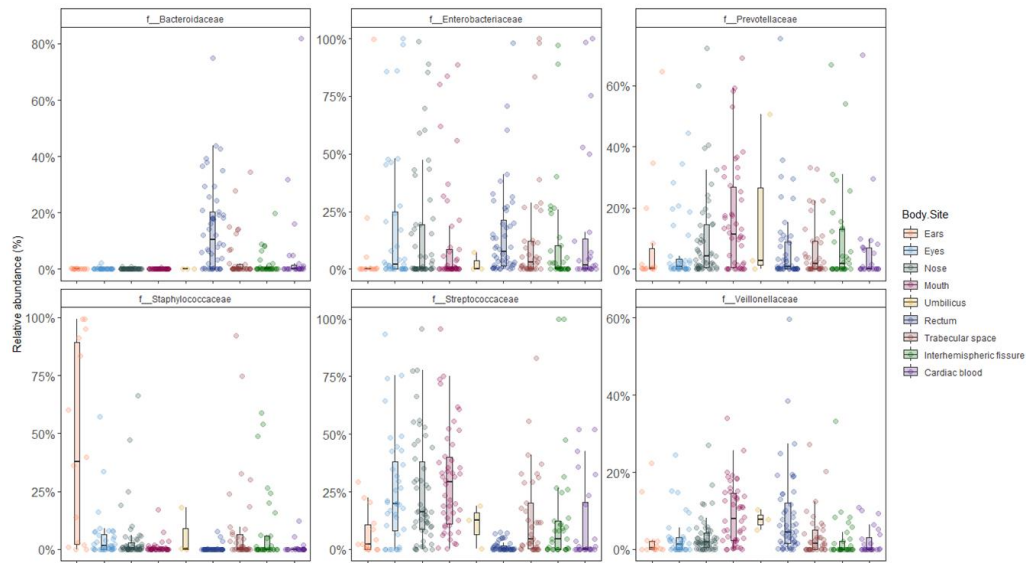


Figure 29. Relative abundance boxplots of the top six family-level taxa grouped by body site.

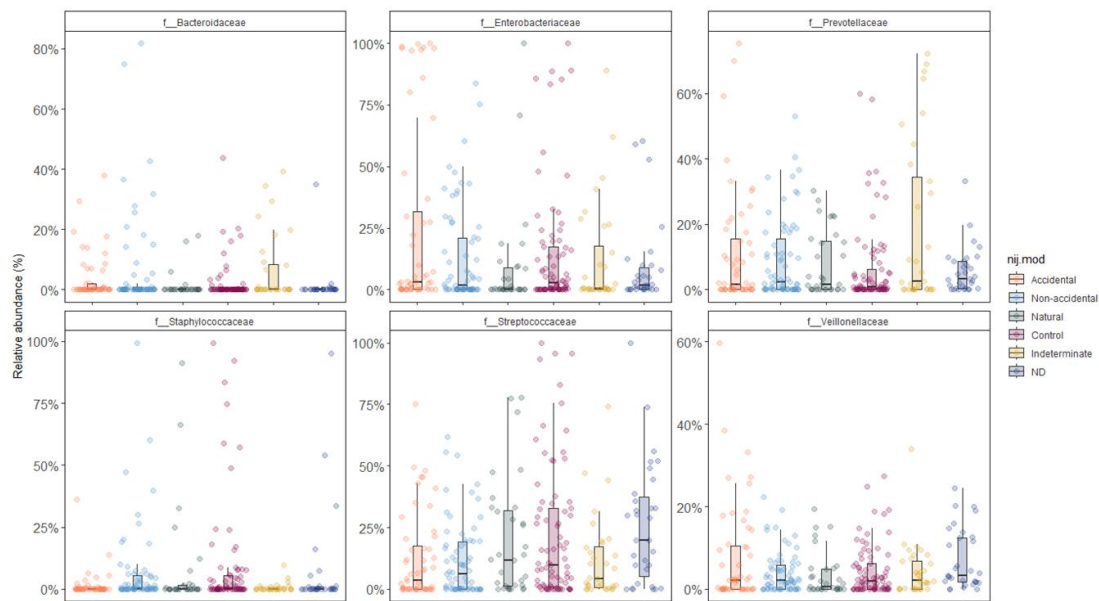


Figure 30. Relative abundance boxplots of the top six family-level taxa grouped by manner of death (MOD).



Figure 31. Total family-level relative abundances grouped by MOD (top) and body site (bottom).

Table 20. Counts and relative abundance of insects caught for the summer and fall.

Order	Family	Species	Summer		Fall		Total n
			n	Relative Abundance	n	Relative Abundance	
Coleoptera			13	3.02%	7	4.29%	20
	Carabidae		1	0.23%	1	0.61%	2
	Coccinellidae		-	-	5	3.07%	5
	Corylophidae		1	0.23%	-	-	1
	Curculionidae		3	0.70%	-	-	3
	Nitidulidae		2	0.46%	-	-	2
	Staphylinidae		6	1.39%	1	0.61%	7
Diptera			138	32.02%	52	31.90%	190
	Anthomyiidae		11	2.55%	3	1.84%	14
	Asilidae		1	0.23%	-	-	1
	Calliphoridae		19	4.41%	23	14.11%	42
		<i>Calliphora vomitoria</i>	-	-	2	1.23%	2
		<i>Cynomya cadaverina</i>	-	-	4	2.45%	4
		<i>Lucilia coeruleiviridis</i>	14	3.25%	5	3.07%	19
		<i>Lucilia illustris</i>	1	0.23%	3	1.84%	4
		<i>Lucilia sericata</i>	-	-	4	2.45%	4
		<i>Lucilia silvarum</i>	3	0.70%	5	3.07%	8
		<i>Phormia regina</i>	1	0.23%	-	-	1
	Ceratopogonidae		-	-	1	0.61%	1
	Chloropidae		29	6.73%	2	1.23%	31
	Dolichopodidae		11	2.55%	-	-	11
	Drosophilidae		2	0.46%	-	-	2
	Faniidae		3	0.70%	5	3.07%	8
	Heleomyzidae		-	-	2	1.23%	2
	Muscidae		19	4.41%	1	0.61%	20
	Mycetophilidae		1	0.23%	-	-	1
	Phoridae		9	2.09%	-	-	9
	Piophilidae		1	0.23%	-	-	1
	Pipunculidae		6	1.39%	-	-	6
	Polleniidae		1	0.23%	-	-	1
	Sarcophagidae		3	0.70%	-	-	3
	Scathophagidae		3	0.70%	9	5.52%	12
	Sciaridae		1	0.23%	2	1.23%	3
	Sepsidae		4	0.93%	-	-	4
	Syrphidae		10	2.32%	-	-	10
	Tachinidae		1	0.23%	-	-	1
	Tephritidae		1	0.23%	-	-	1
	Tipulidae		2	0.46%	2	1.23%	4
	Trichoceridae		-	-	2	1.23%	2
Hemiptera			17	3.94%	9	5.52%	26
	Aphididae		-	-	3	1.84%	3
	Cercopidae		5	1.16%	1	0.61%	6
	Cicadellidae		2	0.46%	-	-	2
	Pentatomidae		9	2.09%	5	3.07%	14
	Reduviidae		1	0.23%	-	-	1
Hymenoptera			36	8.35%	1	0.61%	37
	Apidae		4	0.93%	-	-	4
	Braconidae		2	0.46%	-	-	2
	Chalcididae		1	0.23%	-	-	1
	Cynipidae		1	0.23%	-	-	1
	Formicidae		9	2.09%	-	-	9
	Ichneumonidae		6	1.39%	1	0.61%	7
	Pteromalidae		5	1.16%	-	-	5
	Sphécidae		8	1.86%	-	-	8
Lepidoptera			-	-	1	0.61%	1
	Noctuidae		-	-	1	0.61%	1
Psocoptera			2	0.46%	-	-	2
	Psocidae		2	0.46%	-	-	2
Total			431		163		594